CARBON NANOTUBES AS A THERAGNOSTIC TOOL AGAINST BREAST CANCER（和訳：乳癌の診断・治療のためのカーボンナノチューブの開発）

著者	PRASHANTI JEYAMOHAN
学位授与大学	東洋大学
取得学位	博士
学位の分野	生命科学
報告番号	32663甲第351号
学位授与年月日	2013-09-25
URL	http://id.nii.ac.jp/1060/00006459/

CARBON NANOTUBES AS A THERAGNOSTIC TOOL AGAINST BREAST CANCER

Prashanti Jeyamohan

4R10101003

Doctor Course

Bio-Nano Science Fusion Course

Graduate School of Interdisciplinary New Science

Toyo University, Japan

July 2013

Preface

The new field of nanotechnology, has opened up rapid advances in science and technology, and creates myriad new opportunities for advances in medical science and disease treatment in human health care. Since adequate cancer therapeutics remains elusive, it is required to develop new methods for efficient cancer diagnosis and therapy. Nanoparticle-mediated site targeted drug delivery offers an attractive option to enhance the therapeutic efficacy by delivering optimal drug concentrations to the targeted cancer cells, and with reduced toxicity to the healthy tissues. The integration of nano-materials into cancer therapeutics provides a way of smart drug delivery with high target specificity and greater therapeutic efficacy. Carbon nanotubes (CNTs), due to their unique intrinsic physiochemical properties are extensively explored as novel drug delivery systems for therapy and diagnosis.

In this thesis entitled "**Carbon Nanotubes as a Theragnostic Tool Against Breast Cancer**" comprises of seven chapters and mainly focuses on the use of carbon nanotubes as potential biomedical materials, which show great potential as a targeted and effective drug delivery system for cancer therapy, by grafting it with cell-specific receptors and intracellular targeting molecules.

Chapter 1 explains the scope of nanotechnology in developing target specific carriers to achieve higher therapeutic efficacy, which will significantly contribute to the next generation of medical care and pharmaceuticals in the areas of disease diagnosis, disease prevention and most importantly cancer therapy. This review introduces specific physical and chemical properties of a series of nano-materials, such as nanoparticles, micelles, dendrimers, and with more emphasis on carbon nanotubes, which show great potential as effective drug delivery systems for cancer therapy. In addition to the ability of nanotubes to act as carriers for a wide range of

therapeutic molecules, they are also exploited for the use in photo-thermal destruction of cancer cells. Specifically, this article focuses on the current status, recent advancements, potentials and limitations of functionalized carbon nanotubes as targeted drug delivery carriers for efficient cancer nano-therapeutics.

Chapter 2 discusses the principles behind various instruments and techniques used for characterization of nano-sized structures, and for analysis of biological samples used in our research work.

Chapter 3 explains about a targeted drug delivery system (DDS) based on SWCNTs biofunctionalized with polyethylene glycol (PEG), conjugated with folic acid (FA) as targeting moiety and loaded with anticancer drug doxorubicin (DOX) for selective killing of tumor cells. The prepared nanotubes were characterized for their morphological features and their elemental composition. In this study, in vitro drug release analysis showed that the drug (DOX) binds at physiological pH (pH 7.4) and is released at a lower pH (lysosomal pH 4.0), which is the characteristic pH of the tumor environment. A sustained release of DOX from the SWCNTs was observed for a period of three days, which effectively caused the death of the breast cancer cells. The nanotubes were incubated with breast cancer cells and their biocompatibility and anti-proliferative effects were analyzed. We found that the targeted nanotubes were non-toxic to normal cells but toxic to tumor cells. Cellular uptake of the targeted nanotubes was studied in vitro using confocal microscopy. Time dependent drug effect was also studied on normal cells and tumor cells. Our results show significant internalization and retention of the nanotubes inside the tumor cells, inducing apoptosis. The results indicate that this study with folate conjugated and DOX loaded nanotubes can be a promising targeted delivery vehicle for cancer therapy.

Chapter 4 demonstrates that SWCNTs have a strong optical absorbance in the near-infrared (NIR) region. An approach utilizing the photo-thermal effect of single-walled carbon nanotubes (SWCNTs), in combination with folate as a targeting moiety and DOX an anticancer drug doxorubicin, for selective and accelerated destruction of breast cancer cells is demonstrated. The results of our study show that, under laser irradiation at 800 nm, SWCNTs showed strong light-heat transfer characteristics. These optical properties of SWCNTs provide an opportunity for photo-thermal ablation in cancer treatment. Our observation also showed that the internalization and uptake of folate conjugated nanotubes into cancer cells was by a receptor mediated endocytosis mechanism. In our in vitro experiments, laser effectively caused destruction of cancer cells while sparing the normal cells. When the above laser effect was combined with DOX conjugated SWCNTs, an enhanced and accelerated killing of breast cancer cells was noted. Thus, this targeting nano drug delivery system (NDDS) could effectively kill and suppress the growth of breast cancer cells, showing much higher pharmaceutical efficiency compared to free DOX. This study suggests that Laser + drug + SWCNTs could prove to be a promising selective modality with high treatment efficacy and low side effects for future cancer therapy.

In **Chapter 5** we present a dual drug delivery system consisting of PEG modified SWCNTs conjugated with FA and loaded with two anticancer drugs (DOX) and paclitaxel (PTX), forming DOX-PTX-FA-PEG-SWCNT conjugate. The combination of two or more therapeutic drugs is a feasible means to overcome the limitations of single chemotherapeutic drug in anti-tumor treatment, such as development of high toxicity, drug resistance, and limited regime of clinical uses. The prepared nanotubes were characterized for their morphological features and their elemental composition. Independent and combined drug release behaviors of the

drugs were studied. A time-dependent in vitro cytotoxicity studies were done for studying the cancer killing effect in comparison with free PTX and free DOX in breast cancer (MCF7) cells. A faster drug release was found to be associated with lower pH, which is advantageous for tumor targeted anticancer therapy. Confocal studies were carried out to demonstrate cellular uptake of the targeted nanotubes in tumor cells, while sparing the normal cells. This efficient suppression in tumor cell growth demonstrates a highly synergistic anti-proliferative activity of our developed system in breast cancer cells. The effect of this DDS in combination with laser was also analyzed, and enhanced destruction of breast cancer cells were observed. This nano-carrier might have important potential in clinical implications for co-delivery of multiple anti-tumor drugs with different properties.

Chapter 6 explains the application of another nano-carrier that could be utilized as a drug delivery agent in cancer therapy. Here, an anticancer drug loaded poly-L-Lactic-co-glycolic acid (PLGA)-lecithin-PEG nanoparticles were synthesized and were functionalized with AS1411 anti-nucleolin aptamers for site-specific targeting against tumor cells, which over expresses nucleolin receptors. The results of this study confirmed that the aptamer-labeled PLGA-lecithin-PEG nanoparticles are potential carrier candidates for differential targeted drug delivery.

Chapter 7 concludes the thesis with the summary and future prospects of this research work.

The need to develop target specific carriers to achieve higher therapeutic efficacy with minimal side effects to healthy tissues, is one of the most interesting and challenging endeavors faced in the pharmaceutical field.

Contents

Chapter 1

Opportunities and challenges of single walled carbon nanotubes in cancer therapy

Abstract

The scope of nanotechnology to develop target specific carriers to achieve higher therapeutic efficacy is gaining importance in the pharmaceutical and other industries. Specially, the emergence of nanohybrid materials is posed to edge over chemotherapy and radiation therapy as cancer therapeutics. This is primarily because nanohybrid materials engage controlled production parameters in the making of nanoparticles with specific size, shape and other essential properties. It is widely expressed that these materials will significantly contribute to the next generation of medical care technology and pharmaceuticals in areas of disease diagnosis, disease prevention and most importantly cancer therapy. This review firstly introduces the specific physical and chemical properties of a series of nanomaterials, such as nanoparticles, micelles, dendrimers and carbon nanotubes. It then places great emphasis on the carbon nanotubes, which show great potential as effective drug delivery systems for cancer therapy, as they can be grafted with cell-specific receptors and intracellular targeting molecules for the targeted delivery of therapeutics. In addition to the ability of nanotubes to act as carriers for a wide range of therapeutic molecules, they have also been exploited for use in photothermal destruction of cancer cells. Specifically, this article focuses on the current status, recent advancements, potentials and limitations of functionalized carbon nanotubes as targeted drug delivery carriers for efficient cancer treatment.

Introduction

Currently available technologies have made enormous advancement in cancer research, but an adequate therapy remains elusive.[1] Cancer occurs at a molecular level when multiple subsets of genes undergo genetic alterations, either by activation of oncogenes or inactivation of tumor suppressor genes, allowing cancerous cells to grow and divide uncontrollably.[2] These processes allow cancer cells to acquire properties of malignant proliferations, tissue infiltrations through interactions with surrounding stromal cells, dysfunction of organs by the evasion of immune detection, self-sufficiency in growth signals and resistance to both anti-proliferative and apoptotic agents.[3, 4] Also, in vivo delivery of the therapeutic agents has to overcome physiological barriers, including hepatic and renal clearance, enzymolysis and hydrolysis, as well as endosomal/lysosomal degradation.[5, 6] In addition, the efficiency of anticancer drugs is limited by their unsatisfactory properties, such as poor solubility, narrow therapeutic window, and intensive cytotoxicity to normal tissues, which may be the causes of treatment failure in cancer.[7] Therefore, it would be desirable to develop new methods to detect cancers at their early stage and also design novel therapeutic strategies capable of delivering chemical agents and other therapeutic materials specifically to tumor locations without affecting healthy tissues.[8, 9, 10, 11] With the emerging field of nanotechnology, the integration of nanomaterial's into cancer therapeutics is one of the rapidly growing fields in the development of nanoparticles, nanostructured surfaces and platforms for rapid and early diagnostics, smart drug delivery and for understanding the therapeutic efficacy.[12, 13] Nanomaterials have sizes ranging from about one nanometer up to several hundred nanometers, Materials in this size range exhibit interesting physical

properties, presenting new directions for more effective diagnosis and therapy of cancer.[14, 15]

Types of nanotechnology based nanocarrier systems

Nanocarriers applied as drug delivery systems are synthesized from organic and inorganic materials such as polymeric nanoparticles, micelles, dendrimers, lipid nanoparticles, carbon nanotubes, quantum dots, and nanofibers[16, 17] (Figure 1). They show great potential in cancer therapy by enhancing the performance of medicine and reducing side effects to healthy tissues for improved therapeutic efficiency.

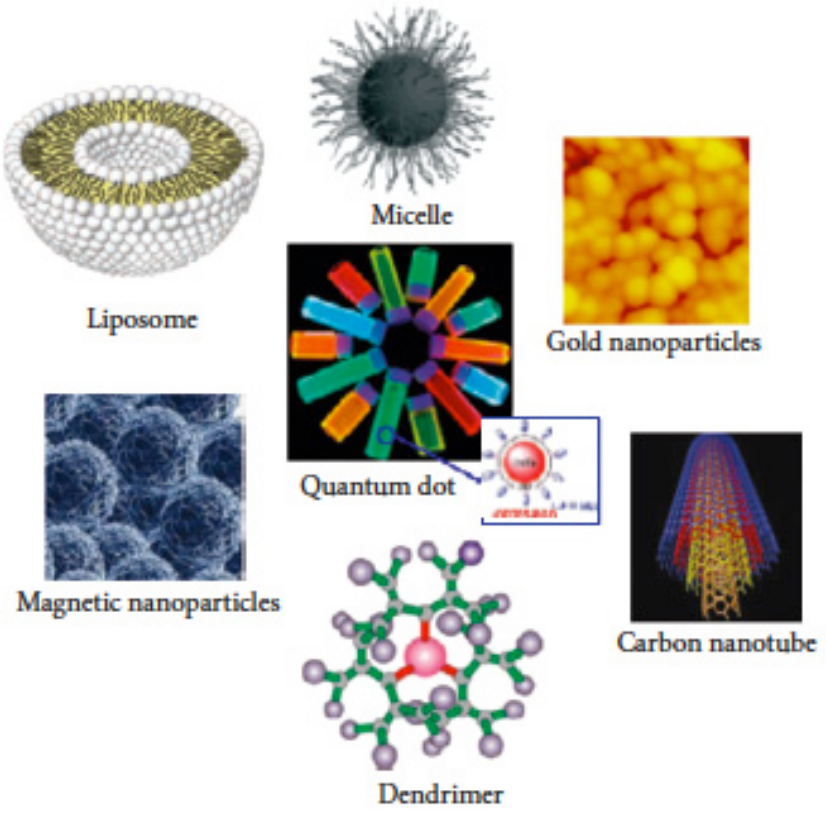

Figure 1. Examples of nanomaterials and nanocarrier systems. [16, 24]

Polymeric nanoparticles

Polymeric nanoparticles are particles less than 1μm in diameter, synthesized from natural or synthetic polymers. Depending on the methods of preparation, matrix-type or reservoir-type structure, namely nanospheres or nanocapsules can be obtained.[18] Natural polymers such as albumin, chitosan, heparin and synthetic polymers such as N-(2-hydroxypropyl)-methacrylamide copolymer (HPMA), polystyrene-maleic anhydride copolymer, polyethylene glycol (PEG), and poly-L-glutamic acid (PGA) have been material of choice for polymeric nanoparticles.[19, 20, 21] They are considered as the promising carriers for drug delivery because they can improve the specificity of drug action by changing their tissue distribution and paharmacokinetics.[22] They have also played important roles in delivering antitumor drugs in a targeted manner to the malignant tumor cells, thereby reducing the systemic toxicity and increasing their therapeutic efficacy. These nanoparticles due to the reticulo-endothelial system (RES) and the effect of enhanced permeation and retention (EPR) effect, can be used for passive delivery to the lymphatic system, brain, arterial walls, lungs, liver, spleen or for long-term systemic circulation.[3, 22, 23] These nanoparticles are also amendable to surface functionalization for active targeting to tumor tissues or cells and for stimulus-responsive controlled release of drug.[24]

The receptor-mediated endocytosis (RME) reveals the selective recognition, high-affinity binding, and immediate internalization for the ligands at a cellular level.[25] Various targeting moieties can be attached to the polymer backbone, which acts as a secondary uptake mechanism following EPR-based primary accumulation (Figure 2) .[4, 26] Liang et al. developed paclitaxel-loaded nanoparticles with galactosamine conjugated on it for targeting liver cancer cells. The nanoparticles appeared most efficient in reducing the size of the tumor when injected into hepatoma-bearing nude

mice, through the specific interaction between galactosamine and asialoglycoprotein receptors.[27] Thermosensitive magnetoliposomes (TMs) encapsulated with methotrexate (MTX) can achieve a good magnetic targeting effect and rapid drug release in response hyperthermia, which implies their great potential in cancer therapy.[28]

Micelles

Spontaneous assembly usually forms polymeric micelles into core-shell structures when its concentration is above critical micelle concentration (CMC). They have a number of unique features, including nanosize, easy manipulation of surface chemistry, core functionalities, as well as ease of fabrication, making them suitable carriers for encapsulation, and delivery of water insoluble agents.[5] The hydrophobic solid-like inner core region serves as a reservoir for hydrophobic drugs, whereas the hydrophilic shell region stabilizes the hydrophobic core and renders the polymers water-soluble.[29] The hydrophilic shell helps the micelles in escaping the recognition of RES and prolongs the blood circulation of drugs. The small size (< 100 nm) allows the efficient accumulation of micelles in pathological tissues with permeabilized vasculature via the enhanced permeability and retention (EPR) effect.[30] Mikhail presented a detailed review on the density and heterogeneity of the vasculature at tumor sites, interstitial fluid pressure, and found that transport of macromolecules in the tumor interstitium are responsible for the extravasation of micelles.[31]

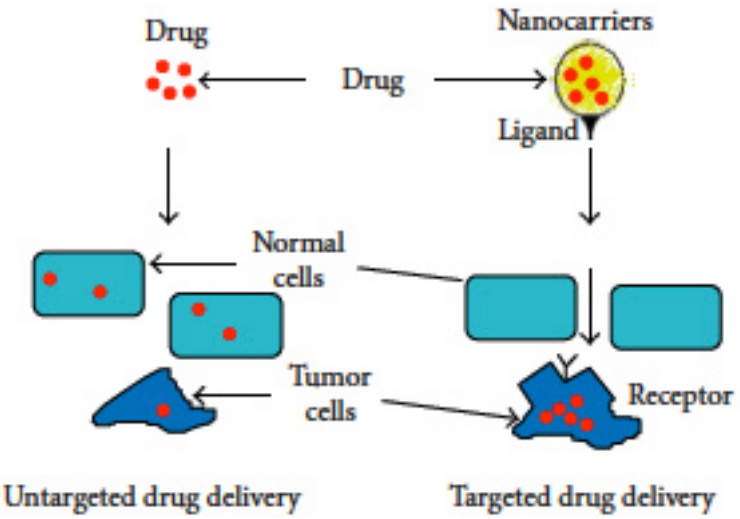

Figure 2. Schematic of nanocarrier systems for site-targeted drug delivery. [25]

Stimuli-responsive polymeric micelles are often designed for controlled release of drug into tumor tissue with external stimuli trigger, like temperature, pH, ultrasound and special enzymes.[32, 33] Among these stimuli, pH and temperature are representative, because the external pH of cancerous tissue tends to be lower and the temperature is higher compared to the surrounding normal tissue, which are caused by abnormal metabolism of cancer tissues.[5] Lower critical solution temperature (LCST) polymers, such as poly (N-isopropylacrylamide) (pNIPAAm) with a cloud point around 32°C or some other poly (N-alkylacrylamide) compounds, were investigated as components of temperature-responsive copolymer micelles.[33] The micelles exhibited rapid and temperature-responsive drug release in cancer cells, which was caused by the destruction of the hydrophobic-hydrophilic balance with the increase of temperature. Licciardi et al. synthesized novel folic acid- (FA-) functionalized diblock copolymer micelles for target delivery of antitumor drugs, and lowering the solution pH to 5 could trigger the rapid release of drug. This strategy combined the targeted delivery of therapeutics together with pH-controlled drug release, which provided a tumor-selective nanocarrier for the efficient delivery of anticancer drugs (Figure) .[34]

Dendrimers

Dendrimers are artificial macromolecules with tree-like structures in which the atoms are arranged in many branches and sub-branches radiating out from a central core.[35, 36] They are synthesized from branched monomer units in a stepwise manner. Thus, able to control their molecular properties, such as size, shape, dimension, and polarity, which depend on the branched monomer units.[36] They offer unique interfacial and functional performance advantages due to their empty internal cavities and surface functional groups.[37] So they have an enormous capacity for solubilization of hydrophobic drugs and can be modified or conjugated with various molecules. Based on these specific properties, the dendrimers have shown great development in anticancer drug delivery systems.[36, 38] To actively target drugs to tumor tissues the dendrimers are used for covalent attachment of special targeting moieties, such as sugar, folic acid, antibody, biotin, therapeutic drugs and epidermal growth factors.[39, 34, 40, 36, 41] Choi and coworkers synthesized a fifth generation polyamidoamine (G5 PAMAM) dendrimers conjugated to fluorescein and folic acid, linked together by complementary DNA oligonucleotides to produce clustered molecules for targeting cancer cells that overexpress the high-affinity folate receptor. In vitro studies indicated that the DNA-linked dendrimer clusters could specifically bind to KB cells and could be used as imaging and therapeutics agents for cancer therapy.[42]

Carbon Nanotubes

Carbon nanotubes (CNT) are synthetic nanomaterials made from carbon and belong to the fullerene family. Carbon nanotubes are made up of thin sheets of benzene ring structured carbon rolled up into the shape of a seamless tubular structure. They can be classified into two general categories based on their structure: single-walled carbon nanotubes (SWCNTs) with a single cylindrical carbon wall having a diameter of 1-2

nm, and length ranging from 50 to several hundred nanometers. Multiwalled carbon nanotubes (MWCNTs) have multiple walled-cylinders nested within other cylinders with a diameter ranging from 5-100 nm.[43] Figure 3 CNTs are generally produced by three major techniques: electric arc discharge, [44] laser ablation[45] and thermal or plasma enhanced chemical vapor deposition (CVD) [46]. These methods involve synthesis at high temperature and pressure in the presence of reaction catalysts, leading to fine structures of CNTs along with some impurities like graphite debris and catalytic particles. Various methods such as oxidation, acid treatment, chromatography, filtration and functionalization are involved in the purification.[47] Compared to other nanomaterials, CNTs have unique physical and chemical properties such as high aspect ratio, ultrahigh surface area, light weight and distinct optical properties, such as, high absorption in the near-infrared (NIR) range and a strong Raman shift, which makes them advantageous for biomedical applications linked to detection and imaging.[48] The combination of these characteristics makes CNT a unique nanomaterial with the potential for diverse applications, in areas of gene therapy, drug delivery, thermotherapy, imaging and anticancer treatments, as explained in the subsequent sections.[25, 49]

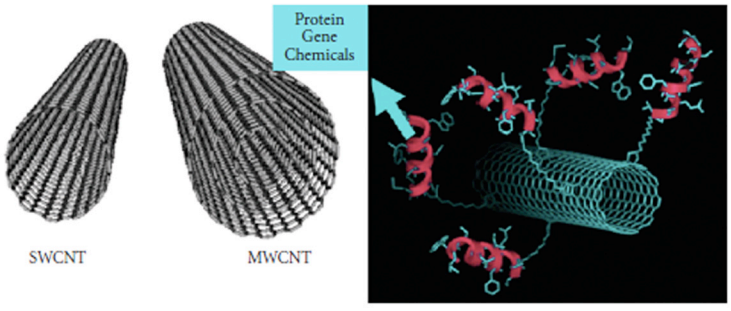

Figure 3. Structure of single-walled carbon nanotubes (SWCNTs) and multiwalled carbon nanotubes (MWCNTs), as well as drug loaded carbon nanotubes (adapted from http://www-ibmc.u-strasbg.fr/ict/vectorisation/nanotubes eng.shtml and http://www-ibmc.u-strasbgfr/ict/vectorisation/vectorisation eng.shtml).

Functionalization of carbon nanotubes for drug delivery and other applications

CNTs are hydrophobic in nature and thus insoluble in water, which limits their application in biomedical and medicinal chemistry. Therefore, various functionalization methods like adsorption, electrostatic interaction and covalent bonding are being utilized with a number of compounds and polymers to render a hydrophilic character to CNTs so as to avoid aggregation and to facilitate their use in biomedical applications.[1] Covalent modifications are carried out by reacting carbon atoms on the sidewall of carbon nanotubes to a therapeutic molecule. In biological applications, oxidation and grafting polymers on the sidewalls of carbon nanotubes are widely employed. During oxidation, pristine CNTs are refluxed in nitric acid, which results in oxygenated functional groups, mainly carboxyl acids.[50, 51] Another covalent modification of CNTs involves 1, 3-dipolar cycloaddition reactions.[52] Using this method, azomethineylides are added on the graphite surface of CNTs, forming pyrrolidine-fused rings. These covalent modifications lead to the generation of various functional moieties on the ends and sidewall of CNTs and enable the conjugation of various fluorescent dyes, drugs, and peptides.[53, 54] Other biocompatible polymers like polyethylene glycol (PEG) can be grafted forming SWCNT-PEG graft copolymer that enhances the solubility of the nanotubes.[55] Figure 4 Non-covalent functionalization of CNTs has also been explored with materials like surfactants, natural polymers, synthetic polyelectrolytes and amphiphilic block polymers or polymeric micelles. The hydrophobic moiety binds to the CNT sidewalls via π-π interactions, helping the CNTs to disperse in aqueous solutions. It was demonstrated that the non-covalent conjugation of pyrene with glycodendrimers via π-π stacking on the sidewall of CNTs, enhances their water solubility.[56] Amphiphilic polymer phospholipid linked PEG (PL-PEG) was used to non-covalently bind to the sidewalls

of SWCNTs, giving rise to a number of biomedical applications.[57]

CNTs as carriers for drugs, genes and proteins in cancer therapy

Most of the research on CNTs has been focused on their potential for anticancer drug delivery. This might be attributed to the transporting capabilities of CNTs combined with appropriate surface modification and their unique physiochemical properties, which lead to the development of a new kind of nanomaterial for cancer therapy.[11]

Drug delivery by CNTs

Functionalized CNTs can cross the mammalian cell membrane by endocytosis or other mechanisms with the help of specific peptides or ligands on their surface to recognize cancer-specific receptors on the cell surface.[58] Cancer cells overexpress folic acid (FA) receptors, and many research groups have designed CNT carriers with engineered surfaces to which FA derivatives can be attached. CNTs are used for targeting lymph node cancers, as they can be retained in the lymph nodes for longer periods of time compared to spherical nanocarriers.[59-62] In a recent study, Yang et al.[63] have loaded the anticancer molecule gemcitabine into magnetic MWCNTs and injected subcutaneously and, they reported high activity against lymph node metastasis in mice. In another study, the poorly water-soluble anticancer drug, camptothecin, has been loaded into polyvinyl alcohol-functionalized MWNTs and was reported to be potentially effective in the treatment of breast and skin cancers.[64] In another approach, PAA-grafted MWCNTs were prepared and subcutaneously injected into the left rear footpad of rat.[65] The biopsy result showed that left popliteal lymph nodes were blacker than other regions, 24 h after the injection. Biopsy experiments did not identify the presence of PAA-g-MWCNTs in the major internal organs such as liver, kidney and lung, which suggests that the PAA-g-MWCNTs may

have the potential to be used as a vital staining dye and can be used for lymph node identification during surgery, even when they are very small.[66]

Dhar and coworkers developed the longboat delivery system, (Figure 5) in which cisplatin and FA conjugate was attached to a functionalized SWCNT via a number of amide bonds to form a "longboat" which is reported to be taken up by cancer cells via endocytosis, followed by the release of the drug and its subsequent interaction with the nuclear DNA. Another platinum anticancer drug, carboplatin, was incorporated into CNT and has been shown to inhibit the proliferation of urinary bladder cancer cells in vitro.[67]

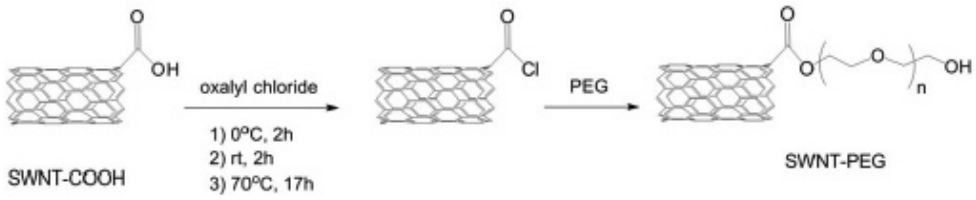

Figure 4. Synthetic scheme of SWNT-PEG graft copolymers. The carboxylic acid functionalized Single Wall Carbon Nanotubes (SWNT–COOH) react with oxalyl chloride to form the acylchloride intermediate, which is further reacted with PEG to form SWNT–PEG. [148]

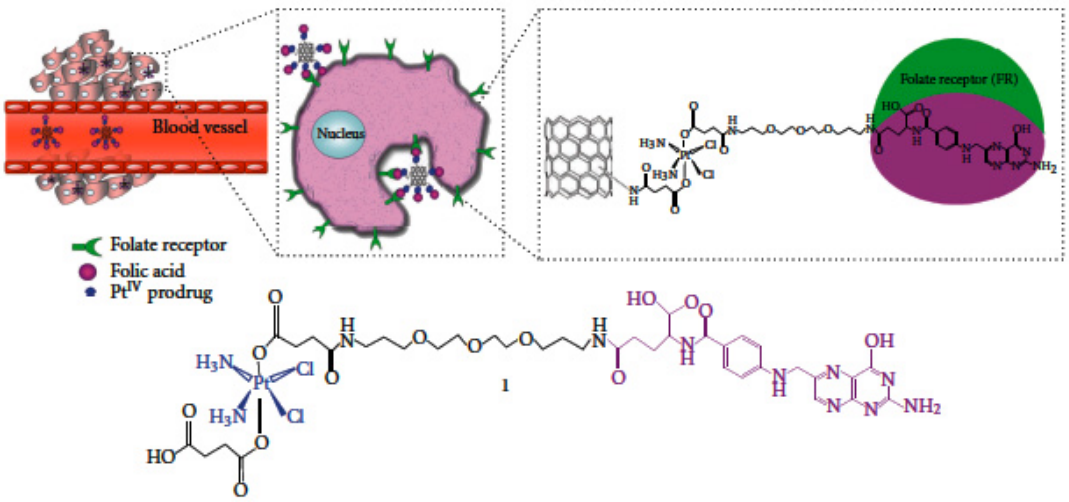

Figure 5. The "longboat" anticancer system in which one end of the chemotherapeutic agent cisplatin is attached from to the FA derivative and the opposite end to a SWCNT via an amide link. [67]

CNTs can carry therapeutic drugs more safely and effectively into the cells, which make them ideal candidates for drug delivery. Recently, novel SWCNT- based tumor-targeted drug delivery systems (DDS) have been developed. These delivery systems generally consist of three parts: functionalized SWCNTs, tumor targeting ligands and anticancer drugs. The complex is taken up efficiently and specifically by cancer cells with subsequent intracellular release of anticancer drugs, which suppressed cancer cell growth more effectively than untargeted controls containing the same drug.[68] Hence, with this novel approach, serious and harmful side effects to healthy tissues can be avoided. Paclitaxel is a poorly water-soluble anticancer drug. In the commercialized paclitaxel product (Taxol), Cremophor EL is used to solubilize the drug. Unfortunately, Cremophor EL itself is toxic. Therefore, finding a suitable alternative is of high priority. Moreover, the circulation time of Taxol is very short. Coating the nanocarriers with hydrophilic polymers such as polyethylene glycol (PEG) has been established as a strategy to prolong the circulation of the nanocarrier in blood by making the carrier highly evasive to the uptake by the macrophages in blood.[69, 70] PEGylation of paclitaxel increases the circulation time in the blood over Taxol.[71] In the research performed by Liu Z. et al., [72] functionalized SWNTs conjugated with paclitaxel through branched PEG chains via a cleavable ester bond was synthesized. This resultant complex was more effective in suppressing tumor growth in vivo than Taxol or paclitaxel-PEG conjugate in a 4T1 breast cancer animal model. PEGylation of the nanotubes is able to prolong the circulation time and greatly enhance cellular uptake of the drug by the cancer cells. Similar findings of anti-cancer activity have been reported when paclitaxel was loaded into PEGylated SWCNTs or MWCNTs using HeLa and MCF-7 cancer cell lines.[73, 74]

Multidrug resistance is a significant obstacle to successful anticancer drug therapy since the P-glycoprotein transporter can interfere with the accumulation of anticancer drugs in the target cells, resulting in reduced effectiveness of therapy.[75, 76] Recently, confocal microscopy has shown the accumulation of PEGylated MWCNTs in multidrug resistant hepatoma cell lines.[77] Liu and coworkers reported that although PEGylation of SWCNTs can prolong blood circulation time of the associated anticancer drug, it may cause an accumulation of the nanotubes in the dermal tissues of mice, suggesting that the extend of PEG coating require optimization.[78]

Biotin-functionalized SWCNTs conjugated with the anticancer agent taxoid using a cleavable linker have also been designed. The drug is transported via endocytosis, released in the cell and interacts with microtubules as evaluated by flow cytometry. This resulted in the formation of a stable microtubule-taxoid complex, which finally caused apoptosis and cell death.[74]

A targeted delivery system of FA-tethered SWCNTs-doxorubicin (DOX) has been designed. Bioadhesive polymers such as chitosan (CHI) and sodium alginate (ALG) were used to enhance the aqueous dispersibility of the nanotubes, while FA was used to improve the targeting properties of the nanotubes (Figure 6). Transmission electron microscopy (TEM) indicated that the drug was released at the low lysosomal pH of the HeLa tumor cells after being transported into the tumor but not at the normal physiological pH of 7.4.[58] Recently, a novel approach by covalently attaching PAMAM dendrimers to FA-treated MWCNTs has been introduced and flow cytometry and confocal microscopy indicated possible targeting of cancer cells that overexpress FA receptors.[79] Li and coworkers designed a novel system referred to as "dual-targeted drug nanocarrier" by conjugating MWCNTs with iron nanoparticles and folate moiety. This system was efficiently loaded with doxorubicin and

demonstrated superior delivery to HeLa cells when compared to free doxorubicin.[80] A list of CNT-based tumor-targeted drug delivery systems (DDS) is given in Table 1.

CNTs as carriers of immunoactive compounds, proteins, and genetic materials

Gene therapy aims to use genetic material to treat diseased cells by repairing the cause of the disease. Since genetic materials are not able to cross the biological membranes, the use of viral or nonviral vectors to carry the gene and internalize it into the cell is necessary. Nonviral vectors are less efficient than viral vectors[81] and short lived, [82] but they are far safer.[83, 84] Pantarotto and coworkers developed novel functionalized SWCNT-DNA complex and reported high DNA expression compared with naked DNA.[85]

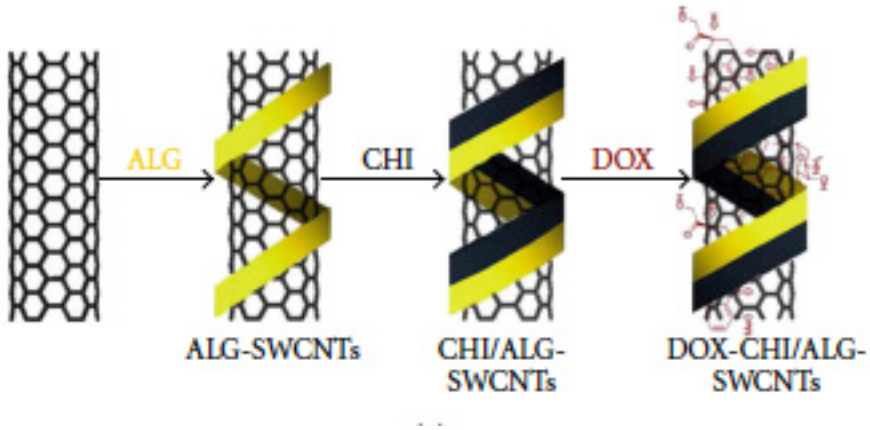

Figure 7. Preparation of SWNTs-DOX after inclusion of bioadhesive polymers to enhance nanotubes dispersability in aqueous phase. [58]

Reference	CNTs	Drug	Tumor-targeted modules	Tumor
Chen et al. [74]	SWNTs	Taxoid	Biotin and a spaces	Leukemia
Heister et al. [149]	SWNTs	Doxorubicin	A monoclonal antibody	Colon cancer
Bhirde et al. [150]	SWNTs	Cisplatin	Epidermal growth factor	Squamous carcinoma
Dhar et al. [67]	SWNTs	Cisplatin	Folate	Nasopharyngeal epidermoid carcinoma etc.
Liu et al. [73]	SWNTs	Doxorubicin	Rgd	Breast cancer, Glioblastoma
Zhang et al. [58]	SWNTs	Doxorubicin	Folate	Cervical carcinoma
Mc Devitt et al. [151]	SWNTs	Radionuclide	Thiolated-antibody	Burkitt lymphoma
Liu et al. [72]	SWNTs	Paclitaxel	–	Breast cancer

Table 1. CNT-based tumor- targeted drug delivery systems (DDS)

Functionalized SWCNTs have been used as suitable non-viral carriers of macromolecules and internalization of such macromolecules into living cells by CNTs has been reported to take place via energy-dependent endocytosis.[86] Confocal microscopy and flow cytometry results have shown much greater fluorescent activity of protein and DNA when conjugated to SWNTs as compared to the naked macromolecules indicating that CNTs are promising vectors for gene and protein.[87] Cai and coworkers introduced an approach to gene delivery named as "carbon nanotube spearing".[88] Plasmid DNA with a fluorescent protein were immobilized onto nickel-embedded CNTs and was "speared" into Bal 17 B lymphoma cells using a magnetic field, which produced high transfection in the target cells.[88] In another study, HeLa cells were exposed to DNA attached SWCNTs at 37°C which resulted in gene internalization. However, at lower temperature (e.g., 4°C), no internalization took place, possibly because gene transport occurs by energy-dependent endocytosis.[87]

Gene silencing, a recent strategy in gene therapy, involves the use of small interfering RNA (siRNA) in the treatment of many diseases, including various cancers. In cancer, antitumor immunity might be inhibited by suppression of cytokine signaling 1 (SOCS1). siRNA can be conjugated to phospholipid-functionalized SWCNTs using a cleavable disulfide linker, resulting in efficient gene silencing and subsequent death

of the targeted cell.[89] In another study, amino-functionalized MWNTs-siRNA complexes have shown successful suppression of tumor and prolonged survival in lung tumor of an animal model.[90] Functionalized SWCNTs have been designed as carrier for siRNA for internalization into K562 cells and subsequent inhibition in the production of cyclinA(2) and treatment of chronic myelogenous leukemia. Many types of cancer (e.g., leukemia) can overexpress cyclinA(2), and suppression of this material using siRNA-CNTs can promote apoptosis in the targeted tumor.[91] In another finding, functionalized SWNTs have been conjugated to telomerase reverse transcriptase (TERT) siRNA which successfully silenced the target gene, and tumor growth was inhibited in vitro using murine tumor cell lines and in vivo using a mouse model.[92] Similarly in another study CNTs cationically functionalized with polyethylene imines have been shown capable of complexing with siRNA and generating a silencing activity of up to 30% and cytotoxicity of up to 60%.[93]

Streptavidin is a protein that has anticancer activity.[94] However, due to its very large molecular weight, it does not penetrate the cells. Kam et al.[95] used a conjugate of streptavidin with SWCNT-biotin, which resulted in internalization of the protein into model cancer cells by adsorption-mediated endocytosis. Transmission electron and confocal microscopy have shown that MWCNTs can act as transporters of the recombinant ricin A chain protein, resulting in high death rates of cancer cells.[96]

Immunotherapy may be an alternative to gene therapy in cancer treatment. Antitumor immunotherapy using CNTs has gained interest among researchers. Tumor-specific monoclonal antibodies, radiometal ion chelates, and fluorescent probe have been conjugated to SWCNTs and successful targeting to tumor has been reported.[97] The antitumor immune response was increased when MWCNTs were conjugated to tumor lysate protein as an antigen.[98]

Glioma is a brain tumor that is able to evade the host immune system.[99, 100] Macrophages have a preferential affinity towards CNTs when compared to glioma cells.[101] Van Handel and coworkers[102] developed an immunotherapy approach using MWNTs against GL261 murine intracranial glioma cancer model, based on the fact that macrophages prefer to engulf CNTs compared with glioma cells. An increase in the influx of macrophages into the glioma cells with MWNTs was reported. Also, an increase in the levels of IL-10 expression was observed, suggesting that immunomodulation using CNTs is a possible strategy to treat cancer.

Reduction in the tumor volume and prolonged survival in animal models was reported when angiogenesis targeting antibodies E4G10 were attached to SWNTs via radiometal ion chelates.[103] Oxidized MWCNTs has been reported to retard tumor growth when injected subcutaneously to a hepatocarcinoma bearing animal to induce an immune response.[104] This suggests that CNTs themselves could possibly be surface-engineered to have anticancer activity by inducing an immune response against tumor.

A major hurdle to effective anticancer therapy is the multidrug resistance caused by enhanced efflux of anticancer drugs by the overexpressed p-glycoprotein, resulting in poor anticancer effect.[75, 76] Li et al. reported that SWCNTs functionalized with p-glycoprotein antibodies and loaded with the anticancer drug doxorubicin demonstrated higher cytotoxicity against K562R leukemia cells compared with free doxorubicin.[105]

CNT mediated photothermal therapy of cancer

CNTs are also welcomed in the field of thermal therapy and considered to be a non-invasive, harmless and highly efficient technique.[106] CNTs are able to absorb light in

the near infrared (NIR) region, resulting in heating of the nanotubes. This unique property of CNTs has been exploited as a method to kill cancer cells via thermal effects.[86, 107-119] According to Gannon et al.[107] The incubation of the nanotubes functionalized using kentera (a polyphenylene ethynylene-based polymer) were studied using hepatic tumor cells followed by application of radiofrequency field, which demonstrated a concentration-dependent thermal destruction and complete necrosis of the tumor cells. By contrast, tumor cells that were injected with the Kentera alone (without CNTs) were viable after the application of the radiofrequency field. Both in vitro and in vivo tests have shown thermal destruction of cancer cells in the presence of SWNTs with exposure to radiofrequency. A formulation based on FA-PL-PEG functionalized SWCNTs was used for targeting cancer cells, which over-express folate receptors.[109] Selective cancer cell destruction was achieved by continuous NIR radiation of SWCNTs. The NIR triggered cell death has been shown to remain nontoxic for neighboring normal cells. [86] This research presented a novel application of CNTs in cancer therapy. Another study utilizing the NIR characteristic of CNTs involved the destruction of breast cancer cells by non-covalently attaching monoclonal antibodies against membrane markers: insulin like growth factor 1 receptor (IGF1R) and human endothelial receptor 2 (HER2). The antibodies were attached using π-π interactions of pyrene rings onto the sidewalls of SWCNTs.[120]

CNTs mediated photodynamic therapy (PDT)

PDT could potentially be an ideal cancer treatment therapy capable of efficiently destroying tumors while at the same time sensitizing the immune system to seek out and destroy metastases.[121] Singlet oxygen is one of the most important agents generated during PDT, which can react rapidly with cellular molecules and mediate cellular toxicity to cause cell damage, ultimately leading to cell death. However the

lifetime and diffusion distance of singlet oxygen are very limited. Zhu et al.[122] synthesized a novel molecular complex photosensitizer, an ssDNA aptamer, and SWCNTs, which were able to control and regulate singlet oxygen generation, whereby more efficient, reliable and selective PDT could be guaranteed.

CNTs for other therapeutic applications

The use of CNTs in therapeutic applications other than cancer is also developing. Surface-engineered CNTs may be able to capture pathogenic bacteria in liquid medium.[123-125] Thus, CNTs themselves might have antimicrobial activity since microorganisms may be adsorbed onto the surfaces of CNTs. It has been reported that the electronic properties of SWNTs may regulate the antibacterial activity in E. coli. The antibacterial effect was attributed to CNT induced oxidation of the intracellular antioxidant glutathione, resulting in increased oxidative stress on the bacterial cells and eventual death.[126] Functionalized CNTs can attach covalently to amphotericin B and transport it into mammalian cells, thus demonstrating their ability to act as carriers for antimicrobial agents.[127, 128]

In vitro and in vivo toxicity of CNTs

Although there are exciting prospects for the application of CNTs in medicine, concerns over adverse and unanticipated effects on human health have also been raised. So far, many studies have been performed to evaluate the toxicological effects of CNTs both in vitro and in vivo.[11] The CNT cytotoxicity was attributed to variability in the doses, physical form like length and type of CNTs, [129] effect of metal catalyst impurities, [130] degrees of functionalization and dispersion of CNTs.[131] Metal catalysts are the main source of cytotoxicity in CNTs.[132, 133] Iron, the most common catalyst for growing CNTs, may boost the free radical reactions in the living cells.[134]

Becker et al.[135] proved that CNTs shorter than 189 +/- 17 nm have greater cytotoxicity. Furthermore, CNTs are required to be hydrophilic as drug carriers. Therefore, the surface chemistry plays an important role in improving the biocompatibility of CNTs. Few reports have demonstrated significant reduction in the cytotoxicity of CNTs due to the high degree of functionalization on CNT side walls.[130, 136, 137] Functionalized SWCNTs (f-SWCNTs) are much less toxic than surfactant-stabilized SWCNTs.[138] In a typical experiment, immunoregulatory cells (macrophages, B and T lymphocytes) were incubated in two types of amino group f-SWCNTs, one being highly soluble and another forming stable suspension in aqueous solution. The activities of the immunoregulatory cells are not influenced by the highly soluble CNTs, whereas proinflammatory cytokines are secreted by macrophages in the CNT suspension.[139] Another group studied the influence of SWCNTs with different degrees of agglomeration on primary cultures derived from chicken embryonic spinal cord (SPC) or dorsal foot ganglia (DRG). [140] Significant decrease in DNA content was more pronounced when cells were exposed to highly agglomerated SWCNTs as compared with better-dispersed SWNT bundles.

Bottini et al.[141] compared the toxicity of pristine and oxidized MWCNTs on human T cells and found that the MWCNTs were more toxic and induced massive loss of cell viability through programmed cell death.

Pulskamp et al.[133] did not observe any acute toxicity on cell viability upon incubation with all CNT products. However, an increase in reactive oxygen species was observed due to the presence of metal particles as well as metalloids in commercial nanotubes, while treatment with a highly ultra-purified form of CNTs had no biological adverse effects.

Yang et al.[142] reported long-term accumulation and low toxicity of SWNTs in

intravenously exposed mice. No acute toxicity was reported by Zeni et al.[143] on administration of SWCNTs. Similarly, other reports show low or no cytotoxic effects due to exposure to CNTs. Huezko and Lange reported null risk of skin irritation and allergy on dermatological trials of CNTs.

Functionalized SWCNTs have been used as drug carriers with paclitaxel.[143, 144] Paclitaxel, being insoluble in water, is currently clinically administered as a highly toxic formulation with Cremophor EL. However, using SWNTs as a carrier allowed for a prolonged circulation of the drug and a 10-fold higher uptake by tumor cells.[144] The high uptake of SWNT complexes by the reticuloendothelial system may endanger liver and spleen as they may suffer toxic effects from SWCNT deposition and accumulation. One of the main problems faced with intravenous administration is the rapid clearance through blood, and another is the toxic effect to other organs and tissues.[145] Another study tested the toxicity of intravenously administered functionalized SWCNTs in mice and demonstrated no evidence of toxicity. PEG-SWCNTs were observed to be gradually removed from the body following an intravenous administration in mouse models with no evidence of toxicity during the excretory process.[146]

Zhuang et al. used PEGylated SWNTs conjugated to RGD peptide that specifically binds to integrin $\alpha_v\beta_3$, expressed on the surface of numerous tumor cells. This formulation was intravenously injected into U87MG tumor bearing mice. The RGD – bound SWCNTs showed a higher tumor uptake as compared to SWCNTs alone.[147]

Conclusion

Nano delivery systems hold great potential to overcome many of the present obstacles of drug delivery, of which carbon nanotubes have been proposed and actively

explored as multipurpose innovative carriers for drug delivery and diagnostic applications. They have many unique physical, mechanical and electronic properties, and these distinct and exceptional properties have made it possible to exploit CNTs as drug delivery systems for biomedical applications. CNTs are promising carriers of both small drug molecules as well as macromolecules such as genes and proteins. Functionalization of CNTs with an organic moiety has made possible their use in diagnostics for imaging as well as for targeting purposes, especially in cancer therapy. Nanotube drug delivery holds future promise for high treatment efficacy combined with minimal side effects for cancer therapy with low drug doses.

Even though CNTs are playing a larger and most promising role in the field of nanomedicine, more research is required to guarantee safety in drug delivery. Functionalized CNTs have been considered biocompatible and safe for drug and biomolecular delivery applications, as they are soluble in physiological media and nontoxic. They have shown no accumulation in the tissues and can be readily excreted through the renal route. Toxicity studies are critical to establish the full in vivo potential of CNTs for drug delivery before their actual application and marketing and in order to understand the toxic impact of the systemic delivery of carbon nanotubes in greater detail, more extensive toxicity, safety and efficacy studies on animal models and in humans over a longer time frame need to be performed. The effects of CNTs aggregation, size, length, functionalization, metal impurities and polymers safety require more thorough research. Functionalization of SWCNTs and its effects on aggregation and consequent genotoxicity also needs to be evaluated. Overall, the use of CNTs for delivery of drugs and biomolecules is a significant development in the field of therapeutic nanomedicine.

References

1. S Prakash, M Malhotra, W Shao, et al. Advanced Drug Delivery Reviews. 63 (2011) 1340-1351.

2. FH Sarkar, S Banerjee, YW Li. Toxicology and Applied Pharmacology. 224 (2007) 3, 326-336.

3. JD Byrne, T Betancourt, L Brannon-Peppas. Advanced Drug Delivery Reviews. 60 (2008) 15, 1615-1626.

4. AK Iyer, G Khaled, J Fang, H Maeda. Drug Discovery Today. 11 (2006) 17-18, 812-818.

5. N Wiradharma, Y Zhang, S Venkataraman, Jl Hedrick, YY Yang. Nano Today. 4 (2009) 4, 302-317.

6. L Jabr-Milane, LV Vlerken, H Devalapally, et al. Nano Today. 130 (2008) 2, 121-128.

7. M Pulkkinen, J Pikkarainen, T Wirth, et al. European Journal of Pharmaceutics and Biopharmaceutics. 70 (2008) 1, 66-74.

8. Y Fukumori, H Ichikawa. Advanced Powder Technology. 17 (2006) 1-28.

9. JK Vasir, V Labhasetwar. Advanced Drug Delivery Reviews. 59 (2007) 718-728.

10. AH Faraji, et al. Medicinal Chemistry. 17 (2009) 2950-2962.

11. S Ji, C Liu, B Zhang, et al. Biochimica et Biophysica Acta. 1806 (2010) 29-35.

12. KK Jain. Clinica Chimica Acta. 358 (2005) 1-2, 37-54.

13. W Qiao, B Wang, Y Wang, et al. Journal of Nanomaterials. (2010) 796303.

14. TC Yih, C Wei. Nanomedicine: Nanotechnology, Biology, and Medicine. (2005) 191-192.

15. I Brigger, C Dubernet, P Couvreur. Advanced Drug Delivery Reviews. 54 (2002) 631-651.

16. W Cai, AR Hsu, ZB Li, X Chen. Nanoscale Research Letters. 2 (2007) 6, 265-281.

17. W Cai, X Chen. Small. 3 (2007) 11, 1840-1854.

18. AK Bajpai, SK Shukla, S Bhanu, S Kankane. Progress in Polymer Science. 33(2008) 11, 1088-1118.

19. C Li. Advanced Drug Delivery Reviews. (2002) 54, 695-713.

20. P Sabbatini, C Aghajanian, D Dizon, et al. Journal of Clinical Oncology. (2004) 22, 4523-31.

21. WJ Gradishar, S Tjulandin, N Davidson, et al. Journal of Clinical Oncology. (2005) 23, 7794-803.

22. C Fonseca, S Simoes, R Gaspar. Journal of Controlled Release. 83 (2002) 2, 273-286.

23. ML Hans, AM Lowman. Current Opinion in Solid State and Materials Science. 6 (2002) 4, 319-327.

24. N Sanvicens, MP Marco. Trends in Biotechnology. 26 (2008) 8, 425-433.

25. T Tanaka, S Shiramoto, M Miyashita, Y Fujishima, Y Kaneo. International Journal of Pharmaceutics. 277 (2004) 1-2, 39–61, 2004.

26. S Sandhiya, SA Dkhar, A Surendiran. Fundamental and Clinical Pharmacology. 23 (2009) 3, 263–269.

27. Y Fukumori, H Ichikawa. Advanced Powder Technology. 17 (2006) 1, 1–28.

28. M Johannsen, U Gneveckow, B Thiesen, et al. European Urology. 52 (2007) 6, 1653–1662.

29. ML Adams, A Lavasanifar, GS Kwon. Journal of Pharmaceutical Sciences. (2003) 92:1343-55.

30. LB Li, YB Tan. Journal of Colloid and Interface Science. 317 (2008) 1, 326–331.

31. AS Mikhail, C Allen. Journal of Controlled Release. 138 (2009) 3, 214–223.

32. GA Husseini, NY Rapoport, DA Christensen, et al. Colloids and Surfaces B. 24 (2002) 3-4, 253–264.

33. N Rapoport. Progress in Polymer Science. 32, 8-9, 962–990.

34. M Licciardi, G Giammona, J Du, et al. Polymer. 47 (2006) 9, 2946–2955.

35. KJ Morrow Jr, R Bawa, C Wei. Medical Clinics of North America. 91 (2007) 5, 805–843.

36. WJ Yang, YY Cheng, TW Xu, et al. European Journal of Medicinal Chemistry. 44 (2009) 2, 862–868.

37. S Svenson, DA Tomalia. Advanced Drug Delivery Reviews. 57 (2005) 15, 2106–2129.

38. ER Gillies, JMJ Frechet. Drug Discovery Today. 10 (2005) 1, 35–43.

39. D Bhadra, AK Yadav, S Bhadra, NK Jain. International Journal of Pharmaceutics. 295 (2005) 1-2, 221–233.

40. AK Patri, A Myc, J Beals, et al. Bioconjugate Chemistry. 15 (2004) 6, 1174–1181.

41. M Hussain, M Shchepinov, M Sohail, et al. Journal of Controlled Release. 99 (2004) 1, 139–155.

42. Y Choi, T Thomas, A Kotlyar, et al. Chemistry and Biology. 12 (2005) 1, 35–43.

43. F Liang, B Chen. Current Medicinal Chemistry. 17 (2010) 10-24.

44. DS Bethune, CH Klang, MS de Vries, et al. Nature. 363 (1993) 605-607.

45. A Thess, R Lee, P Nikolaev, et al. Science. 273 (1996) 483-487.

46. AM Cassel, JA Raymakers, J Kong, H Dai. Journal of Physical Chemistry B 103 (1999) 6484-6492.

47. T Park, S Banerjee, TH Bennya, SS Wong. Journal of Material Chemistry. 16 (2006) 141-154.

48. A Bianco, K Kostarelos, CD Partidos, M Prato. Chemical Communications. (2005) 571-577.

49. L Lacerda, A Bianco, M Prato, K Kostarelos. Advanced Drug Delivery Reviews. 58 (2006) 14, 1460–1470.

50. D Bonifazi, C Nacci, R Marega, et al. Nano Letters. 6 (2006) 1408-1414.

51. B Zhao, H Hu, A Yu, D Perea, et al. Journal of American Chemical Society. 127 (2005) 8197-8203.

52. EB Malarkey, RC Reyes, B Zhao, RC. Haddon, et al. Nano Letters. 8 (2008) 3538-3542.

53. EB Malarkey, RC Reyes, B Zhao, RC Haddon, et al. Nano letters. 9 (2009) 264-268.

54. CL Lay, HQ Liu, HR Tan, Y Liu. Nanotechnology. 21 (2010) 065101.

55. N Tagmatarchis, M Prato. Journal of Material Chemistry. 14 (2004) 437-439.

56. P Wu, X Chen, N Hu, et al. Angewandte Chemie International Edition. 47 (2008) 5022-5025.

57. Z Liu, K Chen, C Davis, et al. Cancer Research. 68 (2008) 6652-6660.

58. XK Zhang, LJ Meng, QH Lu, et al. Biomaterials. 30 (2009) 30, 6041-6047.

59. ST Reddy, A Rehor, HG Schmoekel, et al. Journal of Controlled Release. 112 (2006) 1, 26–34.

60. F Yang, DL Fu, J Long, and QX Ni. Medical Hypotheses. 70 (2008) 4, 765–767.

61. F Yang, J Hu, D Yang et al. Nanomedicine. 4 (2009) 3, 317–330.

62. Y Liu, KY Ng, KO Lillehei. Cancer Control. 10 (2003) 2, 138–147.

63. F Yang, C Jin, D Yang et al. European Journal of Cancer 47 (2011) 12, 1873–1882.

64. NG Sahoo, H Bao, Y Pan et al. Chemical Communications 47 (2011) 18, 5235–5237.

65. JJ Li, F Yang, GQ Guo, et al. Polymer International. 59 (2010) 169–174.

66. M Pramanik, KH Song, M Swierczewska, et al. Physics in Medicine and Biology. 54 (2009) 3291–3301.

67. S Dhar, Z Liu, J Thomale H Dai, SJ Lippard. Journal of the American Chemical Society. 130 (2008) 34, 11467–11476.

68. AA Bhirde, V Patel, J Gavard, et al. ASC Nano. 3 (2009) 307–316.

69. AL Klibanov, K Maruyama, VP Torchilin, L Huang. FEBS Letters. 268 (1990) 1, 235–237.

70. TM Allen, T Mehra, C Hansen, YC Chin. Cancer Research. 52 (1992) 9, 2431–2439.

71. C Li, D Yu, T Inoue et al. Anti-Cancer Drugs. 7 (1996) 6, 642–648.

72. Z Liu, K Chen, C Davis, et al. Cancer Research. 68 (2008) 6652–6660.

73. Z Liu, XM Sun, NN Ratchford, et al. ACS Nano. 1 (2007) 50–56.

74. J Chen, S Chen, X Zhao, et al. Journal of the American Chemical Society. 130 (2008) 49, 16778–16785.

75. JY, W Chan, ACY Chu, et al. Life Sciences. 67 (2000) 17, 2117– 2124.

76. SS Suri, H Fenniri, B Singh. Journal of Occupational Medicine and Toxicology. 2 (2007) 1, 16.

77. J Cheng, MJ Meziani, YP Sun, and SH Cheng. Toxicology and Applied Pharmacology. 250 (2011) 2, 184–193.

78. X Liu, H Tao, K Yang, S Zhang, ST Lee, and Z Liu. Biomaterials. 32 (2011) 1, 144–151.

79. X Shi, HW Su, M Shen et al. Biomacromolecules. 10 (2009) 7, 1744–1750.

80. R Li, R Wu, L Zhao et al. Carbon. 49 (2011) 5, 1797–1805.

81. E Fortunati, A Bout, MA Zanta, D Valerio, et al. Biochimica et Biophysica Acta. 1306 (1996) 1, 55–62.

82. T Rochat, MA Morris. Journal of Aerosol Medicine. 15 (2002) 2, 229–235.

83. FD Ledley. Current Opinion in Biotechnology. 5 (1994) 6, 626–636.

84. C Coutelle R Williamson. Journal of Aerosol Medicine. 9 (1996) 1, 79–88.

85. D Pantarotto, R Singh, D McCarthy et al. Angewandte Chemie International Edition. 43 (2004) 39, 5242– 5246.

86. NWS Kam, M. O'Connell, JA Wisdom, and H Dai. Proceedings of the National Academy of Sciences of the United States of America. 102 (2005) 33, 11600–11605.

87. NWS Kam, Z Liu, and H Dai. Angewandte Chemie International Edition. 45 (2006) 4, 577–581.

88. D Cai, JM Mataraza, ZH Qin et al. Nature Methods. 2 (2005) 6, 449–454.

89. NWS Kam, Z Liu and H Dai. Journal of the American Chemical Society. 127 (2005) 36, 12492–12493.

90. E Podesta, KT Al-Jamal, MA Herrero et al. Small. 5 (2009) 10, 1176–1185.

91. X Wang, J Ren, and X Qu. Chem Med Chem. 3 (2008) 6, 940–945.

92. Z Zhang, X Yang, Y Zhang et al. Clinical Cancer Research. 12 (2006) 16, 4933–

4939.

93. AK Varkouhi, S Foillard, T Lammers et al. International Journal of Pharmaceutics. 416 (2011) 2, 419–425.

94. SL Hussey and BR Peterson. Journal of the American Chemical Society. 124 (2002) 22, 6265–6273.

95. NWS Kam, TC Jessop, PA Wender, H Dai. Journal of the American Chemical Society 126 (2004) 22, 6850– 6851.

96. X Weng, M Wang, et al. Molecular BioSystems. 5 (2009) 10, 1224– 1231.

97. MR McDevitt, D Chattopadhyay, BJ Kappel et al. Journal of Nuclear Medicine. 48 (2007) 7, 1180–1189.

98. J Meng, J Duan, H Kong et al. Small. 4 (2008) 9, 1364–1370.

99. Y Liu, KY Ng, and KO Lillehei. Cancer Control. 10 (2003) 2, 138–147.

100. IF Parney, C Hao, and KC Petruk. Neurosurgery. 46 (2000) 4, 778– 792.

101. B Kateb, M Van Handel, L Zhang, MJ Bronikowski, H Manohara, and B Badie. NeuroImage. 37 (2007) 1, 9–17.

102. M VanHandel, D Alizadeh, L Zhang et al. Journal of Neuroimmunology. 208 (2009) 1-2, 3–9.

103. A Ruggiero, CH Villa, JP Holland et al. International Journal of Nanomedicine. 5 (2010) 1, 783–802.

104. J Meng, M Yang, F Jia et al. Nanotechnology. 21 (2010) 14, 145104.

105. R Li, R Wu, L Zhao, M Wu, L Yang, and H Zou. ACS Nano. 4 (2010) 3, 1399–1408.

106. ME Brennan, JN Coleman, A Drury. Optics Letters. 28 (2003) 4, 266–268.

107. CJ Gannon, P Cherukuri, BI Yakobson et al. Cancer 110 (2007) 12, 2654–2665.

108. SV Torti, F Byrne, O Whelan et al. International Journal of Nanomedicine. 2

(2007) 4, 707–714.

109. F Zhou, D Xing, Z Ou, B Wu, DE Resasco, and W. R. Chen. Journal of Biomedical Optics. 14 (2009) 2, 021009.

110. NH Levi Polyachenko, EJ Merkel, BT Jones, et al. Molecular Pharmaceutics. 6 (2009) 4, 1092–1099.

111. CH Wang, YJ Huang, CW Chang, WM Hsu, CA Peng. Nanotechnology. 20 (2009) 31, 315101.

112. A Burke, X Ding, R Singh et al. Proceedings of the National Academy of Sciences of the United States of America. 106 (2009) 31, 12897–12902.

113. A Burlaka, S Lukin, S Prylutska et al. Experimental Oncology. 32 (2010) 1, 48–50.

114. S Ghosh, S Dutta, E Gomes et al. ACS Nano. 3 (2009) 9, 2667–2673.

115. Y Xiao, X Gao, O Taratula et al. BMC Cancer. 9 (2009) 1471, 351.

116. HK Moon, SH Lee, and HC Choi. ACS Nano. 3 (2009) 11, 3707–3713.

117. N Huang, H Wang, J Zhao, H Lui, M Korbelik and H Zeng. Lasers in Surgery and Medicine. 42 (2010) 9, 638–648.

118. JD Jackson, Classical Electrodynamics, John Wiley & Sons, New York. 3 (1999).

119. J Xu, M Xiao, R Czerw, and DL Carroll. Chemical Physics Letters. 389 (2004) 4-6, 247–250.

120. N Shao, S Lu, E Wickstrom, B Panchapakesan. Nanotechnology. 18 (2007) 315101.

121. CA Robertson, DH Evans, H Abrahamse. Journal of Photochemistry.

Photobiology. B: Biol. 96 (2009) 1–8.

122. Z Zhu, ZW Tang, JA Phillips. Journal of American Chemical Society. 130 (2008) 10856–10857.

123. L Gu, T Elkin, X Jiang et al. Chemical Communications. 7 (2005) 874–876.

124. ASB Esteyez, S Kang, M Elimelech. Small. 4 (2008) 4, 481–484.

125. LR Arias and L Yang. Langmuir. 25 (2009) 5, 3003–3012.

126. CD Vecitis, KR Zodrow, S Kang, M Elimelech, et al. ACS Nano. 4 (2010) 9, 5471–5479.

127. W Wu, S Wieckowski, G Pastorin et al. Angewandte Chemie International Edition. 44 (2005) 39, 6358–6362.

128. M Benincasa, S Pacor, W Wu, et al. ACS Nano. 5 (2011) 1, 199–208.

129. S Lanone, J Boczkowski. Current Molecular Medicine. (2006) 6, 651-666.

130. CM Sayes, F Liang, JL Hudsona. Toxicology Letters. 161 (2006) 135–142.

131. P Wick, P Manser, LK Imbach. Toxicology Letters. 168 (2007) 121–131.

132. VE Kagan, YY Tyurina, VA Tyurin, et al. Toxicology Letters. (2006), 165(1): 88-100.

133. K Pulskamp, S Diabata, HF Krug. Toxicology Letters. (2007) 168(1), 58-74.

134. FQ Schafer, SY Qian, GR Buettner. Molecular Cell Biology. (2000) 46(3): 657-62.

135. ML Becker, JA Fagan, ND Gallant, et al. Advance Material. (2007) 19(7): 939-45.

136. JS Im, BC Bai, YS Lee, et al. Biomaterials. (2010) 31(6): 1414-9.

137. X Chen, UC Tam, JL Czlapinski, et al. Journal of American Chemical Society. (2006) 128(19): 6292-3.

138. H Dumortier, S Lacotte, G Pastorin, Marega et al. Nano Letters. (2006) 6(7): 1522-8.

139. LW Zhang, L Zeng, A Barron, et al. International Journal of Toxicology. (2007) 26(2): 103-13.

140. L Belyanskaya et al. NeuroToxicology. (2009) 30:702-711.

141. M Bottini et al. Toxicology Letters. (2006) 160, 121-126.

142. S Yang et al. Toxicology Letters. (2008) 181, 182-189

143. O Zeni et al. Sensor. (2008) 8, 488-499.

144. W Wu, R Li, X Bian, et al. ACS Nano. 3 (2009) 2740–2750.

145. ML Schipper, N Nakayama-Ratchford, CR Davis, et al. Nature Nanotechnology. 3 (2008) 216–221.

146. L Zhuang, C Davis, W Cai, et al. Proceedings of the National Academy of Sciences. 105 (2008) 1410–1415.

147. Z Liu, W Cai, L He, et al. Nature Nanotechnology. 2 (2007) 47–52.

148. CMJ Hu, S Kaushal, HST Cao, et al. Molecular Pharmacology. 7 (2010) 914–920.

149. E Heister, V Neves, T Carmen, et al. Carbon. 47 (2009) 2152–2160

150. AA Bhirde, V Patel, J Gavard, et al. ACS Nano. 3 (2009) 307–316.

151. MR McDevitt, D Chattopadhyay, BJ Kappel1, et al. Journal of Nuclear Medicine. 48 (2007) 1180–1189.

Chapter 2

Instrumentation

Abstract

An understanding of the structure, surface morphology and elemental composition of the nanoparticles is essential to know the specific properties of the nano-materials under study. This chapter describes the principles of different instruments, which were employed for various characterizations of nanoparticles (NPs) and also analytical instruments used in biological studies. Various microscopic techniques, spectroscopic methods and other characterization techniques are being discussed in this chapter. In addition, the application of nanoparticles in vitro is also visualized with the help of various microscopic techniques. The techniques used for the characterization studies and nanoparticle applications are explained in this chapter.

Introduction

Proper characterization of nanomaterials is highly essential for their accurate analysis. Microscopic techniques and spectroscopic techniques are the common characterization methods for the characterization of various nanoparticles (NPs). Microscopic techniques including both optical and electron microscopes were used in our research. For studying the internal structure and surface morphology of nanoscale materials electron microscopic techniques are inevitable. NPs were characterized for their morphology using Transmission Electron Microscope (TEM), Scanning Electron Microscope (SEM) and Atomic Force Microscope (AFM). The elemental composition studies of the nano samples were carried out using X-ray Photoelectron Spectroscopy (XPS or ESCA), and UV-visible spectrophotometer (UV-Vis spectroscopy) was used to study the electronic excitations. Zetasizer has been used for measuring the zeta potential of the samples. We are discussing in detail about the general working principle and sample preparation of various electron microscopic methods, optical microscopic methods, spectroscopic techniques and other characterization techniques employed to analyze the NPs.

Microscopic techniques

Transmission Electron Microscope (TEM)

Transmission Electron Microscope (TEM) is a scientific microscopy technique, which utilizes a beam of electrons instead of light to analyze the ultra-thin specimens at a significantly higher resolution. This enables the examination of samples even a small single column of atoms can be

observed clearly, which is in the order of few angstroms. TEM analysis provides information regarding the morphology like size, shape and arrangement along with crystallographic and compositional nature of particles at the nanometer scale.

Working principle

TEM is composed of an electron emission source for the generation of electron stream, a vacuum system in which the electrons travel, a series of electromagnetic lenses to guide the beam of electrons and electrostatic plates to manipulate the beam. Imaging devices, which can create an image from the electrons that exit the system, are also required. Electrons are usually generated by thermionie emission from a tungsten filament or alternatively by field electron emission under high vacuum. The electrons are then accelerated by an electric potential which allow them to travel through the vacuum in the column of microscope and are focused by electrostatic and electromagnetic lenses on to the sample, thus allowing the electron beam to travel through the specimen. Depending on the density of materials present, some of the electrons are scattered and disappear from the beam. The transmitted beam contains information about electron density, phase and periodicity. The unscattered electrons hit a fluorescent screen below the specimen, which gives a shadow image of the specimen with its different parts displayed in varied darkness according to their density. This image is then magnified and focused by an imaging device and is detected by a sensor or charge-coupled device (CCD) camera. The TEM used in our studies is JEOL JEM-2200-FS Field Emission Transmission Electron Microscope operating at an accelerating voltage of 200 kV.

Sample preparation

Samples were prepared on a 200 mesh copper (Cu) grid with carbon film coating. The solid sample for TEM observation was prepared by depositing the powder onto the grid with carbon coating surface. For the preparation of liquid samples, the grids were initially subjected to hydrophilic treatment using JEOL Datum HDT- 400 hydrophilic treatment device for 30 seconds. A drop of the sample was then added directly onto the supporting grid and was allowed to air dry at room temperature for further analysis. The grid with the sample was then screwed onto the sample holder and introduced into the sample chamber of the instrument.

Scanning Electron Microscope (SEM)

Scanning Electron Microscope (SEM) images the surface of sample using focused beam of high energy electrons in a raster scan pattern to generate a variety of signals at the surface of samples. The signals that are derived from the electron-sample interactions reveal information regarding the surface morphology, chemical composition, crystalline structure and orientation of materials. SEM has a large depth of field which allows a large amount of the sample to be in focus at one time and produces a two-dimensional image which is a good representation of the three dimensional sample. It also has a magnification range from 15 X to 200,000 X and a resolution of 5 nm. The advantage of SEM analysis is the non-destructive nature, which does not lead to volume loss of the sample, and the same material can be analyzed repeatedly.

Working principle

In a typical SEM, an electron beam is therminionically emitted from an electron

gun fitted with cathode. The electron beam, which typically has an energy ranging from 0.5-40 kV, is focused by one or two condenser lenses to a spot about 04 nm to 5 nm in diameter. Accelerated electrons of high kinetic energy produce a variety of signals by energy dissipation when they hit the sample. These signals include secondary electrons, back-scattered electrons (BSE), diffracted back-scattered electrons (DBSE), photons, visible light and heat, each of which can be detected by specialized detectors. Secondary electrons along with BSE are commonly utilized to produce images of the samples, whereas secondary electrons are most valuable for depicting morphology and topography of samples, while BSE being valuable for illustrating the contrast in composition. DBSE are used to determine crystal structure and orientations of minerals, whereas photons, which have the characteristics of X-rays are used for elemental analysis. Electronic amplifiers of various types are used to amplify the signals, which are displayed as variations in brightness on a cathode ray tube (CRT). The raster scanning of CRT display is synchronized with that of the beam on the specimen within the microscope and the resulting image is therefore a distribution map of the intensity of the signal being emitted from the scanned area of the specimen**.** The image may be captured by photography from a high-resolution cathode ray tube. However, the images are digitally captured, displayed on a computer monitor and saved to the computer's hard disk in the modern machines.

For our SEM studies, we used JEOL JSM-7400F Field Emission Scanning Electron Microscope operating at 5 kV accelerating voltage.

Sample preparation

Solid samples for SEM imaging can be mounted easily and rigidly on a specimen holder using a small piece of double-sided carbon tape or silicon substrate. To

make specimen electrically conducting and electrically grounded, the sample on stubs was coated with platinum (approximately 511 rim thickness) using Hitachi E-1030 ion sputter machine before microscopic examination. This coating helps to prevent the accumulation of static electric charges that occur when the electron beam interacts with the sample during the analysis. For liquid samples a small piece of silicon substrate or mica substrate was mounted on the specimen stub and the sample was dropped over that and allowed to air dry or vacuum dry depending on the solvent used.

Atomic Force Microscope (AFM)

Atomic Force Microscopy (AFM) is a very high-resolution scanning probe microscopy with resolution in the order of fractions of a nanometer. The AFM can be operated in a number of modes depending on the application In general, possible imaging modes are divided into static (also called contact) modes and a variety of dynamic (non-contact or "tapping") modes where the cantilever is vibrated.

Working Principle

The AFM consists of a cantilever with a sharp tip (probe) at its end that is used to scan the specimen surface. The cantilever is typically silicon or silicon nitride with a tip radius of curvature in the order of nanometers. When the tip is brought into the proximity of a sample surface, forces between the tip and the sample lead to a deflection of the cantilever according to Hooke's law. Typically, the deflection is measured using a laser spot reflected from the top surface of the cantilever into an array of photodiodes. Other methods that are used include optical interferometry, capacitive sensing or piezoresistive AFM cantilevers. These cantilevers are fabricated with piezioresistive elements that act as a strain

gauge. Using a wheatstone bridge, strain in the AFM cantilever due to deflection can be measured, but this method is not as sensitive as laser deflection or interferometry. If the tip was scanned at a constant height, there is a risk of the tip colliding with the surface, causing damage. Hence, in most cases, a feedback mechanism is employed to adjust the tip-to-sample distance to maintain a constant force between the tip and the sample. Traditionally, the sample is mounted on a piezoelectric tube, which can move the sample in the *z* direction for maintaining a constant force and the *x* and *y* directions for scanning the sample. Alternatively a 'tripod' configuration of three piezo crystals may be employed with each responsible for scanning in the *x, y* and *z* directions. This eliminates some of the distortion effects seen in a tube scanner observed in newer designs. The tip is mounted on a vertical piezo scanner while the sample is being scanned in X and V using another piezo block. The resulting map of the area $z = f(x.v)$ represents the topography of the sample.

The AFM used in our studies is Asylum Research,

Sample preparation

The samples for AFM analysis was spin coated onto a Si substrate or glass slide.

Confocal Laser Scanning Microscope (CLSM)

Confocal microscopy is an optical imaging technique used to increase the optical resolution and contrast of a micrograph by using point illumination, and a spatial pinhole to eliminate out of focus light in the specimens that are thicker than the focal plane. This microscopy enables the reconstruction of three-dimensional structures from the obtained image.

Working principle

Marvin Minsky patented the principle of confocal imaging in 1957. A

confocal microscope uses point illumination and a pinhole in an optically conjugate plane in front of the detector to illuminate out of focus signal-the name "confocal" stems from this configuration principle. This is better than that of the wide-field microscopes because only light produced by fluorescence very close to the focal plane can be detected yielding to the improved optical resolution of the image. However increased resolution is obtained at the cost of decreased signal intensity, making long exposures a requirement.

CLSM use a pair of mirrors, one at *x* and other at *y*-axis to scan the laser across the samples and descan the image across a fixed pinhole and detector. CLSM can have a programmable sampling density and very high resolution. The thin optical sectioning of CLSM makes it possible to obtain 3D imaging and surface profiling of the samples. Cutting edge developments of CLSM now allows better than video rate imaging by multiple micro electro-mechanical systems based scanning mirrors. The laser light source has the additional benefits of being available in a wide range of wavelengths.

Sample preparation

CLSM images of the biological samples (cell lines) were obtained by growing specific cell lines on a glass-bottom dish. The bright field image is obtained under a normal light source whereas the fluorescent image can be obtained based on the excitation and emission wavelength of the nanoparticles or dyes used in the study. In the case of blue fluorescent NPs and DAPI (dye staining the nucleus of the cells), we have utilized excitation wavelength of 405 nm (blue filter). In the case of green fluorescent materials, Tubulin Marker (dye staining the micro spindles of the cells) and Lysotracker (dye staining the lysosomes of the cells) at excitation of 488 nm is used and for red fluorescent

materials Nile Red dye, 561 nm was used as the excitation wavelength. To study the fluorescence of nanoparticles, they were added onto the cover slips and subjected for analysis**.**

In our studies we have used Olympus IX81 confocal laser scanning microscope.

Phase Contrast Microscope

Phase contrast microscopy is a type of light microscopy, which enhances the contrast of transparent and colorless objects by influencing the optical path of light. It employs an optical mechanism to translate minute variations in phase into corresponding changes in amplitude, which can be visualized as differences in image contrast, and no staining is required to view the samples**.** Most of the details of living cells is undetectable in bright field microscopy, due to lack of contrast between the structures with similar transparency and because of the lack of natural pigmentation in the sample under study. Phase contrast microscopy distinguishes wide variation in refractive index shown by various biological organelles thus yielding an image with better resolution.

Working principle

Only two specialized accessories are required to convert a bright field microscope for phase contrast observation; a specially designed annular diaphragm which is constructed as an opaque flat-black (light absorbing) plate with a transparent annular ring, is positioned in the front focal plane of the condenser so that the specimen can be illuminated by defocused, parallel light wave fronts emanating from the ring, and a phase plate which is mounted in or near the objective rear focal plane in order to selectively alter the phase and amplitude of the surrounding light passing through the specimen. Phase contrast technique allows phase of the light passing through the object under study to be

inferred from the intensity of the image produced by the microscope**.**

For our studies we had used Nikon Eclipse TE2000-U Microscope.

Sample preparation

For phase contrast analysis of biological samples, cells were grown in standard T25 flask or on 6 well plates.

Spectroscopic techniques

UV-Vis Spectroscopy

Ultraviolet-Visible spectroscopy is the optical spectroscopy that investigates the absorption of light in the visible, ultraviolet and near infrared ranges by molecules that are in a gas or vapor state or dissolved molecules/ions. It is ideal for characterizing the optical and electronic properties of various materials such as, powders, monolithic solids, and liquids.

Working principle

Measurements in the UV-Visible region cover wavelengths from about 200 nm to 800 nm. When the light passes through the sample, some of the light energy is absorbed by the sample. The absorption of ultraviolet or visible radiation by a molecule leads to the transitions among the electronic energy levels of the molecule. The optical spectrometer records the wavelength at which absorption occurs. A graph of absorbance against wavelength gives the samples absorption spectrum. It compares the intensity of light before and after passing through the sample and ratio of the intensities is called transmittance. The wavelength at the maximum absorption will give information about the structure of the molecule present in the sample, and the extent of the absorption is proportional to the amount of species absorbing the light.

The UV-Vis spectrophotometer used in our works is Shimadzu UV4100PC/3100PC UV visible spectrophotometer.

Sample preparation

The sample to be measured was dispersed well in a suitable solvent. The chosen solvent alone was taken as the reference agent in one quartz cuvette and the sample solution was taken in another quartz cuvette and kept in the chamber for the measurement.

X-ray Photoelectron Spectroscopy (XPS)

X-ray photoelectron spectroscopy (XPS) is also known as Electron Spectroscopy for Chemical Analysis (ESCA). It is a quantitative spectroscopic technique that measures the elemental composition, empirical formula, chemical state and electronic state of the elements that exists within the material. This instrument measures the relative composition of elements present in the surface of the samples.

Working principle

This spectroscopic technique uses mono-energetic soft X-rays to eject electrons from the inner shell orbitals of atoms. When the X-ray beam hits the sample surface, the energy of X-ray photons is absorbed by the core electrons and results in ionization and emission of photoelectrons from the sample surface with specific kinetic energies. The kinetic energy distribution of the emitted photoelectrons can be measured using any appropriate electron energy analyzer and a photoelectron spectrum can thus be obtained. The photo-ionization and analysis of the kinetic energy distribution of the emitted photoelectrons is utilized to study the composition and electronic state or the surface region of a sample. The energy of photo emitted core electron is a function of its binding energy and is the

characteristics of the element from which it is emitted. When the core electron is emitted from the atom by incident X-rays, the hole is filled by the electron from the outermost orbital. At the same time a second electron gets emitted and is called as auger electron. This auger electron emission occurs within 10^{-14} s after the emission of photoelectrons leading to emission of two types of electrons. The detector detects the kinetic energy of all the collected electrons contributed from both photoelectrons and auger electrons**.** This spectrum from a mixture of elements is approximately the sum of peaks of the individual elements present. The quantitative data obtained from the peak heights or areas and the identification of chemical state can be made from exact analysis of peak positions and separations. XPS detects all elements with an atomic number (Z) of 3 and above. It cannot detect hydrogen (Z = 1) or helium (Z = 2) because the diameter of these orbitals is so small, reducing the catch probability to almost zero.

For experimental studies, we used Kratos Analytical X-ray Photoelectron Spectroscopy IX PSI with monochromatic Al, Ka X-ray source with photon energy of 1487.6 eV. The instrument was operated at 12 kV and 15 mA under high vacuum condition with vacuum pressure maintained below 10^{-9} Torr.

Sample preparation

Powder samples were added onto the double-sided carbon film or white film fixed on to the XPS specimen holder. For liquid samples, a drop of the sample solution was dropped on a small piece of silicon substrate and the sample was allowed to vacuum dry or air dry. The silicon substrate with the dried sample was then mounted on the double-sided tape fixed on the specimen holder.

Other instrumentation techniques

Zetasizer

Zetasizer is commonly used to measure the size, poly dispersity and zeta potential of the NPs to optimize the production processes. The development of a net charge at the particle surface affects the distribution of ions in the surrounding interfacial region, resulting in an increased concentration of counter ions (ions of opposite charge to that of the particle) close to the surface. Thus, an electrical double layer exists around each particle. The liquid layer surrounding the particle exists as two parts; an inner region, called the Stern layer, where the ions are strongly bound and an outer, diffuse region where they are less firmly attached. Within the diffuse layer there is a notional boundary inside which the ions and particles form a stable entity. When a particle move (e.g. due to gravity), ions within the boundary move with it, but any ions beyond the boundary do not travel with the particle. This boundary is called the surface of hydrodynamic shear or slipping plane. The potential that exists at this boundary is known as the Zeta potential.

Working principle

When an electric field is applied across an electrolyte, charged particles suspended in the electrolyte are attracted towards the electrode of opposite charge, whereas viscous force acting on the particles tends to oppose this movement. When the two opposing forces reach equilibrium then the particles move with a constant velocity. The velocity of a particle in an electric field is called the electrophoretic mobility and this knowledge can help us to obtain the zeta potential of the particles. Zeta potential is a consequence of the existing surface charge of the sample, and can also give information on electrical interaction between the

dispersed particles. It is possible to assess the stability of suspensions and emulsions by means of zeta potential. For our research work, we used Malvern Zetasizer Nano-ZS.

Sample preparation

The diluted colloidal solution of NPs was taken in a cuvette and the dip electrode was fitted immersed in the colloidal solution. The cuvette was fitted into the holder and kept undisturbed for 120 s to neutralize the movement of NPs in colloidal solution and the measurement was carried out at 25°C.

Particle size analyzer

Dynamic light scattering (DLS) technique was utilized to analyze the size and the distribution profile of particles suspended in the solution. It is a non-invasive well-established technique for measuring the size of molecules and particles in the submicron region.

Working principle

Particles, emulsions and molecules in suspension undergo Brownian motion. This is the motion induced by the bombardment of solvent molecules that are moving by themselves due to their thermal energy. If the particles or molecules are illuminated with a laser, the intensity of the scattered light fluctuates at a rate that is dependent upon the size of the panicles, as smaller particles are "kicked" further by the solvent molecules and move more rapidly. Analysis of these intensity fluctuations yields the velocity of the Brownian motion and hence the particle size can be assessed using the Stokes-Einstein relationship. The diameter that is measured in DLS is called the hydrodynamic diameter and refers to how a particle diffuses within a fluid. The diameter obtained by this technique is that of a

sphere that has the same translational diffusion coefficient as the particle being measured. The translational diffusion coefficient will depend not only on the size of the particle "core", but also on the surface structure, as well as the concentration and type of ions in the medium. This means that the size can be larger than measured by the electron microscopy, where the particle is removed from its native environment. In most instruments monochromatic coherent He-Ne laser with a fixed wavelength of 633 nm is used as the light source. Light scattered by the particles is detected with only one detector, which is placed at 90° to the incident laser beam. For our research works, we used Malvern Zetasizer Nano-ZS.

Sample preparation

The diluted colloidal solution of NPs was taken in cuvette and the cuvette was fitted into the holder and kept undisturbed for 120 s to neutralize the movement of NPs colloidal solution and the measurement was carried out at 25°C. The resultant profile yields a graphical representation of the size distribution of NPs.

Conclusion

Characterization instruments can easily determine the various properties of the nanomaterials. As the area of research in nanoscience and nanotechnology is expanding rapidly, a need for evolutionary approaches in the field of instrumentation is also required. The instrumentations used in our research are detailed out in this chapter.

Chapter 3

Targeted drug delivery using PEG biofunctionalized folate conjugated SWCNTs against breast cancer cells

Abstract

Medical science and biomedical engineering has advanced to a significant extent, but the therapeutic development of anti-cancer strategies is still limited. In this work, we have developed a targeted drug delivery system (DDS) based on SWCNTs biofunctionalized with polyethylene glycol (PEG), conjugated with folic acid (FA) as targeting moiety and loaded with anticancer drug doxorubicin (DOX) for selective killing of tumor cells. The prepared nanotubes were characterized for their morphological features and their elemental composition. In vitro drug release studies showed that the drug (DOX) binds at physiological pH (pH 7.4) and is released at a lower pH (lysosomal pH 4.0), which is the characteristic pH of the tumor environment. A sustained release of DOX from the SWCNTs was observed for a period of three days, which effectively caused the death of the breast cancer cells. The nanotubes were incubated with breast cancer cells and their biocompatibility and anti-proliferative effects were analyzed. We found that the targeted nanotubes were non-toxic to normal cells while toxic to tumor cells. Cellular uptake of the targeted nanotubes was studied in vitro using confocal microscopy. Time dependent drug effect was also studied using normal cells and tumor cells. Our results show significant internalization and retention of the nanotubes inside the tumor cells, inducing apoptosis, thus indicating that this study with folate conjugated and DOX loaded nanotubes can be a promising targeted drug delivery vehicle for cancer therapy.

Introduction

The emerging field of nanobiotechnology bridges the physical sciences with biological sciences via chemical methods by developing novel tools and platforms for understanding biological systems and in disease diagnosis and treatment.[1-3] Targeted drug delivery is a very potential and desired requirement in cancer nanotherapeutics.[4] Many nanodrug carriers with controlled drug release have already been developed.[5-8] Among the currently available delivery vehicles such as liposomes, [9] polymeric nanoparticles [10, 11] and inorganic nanoparticles,[12] single walled carbon nanotubes (SWCNTs) are emerging as one of the most promising delivery vehicles for cancer diagnosis and chemotherapy. SWCNTs, which comprise of thin sheets of benzene rings rolled up into seamless cylinders, have attracted significant attention for use in biomedical applications due to their significant advantages including good cell membrane permeability, high drug loading capacity, pH dependent therapeutic unloading and prolonged circulation time.[13-21] SWCNT-based drug delivery systems have been designed and prepared, and it has been proved by many in vitro results that these multifunctional SWCNTs could greatly improve the therapeutic efficiency of the drug while reducing their toxicity.[22-25]

Unmodified SWCNTs have highly hydrophobic surfaces and are not soluble in aqueous solutions. For biomedical applications, functionalization is required to solubilize SWCNTs and to render biocompatibility and low toxicity. Surface functionalization of SWCNTs can be made by covalent or non-covalent chemical reactions. Oxidation is one of the most common methods to covalently functionalize SWCNTs, [26] where the CNTS are treated with oxidizing agents like nitric acid. Non-covalent functionalization of SWCNTs can be carried out by coating with amphiphilic surfactant molecules or polymers.[27] Since SWCNTs are insoluble in water, they

aggregate in the presence of salts, and thus cannot be directly used for biological applications due to the high salt content of most of the biological solutions. Further modification can be achieved by attaching hydrophilic polymers such as poly (ethylene glycol) (PEG) to oxidized SWCNTs, yielding SWCNT-polymer conjugates stable in biological environments.[28, 29]

PEGylation is a good strategy to impart various functionalities, high water solubility, biocompatibility and prolonged blood circulation half-lives. PEG is composed of repeating ethylene glycol units $-(CH_2-CH_2-O)_n-$, where the integer n is the degree of polymerization. PEG-coated SWCNTs are obtained by adsorption of amphiphilic polymer functionalized with activated PEG chains onto SWCNTs.[30] Polymers bind to SWCNTs through hydrophobic interactions between the lipophilic moieties and the graphitic SWCNT sidewalls, leaving the PEG chains and other hydrophilic groups projecting from the sidewall, thus imparting water solubility and biocompatibility.[31] PEGylation also reduces non-specific uptake by cells within the recticuloendothelial system, thereby increasing the circulation in blood.

In this work, harnessing the advantages of PEGylated SWCNTs, we have developed a SWCNT-based tumor targeted NDDS which consist of PEG modified SWCNT functionalized with folic acid as a targeting group for the targeted delivery of anticancer drug doxorubicin (DOX). Doxorubicin is a broad-spectrum anti-cancer drug. Although it continues to be used extensively in the treatment of different cancers, its clinical value is limited due to the toxicity to healthy tissues. The aim of our work is to minimize the disadvantages of systemic administration of doxorubicin, which kills healthy cells. [32-34]

Folate receptors may be over-expressed on the surfaces of certain cancer cells. Therefore, folate-functionalized SWCNTs conjugated with the anticancer agent

become a highly desirable targeted drug delivery system. The folate-conjugated drug has shown the ability to be transported via endocytosis, get released in the cell and finally cause apoptosis and cell death. [35-38].

Experimental section

The SWCNTs (length 0.5- 100 μm, diameter of 1-2 nm), DSPE-PEG_{2000}-NH_2-FA (1,2-distearoyl-sn-glycero-3-phosphoethanolamine-N-(polyethylene-glycol-2000) folate), DSPE-PEG_{2000}-NH_2(1,2-distearoyl-sn-glycero-3-phosphoethanolamine-N-amine (polyethylene glycol) 2000), and Doxorubicin Hydrochloride was obtained from Wako Chemicals (Osaka, Japan). All reagents were purchased from Fisher Scientific (Fairlawn, NJ). Chemicals for cell culturing work - Lyso-tracker, Trypan Blue, Trypsin (0.25%), Dulbecco's modified Eagle's medium (DMEM) and fetal bovine serum (FBS) were purchased from Sigma-Aldrich, USA and Gibco, Japan. Invitrogen (USA, Japan) supplied Alamar Blue stain.

Purification of SWCNTs

Purification of SWCNTs was carried out according to previously reported procedure. [39] The SWCNTs (30 mg) were added to a solution containing 96% H_2SO_4 and 70% HNO_3 (3:1, V/V; 120 mL) and subjected to sonication at 0˚C for 24 h. Then the SWCNTs were thoroughly washed with deionized water and filtered through a micro-porous filtration membrane (0.22 μm). After filtration, they were redispersed in HNO_3 (2.6 M, 200 mL) and refluxed for 24 h, collected by filtration and washed with ultrapure water to neutrality. The obtained product was then dried at 50°C for 24 h.

Synthesis of PEGylated SWCNTs

Purified SWCNTs (0.2 mg) were sonicated in (0.10 mL) of dimethyl formamide (DMF) for 2 h to give a homogenous suspension. Oxalyl chloride (0.008 mL) was

added drop wise to the purified SWCNT suspension at 0˚C under N_2 atmosphere. The mixture was stirred at 0˚C for 2 h and then at room temperature for another 2 h. Finally, the temperature was raised to 70˚C and the mixture was stirred overnight on a magnetic stirrer to remove excess oxalyl chloride. Folate conjugated PEG (FA-PEG) dispersed in chloroform and methanol was used for bio-conjugation. FA-PEG (0.2 mM) was added to the SWCNT suspension and the mixture was stirred at 100˚C for 5 days. After it was cooled to room temperature, the mixture was filtered through a 0.2 μm pore-size membrane and washed thoroughly with ethyl alcohol and deionized water (DI). The PEGylated SWCNTs were collected on the membrane and dried overnight under vacuum.[40]

DOX loading onto the PEGylated SWCNTs

DOX loaded PEGylated nanotubes were prepared for anticancer treatment. The drug loading efficiency and its release profile from the PEGylated nanotubes were studied. Doxorubicin hydrochloride (15 mg) was stirred with the PEGylated nanotubes (5 mg) dispersed in a PBS (Phosphate buffered saline) buffered solution of pH 7.4 (10 mL) and stirred for 16 h at room temperature in dark condition to generate the targeted drug delivery system (DOX-FA-PEG-SWCNTs). Unbound excess DOX was removed by repeated centrifugation and washing with water until the filtrate was no longer red (red color corresponds to free DOX). Then the resulting DOX-FA-PEG-SWCNT complexes were finally centrifuged at 12,000 rpm for 10 min, the supernatant was decanted and the DOX-FA-PEG-SWCNT complexes were freeze dried.[36]

Characterization of the modified nanotubes

Morphological features of pristine and purified SWCNTs were characterized using field emission transmission electron microscope (TEM) (JEM 2200 FS, JEOL, Japan). One drop of nanotube suspension was dropped on carbon coated copper grid after

hydrophilizing the grid for 30 s in TEM grid hydrophilizer (JEOL DATUM, HDT-400) and dried thoroughly. Nanotubes were observed using TEM at 200 kV and the tubular nature of the SWCNTs were observed and images were recorded. Surface characteristics of the nanotubes were analyzed using scanning electron microscope (SEM) (JSM 7400F, JEOL, Japan). Nanotube samples were prepared on silica substrates and were sputter coated with platinum by an Auto Fine Coater (JEOL, Tokyo, Japan) for 50 seconds then the silica substrates were fixed to sample stubs using double-sided carbon tape, and were viewed at an accelerating voltage of 3-5 kV under SEM. For atomic force microscopy (AFM), the sample was deposited on a glass surface and vacuum dried. Tapping mode of the cantilever was used in the AFM analysis (MFP-3D-CF AFM, Asylum Research, USA). The presence of FA-PEG on FA-PEG-SWCNT was confirmed by studying the characteristic absorption peaks associated with functional groups of SWCNT, folic acid and PEG using X-ray photoelectron spectroscopy (XPS) (AXIS His-165 Ultra, Kratos Analytical, Shimadzu Corporation, Japan). Analysis was carried out under a basic pressure of $1.7x10^{-8}$ Torr and the X-ray source used was anode mono-Al with pass energy of 40. XPS spectra for FA-PEG-SWCNT with peaks of C, O and N were obtained. The zeta potential (Zetasizer Nano, Malvern Instruments Ltd.) of pristine SWCNT, purified SWCNT and PEGylated SWCNT was analyzed to confirm the change in their surface potential occurring due to the proper bio-functionalization. The DOX conjugation to the PEGylated SWCNTs was determined by UV/Vis absorption spectrophotometry (UV-3100, Shimadzu, Japan).

Drug loading efficiency analysis

The amount of DOX loaded onto the PEGylated nanotubes was quantified[41] spectrophotometrically with the help of UV/Vis absorption spectroscope at an

absorbance of 490 nm based on a standard curve of DOX.[42] Initially, a standard absorbance curve was plotted using standard concentrations of DOX in PBS solution to determine the exact amount of the drug loaded onto the nanotubes (data not shown). To calculate the loading efficiency of the drug, 100 μL of the drug-loaded samples were drawn before and after centrifugation step and analyzed. The following formula was used for calculating the drug efficiency:

$$\text{Drug loading efficiency}(\%) = \frac{A\text{total drug} - A\text{free drug}}{A\text{total drug}} \text{ X } 100$$

where, A total drug is the initial drug concentration and A free drug is the free drug concentration in the supernatant.

In vitro drug release studies

The in vitro drug release profile of DOX from DOX-PEG-SWCNT was studied at the physiological temperature of 37°C and pH of 7.4, 5.3 and 4.0 in PBS. The pH 5.3 and 4.0 (the endosomal pH of cancer cells) and pH 7.4 (the physiological pH) were selected for in vitro drug release studies. All experiments were performed in triplicates. Suspensions of the DOX-loaded SWCNTs (1 mg) were prepared in 5 mL, of phosphate buffer solutions and maintained at 37°C under a continuous shaking of 100 rpm for 3 days. At predetermined intervals, 1 mL of the sample supernatant was collected and centrifuged and the concentration of released DOX in the supernatant was estimated by UV/Vis spectrophotometer at 490 nm. At the same time, the suspension was compensated with 1 mL of fresh PBS. The concentration of drug released at a given time was calculated using a DOX standard curve.

Cell culture studies

Breast cancer cell lines (MCF7) and mouse fibroblast cell lines (L929) cells, obtained from Riken bioresource Center, Japan were cultured in monolayers to 80% confluence by maintaining in Dulbecco's minimal essential medium (DMEM, Gibco) supplemented with 10% fetal bovine serum (FBS) and 1% penicillin-streptomycin solution in a 5% CO_2 -humidified atmosphere at 37 °C. For use in experiments, 1 x 10^4 cells/mL per well were seeded in glass based dish for confocal studies, approximately 5000-7000 cells were seeded in 96 well plates for cytotoxic studies, 3×10^4 cells were plated in 25 mL flask for phase contrast studies.

Biocompatibility studies of PEGylated SWCNTs

Biocompatibility studies were carried out using phase contrast microscopy and Alamar blue assay. Phase contrast microscopy was studied to analyze the biocompatibility of the PEGylated nanotubes. MCF7 and L929 cells were plated onto 6 well plates and the plates were incubated at 37°C in CO_2 incubator with 5% CO_2 and allowed to grow to 70% confluency. The PEGylated nanotubes were added at a concentration of 0.1 mg/mL on day 2. The cells were again incubated for 24 h and washed before viewing under inverted phase contrast microscope (TE2000-U, Nikon ECLIPSE, Japan).

The biocompatibility of pristine and PEGylated nanotubes was also estimated by Alamar blue assay. Three different concentrations (0.1, 0.5 and 1.0 mg/mL) of pristine and PEGylated nanotubes were dispersed in PBS and treated with MCF7 and L929 cells grown in 96 well microplate for 24 h. After the addition of the nanotubes, these plates were further incubated for 24 h. After the addition of 10% Alamar blue dye to each well, the plates were incubated for 4 h and the viability was assessed

using a microplate reader (Multidetection microplate scanner, Dianippon Sumitomo Pharma, Japan) by measuring the absorbance and fluorescence intensity of the resultant product. Experiments were conducted in triplicates.

In vitro cytotoxicity studies

The in vitro cytotoxicity profile of the DOX-FA-PEG-SWCNT in comparison with free DOX was studied using Alamar Blue assay. MCF7 cells were exposed to three different concentrations (0.1, 0.5 and 1.0 mg/mL) for the above two samples for 72 h. Experiments were conducted in triplicates. Alamar blue assay evaluates the proliferation and metabolic activity of cells. In living cells, the mitochondrial reductase enzymes are active and reduce Alamar blue to form a different colored product form the blue dye. This reducing ability of the cells explains the active metabolism that takes place within the cells. When the samples added to the cells are toxic in nature, the reducing ability of the cells to reduce the dye decreases. The fluorescence intensity of Alamar blue assay was quantified at 590- 620 nm. 5000-7000 cells per well were plated and incubated for 24 h before the addition of the nanoparticles. The nanoparticles dissolved in media were added and incubated for 24 h and assayed. The experiment was conducted in triplicate and the viability was assessed using a microplate reader (Multidetection microplate scanner, Dianippon Sumitomo Pharm) by measuring the absorbance and fluorescence intensity of the resultant product.

The relative cell viability was calculated using the formula:

$$\% \text{ of cell viability} = \frac{A \text{ sample}}{A \text{ control}} \times 100$$

where, A sample is the absorbance of the sample used and A control is the absorbance of control sample.

Confocal microscopy

The uptake of nanoparticles was studied using confocal microscopy. All the images were taken using a 100X oil immersion objective lens. Cells were seeded in a glass base dish with standard medium and incubated at 37ºC. After 24 hours of growth, nanoparticles both targeted and non-targeted, at a fixed concentration of 0.1 mg/mL were added to the cells and incubated for 2 hours at 37ºC for uptake by the cells. At the end of the incubation period, the nutrient media was removed and the cells were washed with PBS buffer (0.01 M, pH 7.4) thrice and stained with Lysotracker to mark the location of lysosomes within the cells to understand the localization of nanotubes within the cell. Fresh PBS (0.01 M, pH 7.4) buffer was added to the plates and the cells were viewed under confocal microscopy (Leica TCS SP5, Leica Microsystems GmbH, Germany) or (Olympus 1x81 under DU897 mode).

Results and Discussions

Nanotube characterization analysis

An ideal NDDS should have high drug loading capability, strong affinity for target cells and should release drugs triggered by a characteristic feature of the diseased cells, thus improving the efficacy of the drug and minimizing the systemic toxicity. Here, the SWCNTs were purified before using as delivery vehicles for chemotherapy as the metal catalysts used for the synthesis of CNTs have been proven to be toxic. The SWCNTs can be purified or surface modified by exposing them to oxidizing conditions (solutions containing sulfuric acid and nitric acid). This results in the formation of carboxylic groups on the surface of SWCNTs, which increases their dispersibility in aqueous solutions.

By TEM and SEM observations, we found that the purified nanotubes are dispersed

individually or in small bundles as compared with pristine SWCNTs, which were bundled, and aggregated with black metal catalyst and amorphous carbon particles. We have observed a concomitant decrease in the quantity of metal particles and amorphous carbon in the purified nanotubes when compared to pristine SWCNTs (Figure 1a- d) and (Figure 2a and b) respectively.

To analyze the effect of PEGylation on the morphology of SWCNTs, we carried out SEM and AFM analysis of the PEGylated SWCNTs. On SEM and AFM analysis, we observed uniformly distributed PEGylated SWCNTs (Figure 3a and b). These pictures clearly showed that PEGylated SWCNTs are well dispersed and distributed.

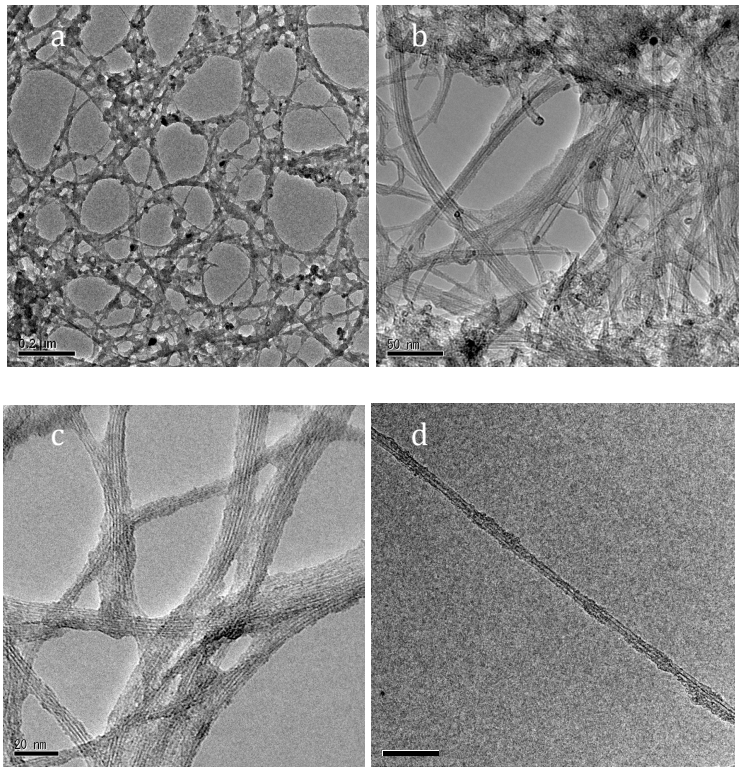

Figure 1. Transmission electron microscopy images of (a, b) Pristine and (c, d) Purified SWCNTs.

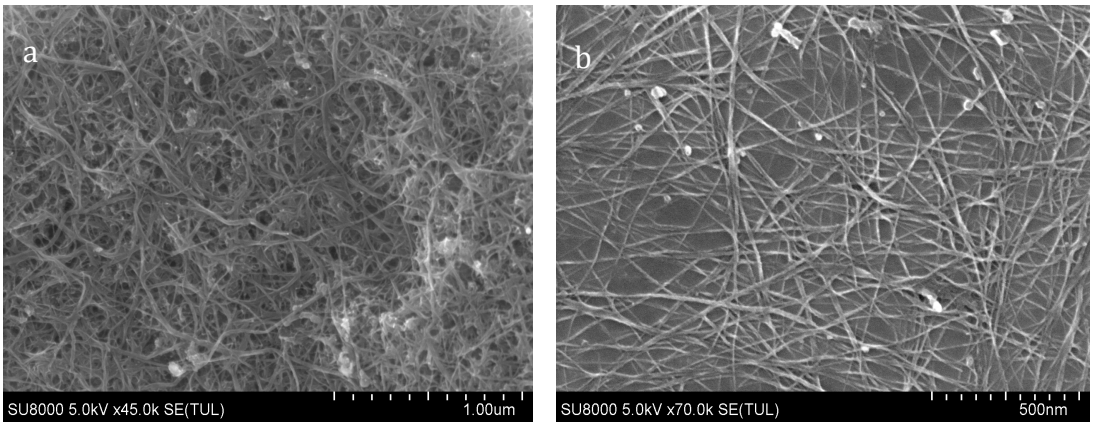

Figure 2. Scanning electron microscopy images of (a) Pristine and (b) Purified SWCNTs.

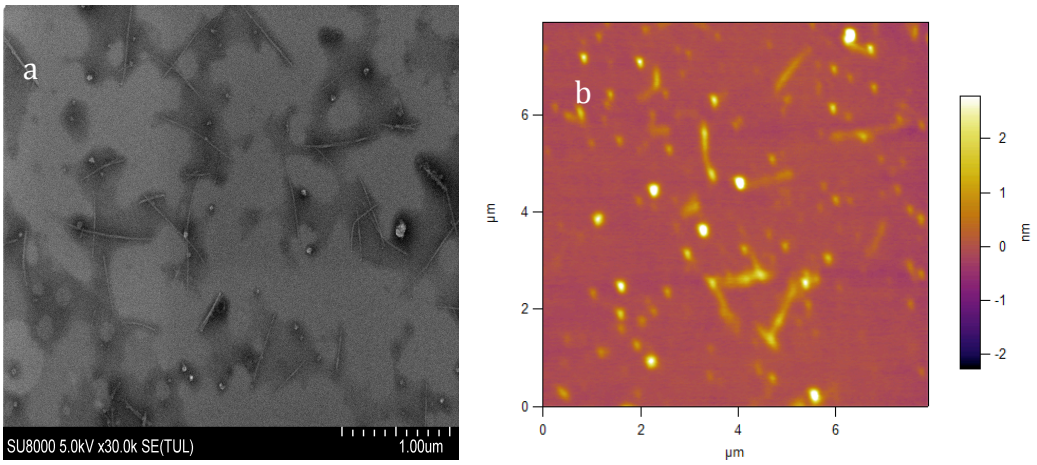

Figure 3. (a) Scanning electron microscopy and (b) atomic force microscopy images of PEGylated SWCNTs.

Particles	Zeta potential
Pristine SWCNT	-26.9 mV
Purified SWCNT	-54.2 mV
PEGylated SWCNT	-34.2 mV

Table 1. Zeta potential analysis of pristine, purified and PEGylated SWCNTs.

To study the change in the surface properties of the modified SWCNTs by PEG coating, we have analyzed the zeta potential of the pristine, purified and PEGylated nanotubes. The zeta potential is an indicator of the stability of colloidal systems. The pristine SWCNTs have a zeta potential of -26.9 mV. The zeta potential was increased to -54.2 mV in purified SWCNTs and this may be due to the existence of many COO^- groups on the sidewalls of SWCNTs.[36] The PEGylated SWCNTs showed a zeta potential of -34.2 mV. PEGylated SWCNTs has less negative potential than purified SWCNTs since PEGylation converts the carboxylic acid groups into esters.[40] The solubility of biofunctionalized SWCNTs was increased, presumably due to oxygen containing glycol chain, which can form hydrogen bonds with the water molecules and capture cations present in the solution.[40] The shift towards more negative potential for PEGylated SWCNTs clearly proves the conjugation of PEG moieties on to the SWCNTs.

Electron Spectroscopy for Chemical Analysis (ESCA) was used to confirm the presence of functional groups on the oxidized SWCNTs. The attachment of FA-PEG to oxidized SWCNTs was confirmed by N_2 peak. The wide spectrum obtained clearly shows the peaks corresponding to carbon, oxygen and nitrogen. Nitrogen peak is absent in oxidized SWCNTs and the presence of nitrogen peak in the PEGylated SWCNTs[43] confirms the PEGylation of the oxidized SWCNTs (Figure 4).

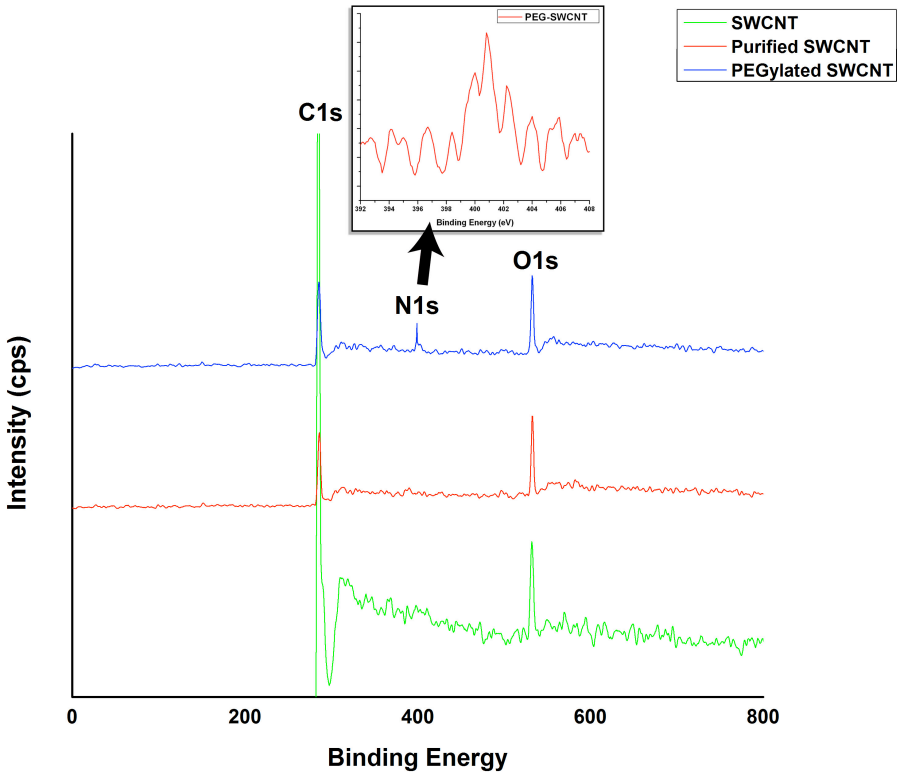

Figure 4. X-ray photoelectron spectroscopy (XPS) peaks of the SWCNTs. (a) Wide scan spectra of Pristine SWCNT (b) Purified SWCNT (c) PEGylated SWCNT. Inset corresponds to N1s signal spectra of PEGylated SWCNTs that has been shown separately outside.

DOX loading onto the PEGylated nanotubes

DOX loading onto the PEGylated SWCNTs was monitored by UV-Vis absorption spectroscopy. Figure 5 shows the absorption spectra of pristine SWCNT, plain DOX and DOX loaded onto PEGylated SWCNTs. Plain DOX in water displays absorption at 490 nm. The stacking of DOX onto PEGylated nanotubes was evident from the UV-Vis spectrum, which clearly shows the characteristic absorption peaks of DOX indicative of the interaction between DOX and SWCNTs.[41]

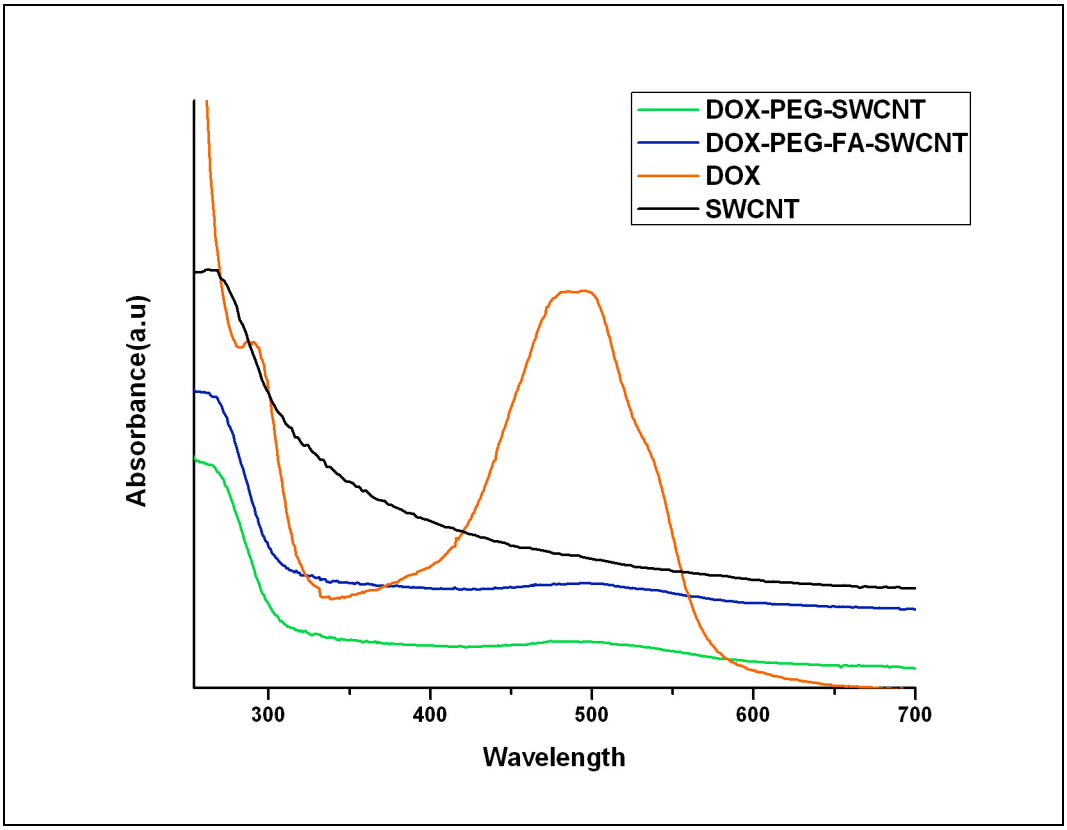

Figure 5. UV-Vis absorbance spectra of pristine SWCNT, plain DOX, DOX-FA-PEG-SWCNT and DOX-PEG-SWCNT.

Drug loading efficiency studies

The loading of DOX onto the nanotubes can be determined by the analysis of the supernatant for free drug using UV-Vis spectrophotometer after ultracentrifugation of the DOX loaded SWCNTs. We obtained a DOX loading efficiency of 58% onto the PEGylated nanotubes.

In vitro drug release studies

The drug release profile of DOX from the DOX loaded nanotubes was studied at 37°C in PBS at three different pH conditions 7.4, 5.3 and 4.0, with a continuous shaking of 100 rpm for 72 h. The temperature of 37ºC was selected for drug release response because it is close to the physiological temperature. The pH of 7.4 corresponds to physiological pH and pH of 4.0 and 5.3 corresponds to lysosomal pH

of cancer cells. The drug release curves (Figure 6) indicate that the release of DOX from the PEGylated nanotubes is pH triggered, and the drug release studies were carried out till it reached the stationary phase. At pH 7.4, the drug release curve shows that DOX loaded on SWCNTs is released at a very low and slow rate for 6 h and attains a stationary phase in the ensuing hours with very minimum drug release up to 24 h. However, at pH 4.0, the DOX release rate has been significantly enhanced during the initial 6 h. We have observed an initial burst of drug release up to 4 h followed by a sustained release pattern till 12 h. The above drug release pattern was repeated again with a small burst of drug after 12 h and again followed by a sustained release till 72 h. The drug release profile at pH 5.3 overlapped with that of pH 4.0. The above results can be ascribed to the hydrogen-bonding interaction between DOX and SWCNT, which is stronger under neutral conditions, resulting in a controlled release. However, the drug release pattern under acidic media indicates higher amount of DOX release than at neutral conditions. Under acidic conditions, the amine ($-NH_2$) groups of DOX get protonated resulting in the partial dissociation of hydrogen-bonding interaction; hence the amount of DOX released from SWCNTs is much higher. This efficient loading and release of DOX indicates strong π-π stacking interaction between SWCNTs and DOX.[44, 45]

The loading and release of DOX depends upon the hydrogen bonding interaction with SWCNT and is a function of pH. At pH 7.4, four possibilities of hydrogen bonding have been expected: (a) -COOH of SWCNT and -OH of DOX, (b) -COOH of SWCNT and the $-NH_2$ of DOX, (c) -OH of SWCNT and -OH of DOX and (d) -OH of SWCNT and $-NH_2$ of DOX. This overall hydrogen bonding interaction between SWCNT and DOX is higher at pH 7.4.[44, 41] Under acidic conditions, two kinds of hydrogen bonding can be expected (a) -COOH of SWCNT and-OH of DOX, and (b)

between -OH of SWCNT and the -OH of DOX. Also the $-NH_2$ of DOX forms $-NH_3^+$ with H^+, which cannot participate in hydrogen bonding. Furthermore, at low pH the H^+ in solution would compete with the hydrogen bond forming group and weaken the above outlined hydrogen bonding interaction, which may lead to a greater release of DOX.[44] Around 70% of the drug was released within 72 h in pH 4.0 buffer, whereas only 17% of the drug was released in pH 7.4 buffer indicating a higher percentage of release of DOX under acidic conditions. In summary, the FA-PEG-SWCNT displayed pH sensitive release of DOX, suggesting it to be a promising delivery vehicle for the anticancer drug, and showing potential for tumor targeting and controlled release applications.

Biocompatibility studies

Phase contrast studies were carried out to analyze the biocompatibility of functionalized SWCNTs. L929 cells and MCF7 cells were plated onto 6 well plates until it attained 70% confluency. Pristine SWCNTs and PEGylated SWCNTs (PEG-SWCNT) at a concentration of 0.1 mg/mL was added to each well and the plates were incubated for 24 h. The biocompatibility of the functionalized SWCNTs can be seen in the phase contrast images taken after 24 h in Figure 7 (a-f). The image clearly shows the PEGylated SWCNT treated cells growing competently at par with the control cells. However, some dead cells were observed in the cells treated with pristine SWCNTs. The biocompatibility of the pristine and PEGylated nanotubes was further studied using Alamar blue assay (Figure 8). The above-mentioned samples were incubated with L929 cells and MCF7 for 24 h. The viability of L929 cells and MCF7 when treated with the highest concentration of 1 mg/mL of pristine SWCNT were found to be 64% and 59% respectively. However, the viability of the cells increased to 87% and 84% in L929 and MCF7 cells, when treated with the same

highest concentration i.e., 1 mg/mL of PEGylated SWCNTs thereby, indicating successful PEGylation of the SWCNTs with PEG. Thus, we can confirm that the PEGylated SWCNTs are highly biocompatible and least cytotoxic in nature.

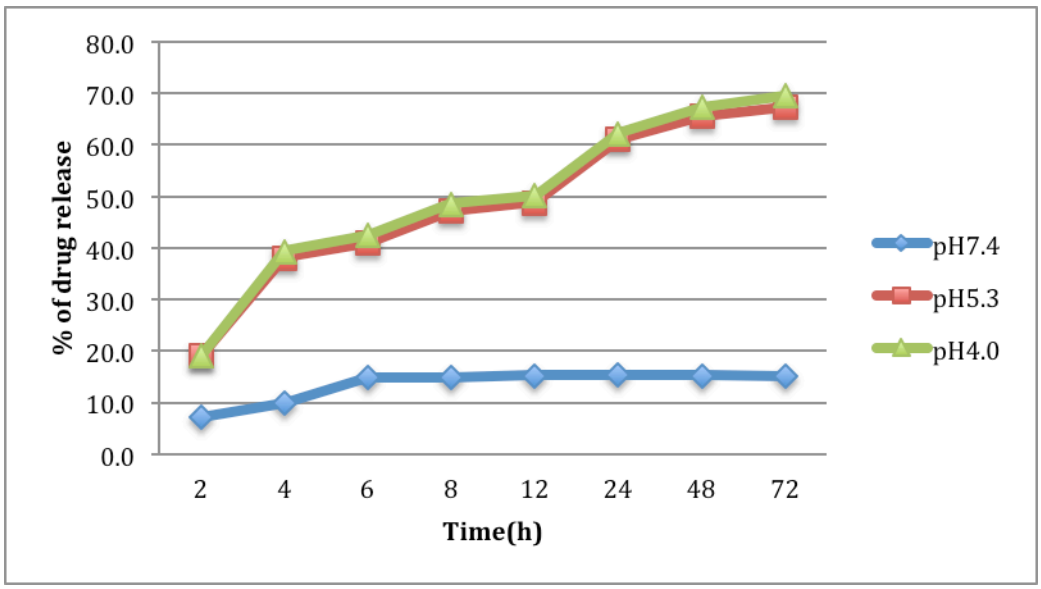

Figure 6. In vitro drug release profile of DOX from DOX-FA-PEG-SWCNT in phosphate buffered saline at pH 7.4, 5.3 and 4.0.

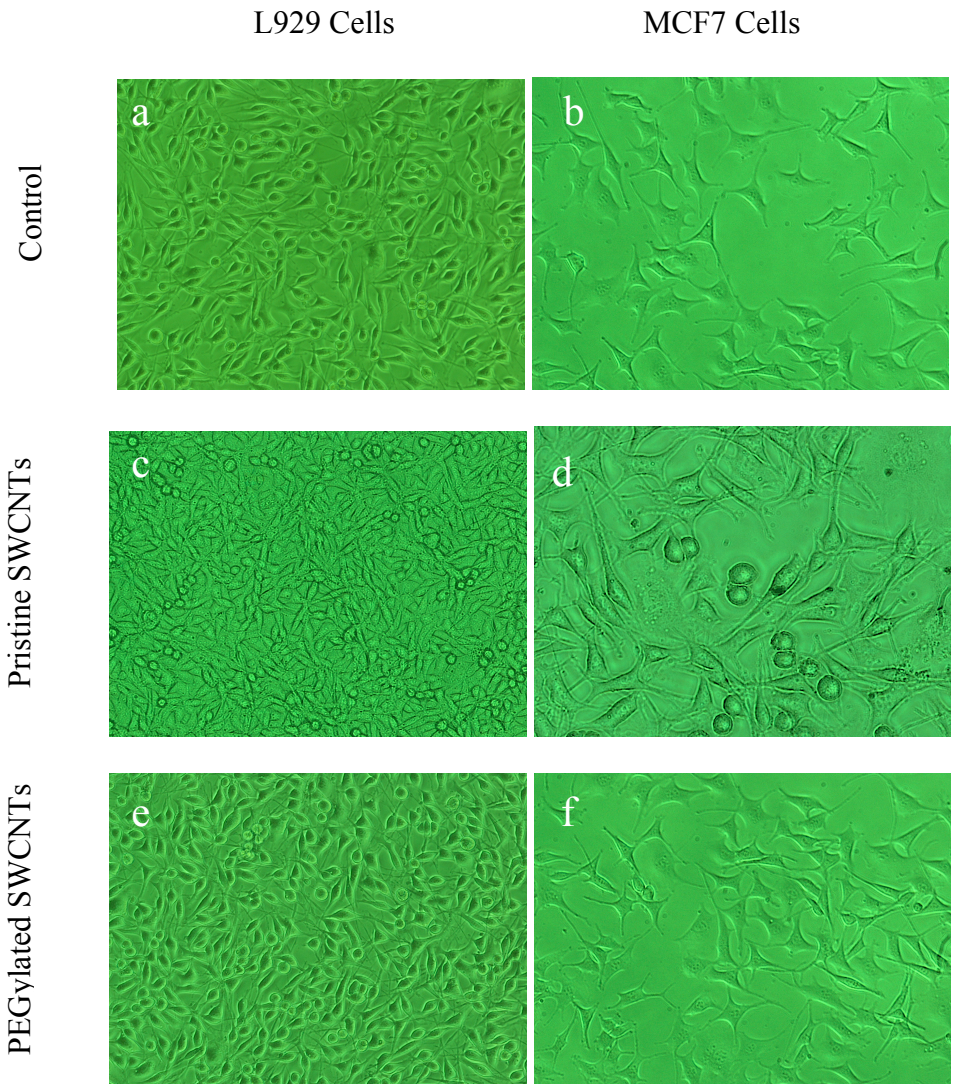

Figure 7. Phase contrast microscopic images of normal (L929) and cancer (MCF7) cells treated with pristine SWCNTs and PEGylated SWCNTs after 24h. Control images of (a) L929 and (b) MCF7 cells. (c & d) are images of cells treated with pristine SWCNTs. (e & f) are images of cells treated with PEGylated SWCNTS and showing biocompatibility of cells after 24h of incubation.

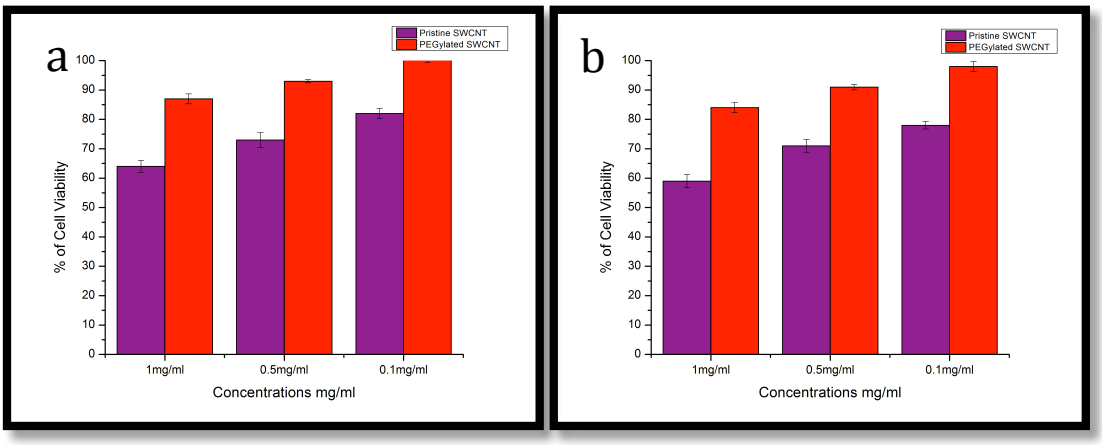

Figure 8. Results of Alamar blue assay. Both (a) normal cells L929 and (b) cancer cells MCF7 were treated with different concentrations of Pristine SWCNTs and PEGylated SWCNTs.

Confocal studies

To confirm the cellular uptake of particles and their localization within the cells, confocal laser scanning microscopy was performed. The DOX-FA-PEG-SWCNTs and DOX-PEG-SWNTs were incubated with human breast cancer cells and analyzed by fluorescence microscopy allowing the DOX to be located as it emits red fluorescence under irradiation. To further elucidate the endosome-mediated pathway of the nanotubes, lysosomal staining was performed with green colored Lysotracker. The overlapping signals of red signal from the DOX-FA-PEG-SWCNT and green signal from lysosomes confirm the receptor-mediated endosomal uptake of the nanotubes into the cells. High targeting capability is vital for the selective destruction of cancer cells. It means that the targeting agents would bind to cancer cells at a much higher rate than to normal cells. To demonstrate the targeted delivery of DOX by SWCNTs, we conjugated folate as the targeting moiety that targets folate receptors of cancer cells. Increased DOX fluorescence was observed in MCF7 cells with DOX-FA-PEG-SWCNT, compared to L929 cells, which showed minimum internalization

of the nanotubes (Figure 9). Thus, it indicates that the FA conjugated nanotubes is taken up more efficiently into the MCF7 cells and suggests that the DOX-FA-PEG-SWCNT is internalized via the FA receptor mediated pathway, pointing to the significant role of folate in cellular uptake.

In vitro cytotoxicity studies

In vitro cytotoxicity profile of the DOX-FA-PEG-SWCNT in comparison with free DOX was studied using Alamar Blue assay. MCF7 cells were used for the cytotoxicity analyses. Three different concentrations of each of the DOX-FA-PEG-SWCNT and DOX as test sample were used. The assays were carried out for 72 h and the fluorescence and absorbance readings were taken for analyses. Figure 10 a and b show the percentage of cell viability measured for free DOX and DOX-FA-PEG-SWCNTs respectively, using Alamar blue assay. In the case of DOX-FA-PEG-SWCNT, we observed that the cell viability decreased with increasing concentration for the initial 24 h. After 24 h, there was sustained release of drug resulting in a slower mortality rate. The viability was abruptly reduced to 59% even at the lowest concentration (0.1 mg/mL) in 24 h. The viability of the cancer cells was further decreased to 29% in 72 h at the same minimum concentration. DOX-FA-PEG-SWCNTs induced serious cytotoxicity, even at a dose much lower than free DOX. In the following study, when 1mg/mL of free DOX was used, cell viability was 75% after 24 h and 63% of cells were viable after 72 h. This is because the permeability of cells to free DOX is very poor, and so cannot effectively kill the cancer cells. We also found that with increase in concentration, the viability of DOX-FA-PEG-SWCNTs treated cells decreased apparently, indicating that the therapeutic efficiency of DOX-FA-PEG-SWCNT was dosage dependent.

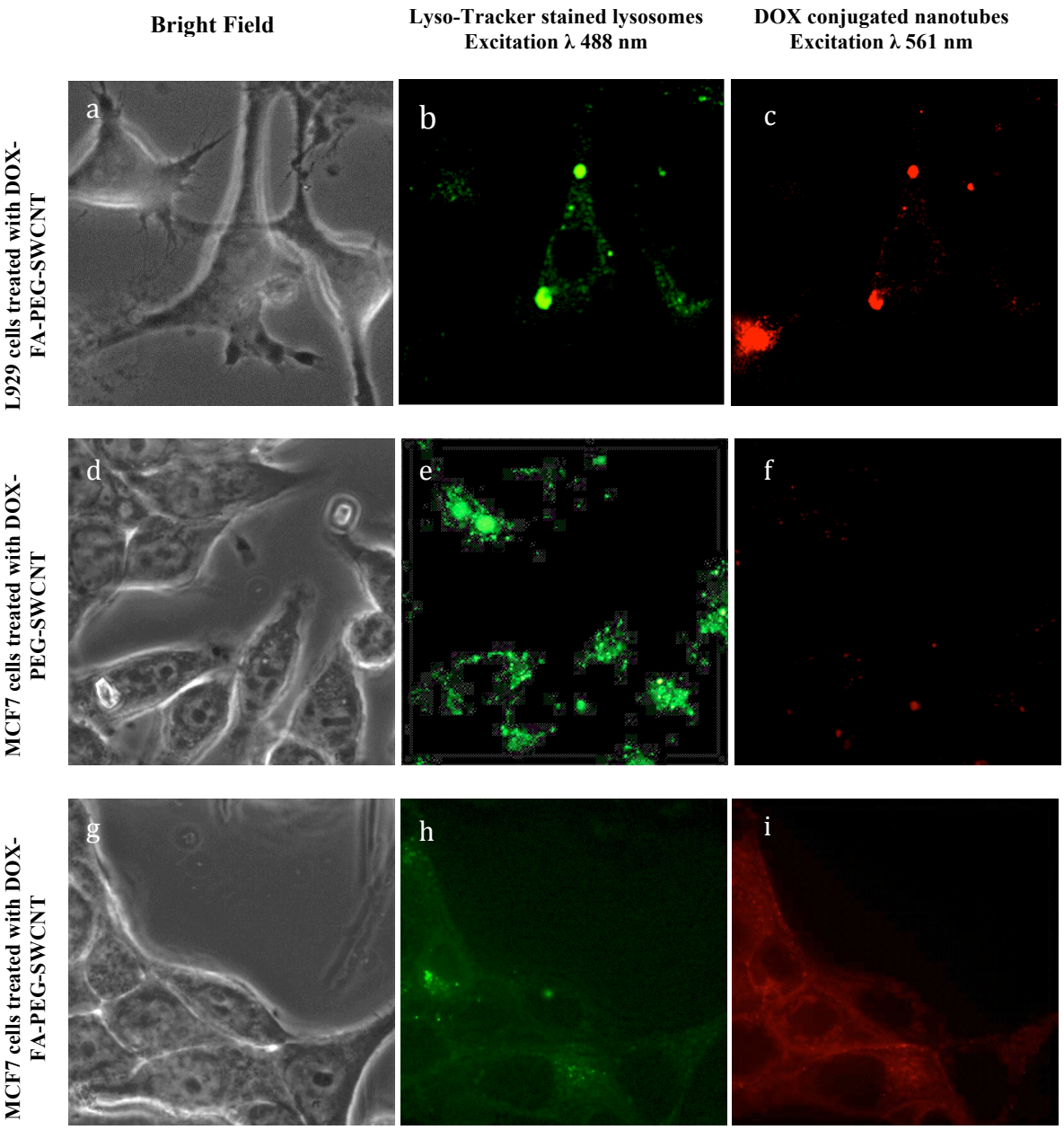

Figure 9. Confocal laser scanning microscopy (CLSM) images showing the selective internalization of SWCNTs by L929 and MCF7 cells. (a, d, g) Bright field images of the cells treated with nanotubes, (b, e, h) shows the green fluorescence of the lysosomal staining of the cells with Lysotracker dye, (c, f, i) shows the red fluorescence images of cells internalized with DOX conjugated nanotubes.

The high efficiency of DOX-FA-PEG-SWCNTs may be due to the following reasons: (1) the folate attached SWCNTs could target the DOX-FA-PEG-SWCNTs conjugates to the targeted sites while free DOX is non-specific and damages normal tissues leading to serious side effects,[44, 36] (2) DOX could easily enter cancer cells after conjugation onto SWCNTs because of their high cell membrane permeability,[46, 47] and (3) the release of DOX from the SWCNTs is pH triggered which explains the abrupt decrease in cancer cell viability at 24 h and which then follows a slow drug release pattern and therefore, slower killing rates up to 72 h. From the results obtained, it can be concluded that DOX-FA-PEG-SWCNT proves to be the most cytotoxic to cancer cells, while not damaging the normal tissues, when compared to free DOX.

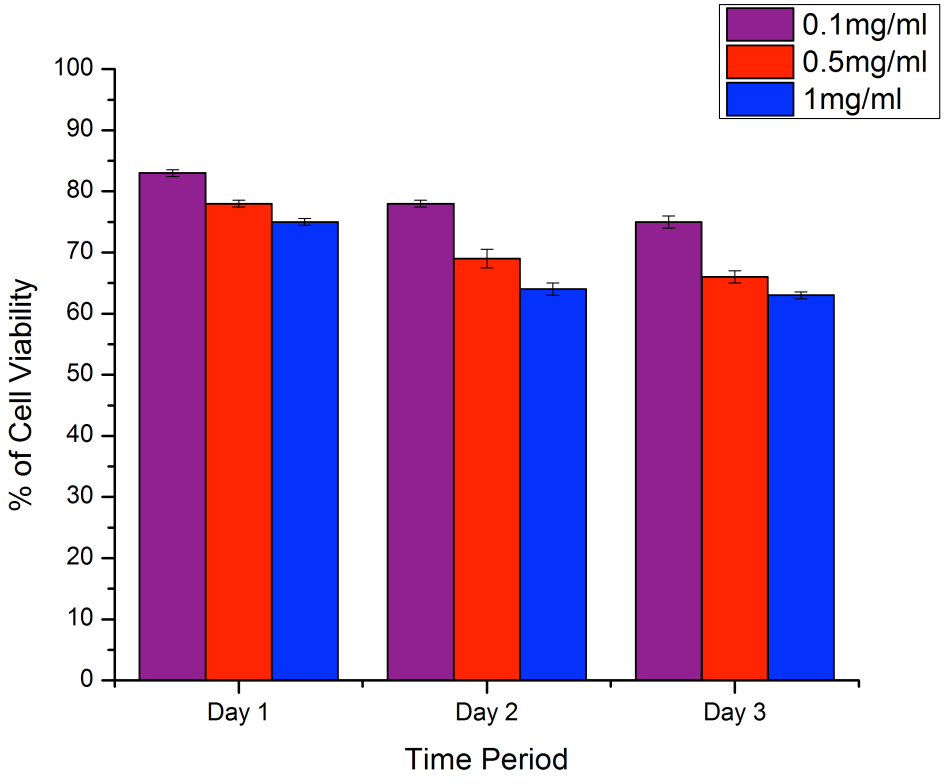

Figure 10 (a). Results of Cytotoxicity Assay of 3 day study of plain DOX on MCF7 cells.

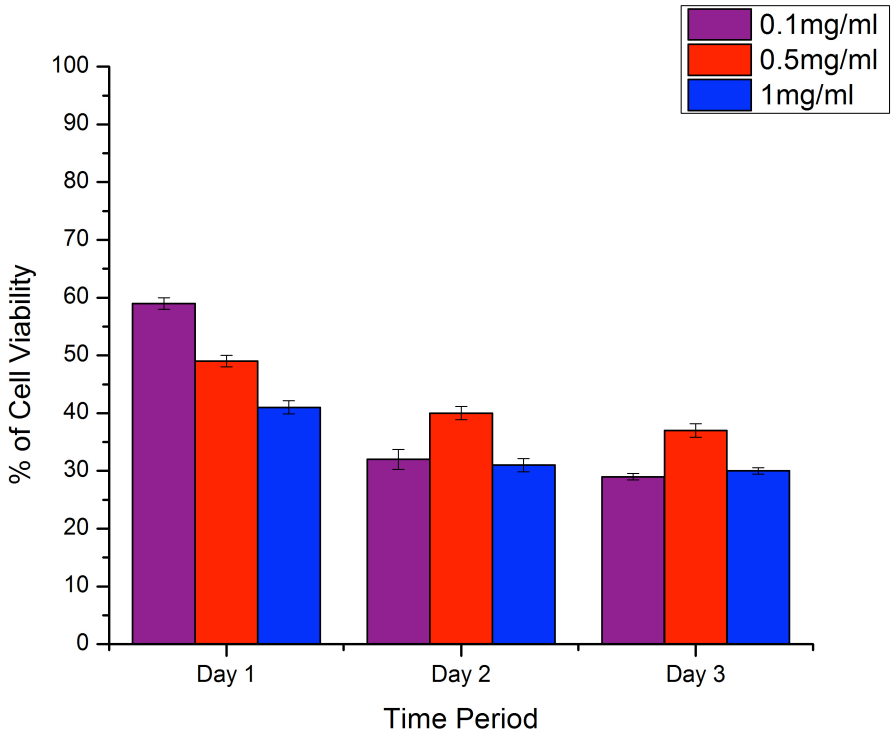

Figure 10 (b). Results of Cytotoxicity Assay of 3 day study of DOX-FA-PEG-SWCNTS on MCF7 cells.

Conclusion

CNTs appear to accumulate in cancerous tumor tissues much more than in normal tissues, partly due to the enhanced permeability and retention (EPR) effect. In summary, we successfully synthesized a highly effective targeted NDDS based on PEG functionalized SWCNTs and then further functionalization was facilitated with a targeting group (FA) and an anticancer drug (Doxorubicin). The obtained system (DOX-FA-PEG-SWCNT) displays excellent stability under physiological conditions. It was found that it could also effectively release DOX at reduced pH typical of the tumor environment of intracellular lysosomes and endosomes. We conclude that this nanoscale drug delivery system is more selective and effective than the free drug and it should result in enhanced therapeutic effects, with reduced general toxicity and

hence reduced side effects in patients. Considering these positive in vitro drug delivery results, the application of DOX-FA-PEG-SWCNT could be extended to enhance the efficiency of cancer therapy in vivo.

References

1. GM Whitesides. et al. Nature Biotechnology. (2003) 21, 1161-1165.

2. CR Lowe, et al. Current Opinion Chemical Biology. (2000) 10, 428-434.

3. L Wang, W Zhao, W Tan. Nano Research. (2008) 1, 99-115.

4. Z Ji, G Lin, Q Lu, et al. Journal of Colloid Interface Science. (2012) 365,143-9.

5. R Ravichandran. NanoBiotechnology. (2009) 5, 17.

6. B Bob. Innovative Pharmaceutical technology. (2004) 1, 58.

7. SK Sahoo, S Praveen, J Panda. Journal of Nanomedicine Nanotechnology Biology and Medicine. (2007) 3, 20.

8. M Rawat, D Singh, S Saraf. Biological & pharmaceutical bulletin. (2006) 29,1790.

9. XM Li, LY Ding, YL Xu, et al. International Journal of Pharmaceutics. 373 (2009) 116.

10. XB Xiong, ZS Ma, R Lai, A Lavasanifar. Biomaterials. 31 (2010) 165.

11. ZH Xu, ZW Zhang, Y Chen, et al. Biomaterials. 31 (2010) 757.

12. M Prabaharan, JJ Grailer, S Pilla, et al. Biomaterials. 30 (2009) 6065.

13. K Kostarelos, A Bianco, M Prato. Nature Nanotechnology. 4 (2009) 627.

14. M Prato, K Kostarelos, A Bianco. Accounts of Chemical Research. 41 (2008) 60.

15. R Singh, JW Lillard. Experimental and Molecular Pathology. 86 (2009) 215.

16. A Bianco, K Kostarelos, M Prato. Current Opinion Chemical Biology. 9 (2005) 674. 38.

17. PA Tran, LJ Zhang, TJ Webster. Advance Drug Delivery Reviews. 61 (2009) 1097.

18. WR Yang, P Thordarson, JJ Gooding, et al. Nanotechnology. 18 (2007).

19. SS Li, H He, QC Jiao, et al. Progress in Chemistry. 20 (2008) 1798.

20. L Lacerda, A Bianco, M Prato, K Kostarelos. Journal of Material Chemistry. 18 (2008) 17.

21. Z Liu, S Tabakman, K Welsher, HJ Dai. Nano Research. 2 (2009) 85.

22. XK Zhang, LJ Meng, QG Lu, et al. Biomaterials. 30 (2009) 6041.

23. S Dhar, Z Liu, J Thomale, HJ Dai, et al. Journal of American Chemical Society. 130 (2008) 11467.

24. Z Liu, XM Sun, N Nakayama-Ratchford, HJ Dai. ACS Nano. 1 (2007) 50.

25. NWS Kam, HJ Dai. Journal of American Chemical Society. 127 (2005) 6021.

26. ID Rosca, F Watari, M Uo. Carbon. (2005) 43, 3124-3131.

27. VC Moore, MS Strano, EH Haroz, RH Hauge. Nano Letters. (2003) 3, 1379-1382.

28. G Pastorin, W Wu, S Wieckowski et al. Chemical Communications. (2006) 1182-4.

29. B Massimo, R Nicola, B Nunzio. Biomacromolecules, (2011) 12, 3381–3393.

30. MA Mamon, ME Itkis, S Niyogi, et al. Journal of American Chemical Society. (2001) 123, 11292-11293.

31. JJ Sudimack, RJ Lee. Advance Drug Delivery Reviews. (2000) 41, 147-162.

32. B Kalyanaraman, J Joseph, S Kalivendi, et al. Free Radical Research Center. (2002) 119-124.

33. ME O'Brien, N Wigler, M Inbar, et al. Annals of oncology (2004) 440-449.

34. HL Wong, R Bendayan, AM Rauth, XY Wu. Journal of pharmaceutical sciences 93 (8) (2004) 1993-2008.

35. J Chen, S Chen, X Zhao, LV Kuznetsova. et al. Journal of American Chemical Society. (2008) 16778–16785.

36. X Zhang, L Meng, Q Lu, Z Fei, PJ Dyson. (2009) 6041–6047,

37. X Shi, H W Su, M Shen, et al. Biomacromolecules. 10 (2009) 1744–1750,

38. R Li, R.Wu, L Zhao, et al. Carbon. (2011) 1797–1805,

39. J Liu, AG Rinzler, H Dai, JH Hafner, et al. Fullerene Pipes Science. (1998) 280, 1253-1256.

40. B Zhao, H Hu, A Yu, D Perea, et al. Journal of American Chemical Society. (2005) 127, 8197-8203.

41. H Huang, Q Yuan, JS Shah, RDK Misra. Advanced Drug Delivery Reviews. (2011) 63, 1332-1339.

42. YJ Gu, J Cheng, J Jin, SH Cheng, et al. International Journal of Nanomedicine (2011) 6, 2889-2898.

43. S Chen, Y Jiang, Z Wang, et al. Langmuir. (2008) 24, 9233–9236.

44. D Depan, J Shah, RDK Misra, J Shah. Materials science and engineering. (2011) C 31, 1305-1312.

45. Z Liu, X Sun, N Nakayama-Ratchford, et al. ACS Nano. (2007). 1, 50–56.

46. K Kostarelos, L Lacerda, G Pastorin, et al. Nature Nanotechnology. (2007) 2, 108-13.

47. JP Cheng, KAS Fernando, LM Veca, et al. ACS Nano. 2 (2008), 2085.

Chapter 4

Accelerated killing of cancer cells using multifunctional SWCNTs based system for targeted drug delivery in combination with photothermal therapy

Abstract

The photothermal therapy using nano-materials has recently attracted attention as an efficient strategy for the next generation of cancer treatments. Single walled carbon nanotube (SWCNT) is an upcoming potent candidate for the photothermal therapeutic agent since it generates significant amounts of heat upon excitation with near-infrared light. Photothermal effect can be employed to induce thermal cell death in a noninvasive manner. Photothermal effect of single-walled carbon nanotubes (SWCNTs) in combination with an anticancer drug doxorubicin (DOX) for targeted and accelerated destruction of breast cancer cells has been demonstrated in this chapter. A targeted drug delivery system was developed for selective killing of breast cancer cells with polyethylene glycol (PEG) biofunctionalized and DOX loaded SWCNTs conjugated with folic acid (FA). SWCNTs have strong optical absorbance in the near-infrared (NIR) region. In this special spectral window, biological systems are highly transparent. Our study reports that under laser irradiation at 800 nm, SWCNTs exhibited strong light-heat transfer characteristics. These optical properties of SWCNTs open the way for selective photothermal ablation in cancer therapy. It was also observed that, the internalization and uptake of folate-conjugated nanotubes into cancer cells was achieved by a receptor mediated endocytosis mechanism. Results of the in vitro experiments show that laser was effective in destroying the cancer cells, while sparing the normal cells. When the above laser effect was

combined with DOX conjugated SWCNTs, we have found an enhanced and accelerated killing of breast cancer cells. Thus this nano drug delivery system (NDDS) consisting of laser, drug and SWCNTs, proves to be a promising selective modality with high treatment efficacy and low side effects for use as future cancer therapeutics.

Introduction

Chemotherapy is used in cancer treatment to destroy cancer cells for maximum treatment efficacy but with side effects to healthy tissues.[1] Although the medical science and biomedical engineering has advanced to a significant extent, the therapeutic development of anti-cancer strategies is still limited[2] due to reduced solubility, poor non-selective biodistribution and restriction by dose-limiting toxicity. Thus, detecting cancer in its early stage, in combination with controlled and targeted therapeutics may provide a more efficient and less harmful solution to overcome the limitations of conventional techniques.[3, 4] Nanomedicine, an emerging research area that integrates nanomaterials and biomedicine, has attracted increasing interest as novel therapeutic strategy in cancer. Nano drug delivery systems (NDDS) have been developed to overcome the above limitations and to improve the pharmacological and therapeutic effects of the anticancer drugs. NDDS provides advantages like site-directed drug targeting[5] for improving drug efficiency, decreased side effects, early stage cancer detection,[6] improving the drug loading capacity and controlled drug release rates. A tumor targeted NDDS generally combines tumor recognition moiety with drug-loaded nanoparticles.[7-13] In recent years, various nano-sized drug delivery vehicles have been evaluated[14-16] of which carbon nanotubes[17, 18] have been shown to be advantageous to cancer therapy and imaging. Single-walled carbon nanotubes (SWCNTs), which are thin sheets of benzene rings rolled up into seamless cylinders, have many unique physical and chemical properties and attracted significant attention as promising drug delivery nano-vehicles for cancer diagnosis and chemotherapy due to their advantages like remarkable cell membrane penetrability, high drug loading capacity, pH-dependent therapeutic unloading and prolonged circulation half-lives.[19-21] SWCNT based NDDS have already been investigated as potential delivery vehicles

for intracellular transport of nucleic acids,[22, 23] proteins[24-26] and drug molecules,[27-30] and it has been repeatedly and independently proven by many in vitro results that the multifunctional SWCNTs could greatly improve the therapeutic efficiency of the drug while reducing their toxicity.[30-32] Thus, considering the advantages of SWCNTs, its potential as a nanocarrier for effective and safe transport for drug therapy is very promising. Carbon nanotubes especially SWCNTs, consisting of quasi one-dimensional quantum wires,[33] have many interesting inherent optical properties that can be useful in biomedical imaging.[34-38] SWCNTs have strong optical absorption from UV to NIR regions, which can be utilized for photothermal therapy[17, 35, 39, 40] and photoacoustic imaging[41, 42] from the heat they generate from NIR light absorption. Semiconducting SWCNTs with small band gaps of the order of 1 eV show photoluminescence in the NIR to IR-A range, which covers the tissue transparency window, and is therefore suitable for fluorescence imaging in biological systems.[43, 44] Therefore, SWCNTs appear to be an excellent platform for biomedical molecular imaging. Photothermal therapy for cancer has been widely investigated as an ideal, local, non-invasive treatment approach in comparison with other methods,[45] due to its precise energy delivery to target cells and the sensitivity of tumor cells to temperature elevation.[46] Laser light in the near-infrared (NIR) region is highly beneficial for in vivo use because of the low absorbance of biological tissues in the NIR region, thus making it a more promising approach towards cancer cell destruction with negligible side effects to healthy tissues. In bio-nanotechnology based cancer therapy, nanostructures with unique photothermal properties have been considered for the destruction of cancer cells.[17, 18, 29, 47, 48] The intrinsic properties of SWCNTs are suitable for these techniques, due to their strong optical absorbance in the NIR region,

which could release significant heat and enhance thermal destruction of cells during NIR laser irradiation.

PEGylation is a common strategy to impart versatile functionalities, high water solubility, biocompatibility and prolonged circulation in blood. PEG is composed of repeating ethylene glycol units -(CH_2-CH_2-O)$_n$-, where the integer 'n' is the degree of polymerization. PEG-coated SWCNTs are obtained by adsorption of amphiphilic polymer functionalized with activated PEG chains onto SWCNTs.[49] This is highly desirable for biological applications because it reduces their non-specific uptake by cells within the recticulo-endothelial system, which diminishes their phagocytosis, thus leading to prolonged circulation time in blood.[50] PEGylation of SWCNTs does not disrupt the π network of SWCNTs, thus preserving their physical properties, which are promising for multiple biomedical applications including imagining.[3]

Doxorubicin is one of the first identified anthracyclines and was isolated from the pigment-producing *Streptomyces peucetius* in the 1960s. It is also known as adriamycin and hyrdoxydaunorubicin. Doxorubicin is an essential component in the treatment of a wide variety of cancers, including hematological malignancies, many types of carcinoma and soft tissue sarcomas. The mechanisms of action of doxorubicin in cancer cells is brought about by the intercalation of doxorubicin into DNA base pairs, which inhibits the progression of the enzyme, topoisomerase II, to stabilize topoisomerase II complex and eventually impedes DNA resealing. The resulting DNA fragmentation leads to cell death.[51-53] However, the clinical use of doxorubicin soon proved to be hampered by serious problems such as the development of resistance in tumor cells or toxicity in healthy tissues. The development of effective approaches to limit toxicity to normal cells while maintaining a high anti-cancer efficacy of doxorubicin in tumor cells has become a

focus in recent years with efforts being made to develop tumor-targeted formulations. Folate (FA) as targeting moiety was selected, since folate receptors are over expressed on many tumors including ovarian, breast, brain, kidney, lung and liver. [55] The nanoparticles-folic acid conjugates have shown the ability to enter some tumor cells via the folic acid receptor mediated pathway,[54-58] and following internalization; the drug is selectively released into the acidic environment of the lysosomes and endosomes.[3] The uptake of folate-conjugated SWCNTs into cancer cells was investigated using confocal fluorescence imaging. In vitro cytotoxicity of PEGylated SWCNTs conjugated with folate as a targeting moiety and loaded with an anticancer drug doxorubicin along with laser irradiation were tested in MCF7 cells.

The ability to kill tumor cells by our system (DOX-FA-PEG-SWCNT) has been further enhanced through NIR irradiation mediated targeted cancer destruction by using the photothermal effect of the SWCNTs. This approach, which uses a combination of DOX and photothermal properties of SWCNTs, might provide a mechanism for enhanced cancer therapy and biological imaging applications.

Experimental details

The SWCNTs (length 0.5- 100 μm, diameter of 1-2 nm), fluorescein-FA-PEG and fluorescein-PEG-amine were obtained from Sigma Aldrich, Japan. Doxorubicin Hydrochloride was obtained from Wako Chemicals (Osaka, Japan). Concentrated acids and all other reagents were purchased from Fisher Scientific (Fairlawn, NJ). Chemicals for cell culturing work - Lyso-tracker, Trypan Blue, Trypsin (0.25%), Dulbecco's modified Eagle's medium (DMEM) and fetal bovine serum (FBS) were purchased from Sigma-Aldrich, USA and Gibco, Japan. Alamar Blue toxicology kit

was purchased from Invitrogen, USA. All chemicals used for this work were of reagent grade.

Preparation and characterization of DOX loaded SWCNTs

A SWCNT-based tumor targeted NDDS which consist of PEG modified SWCNT functionalized with folic acid as a targeting group for the targeted delivery of anticancer drug doxorubicin (DOX) was developed and characterized as previously described in Chapter 3.

Synthesis of fluorescent SWCNTs

FITC-FA-PEG was used to label SWCNTs. FITC-FA-PEG (1 mM) was sonicated with 0.25 mg/mL of SWCNTs in water for 1 h, and the resulting black suspension was centrifuged at 25,000 g for 6 h. The pellet formed at the bottom of the centrifuge tube containing aggregated CNTs and impurities were discarded. The supernatant was collected and filtered through a centrifugal filter (100 kDa molecular weight cut off, Millipore Amicom). The sample was washed several times with water to remove the excess PEGylated fluorescein and re-suspended in water and stored for further NIR laser studies.[59] UV-Vis measurements of FITC- FA-PEG-SWCNT, SWCNT and FITC-FA-PEG were carried out.

Laser measurements

For in vitro experiments, SWCNT solution were irradiated by 800 nm laser at 0.5-1 W/cm^2 for 3 min, and the temperature was measured with an infrared thermal camera (TVS200EX, NEC, Japan). All the experiments were conducted at room temperature.

Cell culture studies

Breast adenocarcinoma cells (MCF7) and mouse connective tissue (L929) fibroblast cells were procured from RIKEN Bioresource Center, Japan. Breast cancer cell lines (MCF7) and mouse fibroblast cell lines (L929) were cultivated for in vitro

experimental studies. MCF7 cells and L929 cells were cultured in T25 flasks and maintained separately in monolayers to 80% confluence using DMEM supplemented with 10% FBS and 1% penicillin-streptomycin solution in a 5% CO_2 humidified atmosphere at 37°C. For use in experiments, the respective cells were trypsinized, counted and loaded onto their respective plates for testing. Cells were seeded into 96 well plates for cytotoxic studies and in 33 mm glass base dish for confocal studies. For cytotoxicity studies, 5000 cells/well were seeded and for confocal studies, 30,000 cells/glass base dish were plated and grown for 24 h before treating them with the nanoparticles.

Alamar blue assay evaluates the proliferation and metabolic activity of cells. In living cells, the mitochondrial reductase enzymes are active and reduce blue colored Alamar blue to a different colored product. This reducing ability of the cells explains the active metabolism that takes place within the cells. When the samples added to the cells are toxic in nature, the reducing ability of the cells to reduce the dye decreases. The fluorescence intensity of Alamar blue assay was quantified at 590- 620 nm.

Selective internalization of SWCNTs into cancer cells

The internalization of the nanotubes with cancer MCF7 and control L929 cells were studied using confocal laser scanning microscopy. Cells were seeded in a glass base dish with standard medium and incubated at 37ºC for imaging studies. After 24 hours of growth, 0.1 mg/mL of DOX-PEG-SWCNT and DOX-FA-PEG-SWCNT nanotubes were suspended in the medium and from the above concentration 20 µL were taken and added to the cells and incubated for different time intervals (1, 3 and 5 h) at 37ºC for uptake by the cells. At the end of the incubation period, the media was removed and the cells were washed thrice with PBS buffer. To mark the location of lysosomes within the cells and to understand the localization of nanotubes within the cells, the

cells were stained with Lysotracker as per the manufacturer's instructions. In addition, the endosome-mediated uptake of the nanotubes was also confirmed. All the images were taken using a 100X oil immersion objective lens. The cells were viewed under a confocal microscope (Olympus 1X 81 in DU897 mode). Emission filter of 561/488 nm were used to observe the fluorescence emitted by the DOX conjugated nanotubes and Lysotracker.

Cancer destruction using the NIR effect of SWCNTs

In this study, we explored the effects of irradiation using an 800 nm laser on FITC-FA-PEG-SWCNT. The accelerated and combined destructive effects of DOX-FA-PEG-SWCNT on excitation with laser were analyzed. SWCNTs can efficiently convert 800 nm laser energy into heat, and selectively destroy target cells. The effect of NIR laser was studied using MCF7 cancer cell lines. Untreated cells were used as controls. Cells were seeded at a density of 1.6 X 10^4 cell/mL in 35 mm petri dishes. After 24 h of growth, MCF7 cells without SWCNT, with FITC-FA-PEG-SWCNT and DOX-FA-PEG-SWCNT at concentration of 0.1 mg/mL were added to the cells and again incubated for 3 h, rinsed with PBS, and stained with Lysotracker as per the manufacturer's instructions. The cells were again washed and placed in fresh medium and irradiated by 800 nm laser at 0.5-1 W/cm^2 for 3 min, and the temperature changes were recorded using an infrared thermal camera (TVS200EX, NEC, Japan). All the experiments were conducted at room temperature. The cells were viewed under confocal microscope before and after the laser treatments using a 100X oil objective and 488/561 nm excitations.

In vitro cytotoxicity assays of nanotubes under laser irradiation

The in vitro cytotoxicity profile of the MCF7 cells without SWCNTs and with FITC-FA-PEG-SWCNT and DOX-FA-PEG-SWCNT after laser irradiation was studied

using Alamar Blue assay. MCF7 cells were exposed to 0.1 mg/mL of the functionalized SWCNTs for the above two samples. Untreated cells were used as controls. Experiments were conducted in triplicates. The experiments were carried out for a time interval of 6 h, 12 h and 24 h. The fluorescence intensity of Alamar blue assay was quantified at 590-620 nm.

Results and Discussions

An ideal NDDS should have high drug loading, strong affinity for target cells and should release drugs triggered by a characteristic feature of the diseased cells, thus improving the efficacy of the drug and minimizing the systemic toxicity. In this study, Figure 1 shows the schematic representation of a targeted drug delivery system based on SWCNTs, biofunctionalized with polyethylene glycol (PEG), conjugated with folic acid (FA) as targeting moiety and loaded with DOX for selective killing of tumor cells was developed. Also, the photothermal effect of SWCNTs in combination with an anticancer drug DOX for targeting and selective destruction of breast cancer cells is demonstrated.

Characterization of the fluorescent SWCNTs

The functionalization of SWCNTs with FITC-PEG was analyzed by UV-Vis absorption spectroscopy. Figure 2 a, b and c shows the absorption spectra of pristine SWCNTs, FITC-PEG and FITC-PEG-SWCNT. The absorbance peaks of FITC-PEG-SWCNT at 250 nm and 550 nm corresponds to the characteristic peaks of SWCNT and FITC-PEG, respectively.

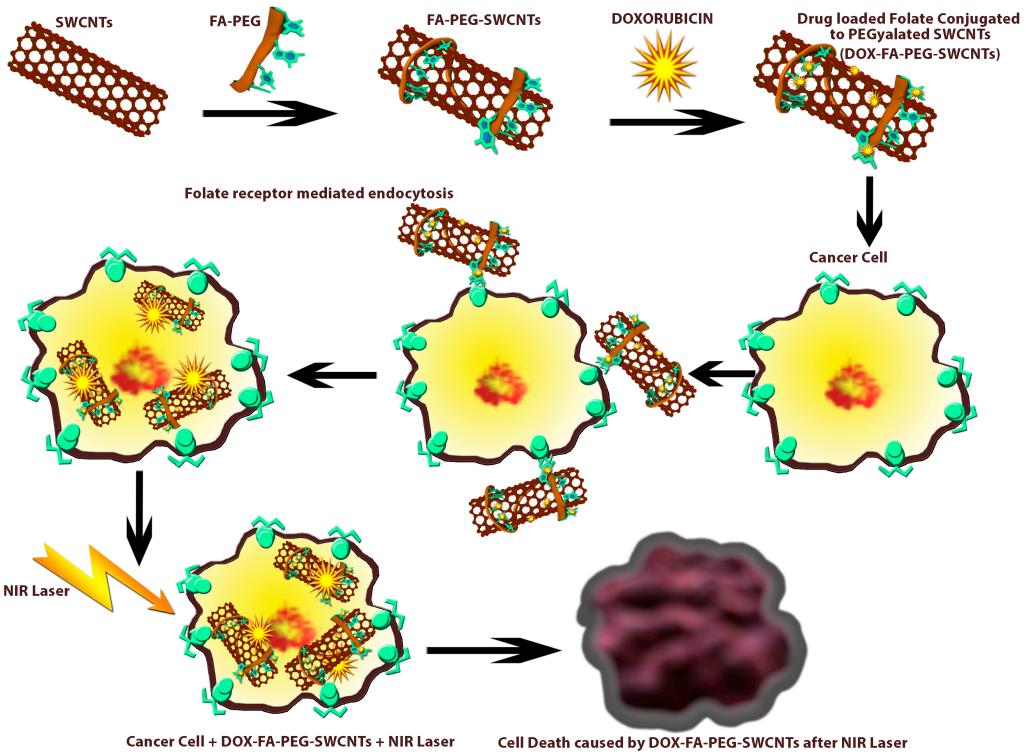

Figure 1. Schematic representation of an NDDS based on SWCNTs, biofunctionalized with PEG, conjugated with FA and loaded with DOX along with photothermal therapy for selective killing of tumor cells.

a **b** **c**

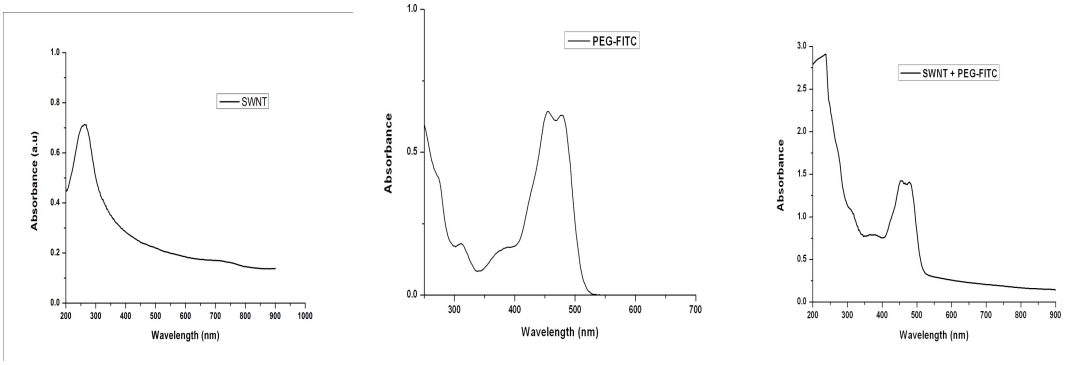

Figure 2. UV-Vis spectra of (a) Pristine SWCNT (b) FITC-PEG (c) FITC-PEG-SWCNT.

Temperature measurement during NIR radiation

To detect the effects of 800 nm optical excitation of SWCNTs, we carried out two different sets of control experiments. First set was carried out by irradiating DMEM without and with SWCNTs, ex vitro. Three different nanotube concentrations (0.1, 0.5 and 1 mg/mL) were selected. We observed that irradiation of DMEM without SWCNTs caused temperature increase from 20.1 to 20.5°C. However, DMEM with SWCNTs at 0.1, 0.5 and 1 mg/mL concentrations irradiated by 0.5-1 W/cm^2, 800 nm laser for 3min caused the temperature to elevate from 21.4 to 45.3°C, 21.5 to 69.2°C and 21.1 to 85.7°C, respectively (Figure 3a). In the second set of experiment, MCF7 cancer cells were seeded at a density of 1.6 X 10^4 cell/mL in 35 mm petri dishes. After 24 h of growth, MCF7 cells without SWCNTs and MCF7 cells with FITC-PEG-SWCNT and FITC-FA-PEG-SWCNT at a concentration of 0.1 mg/mL were added to the cells and again incubated for 3 h, rinsed with PBS to remove the unbound SWCNTs, and followed by irradiation with a 800 nm laser for 3min. We observed a temperature increase from 20.6 to 20.8°C for MCF7 cells without SWCNTs, whereas temperature elevation from 21.3 to 26°C and 21 to 45.1°C for MCF7 cells with FITC-PEG-SWCNT and with FITC-FA-PEG-SWCNT, respectively, were noted (Figure 3b). These findings clearly demonstrated the strong light-heat transfer characteristics of the FITC-FA-PEG-SWCNT by 800 nm light. Also, the heating efficiency of FITC-FA-PEG-SWCNT relies strongly on time and dose, indicating that with increasing concentration and time, the temperature was significantly higher.

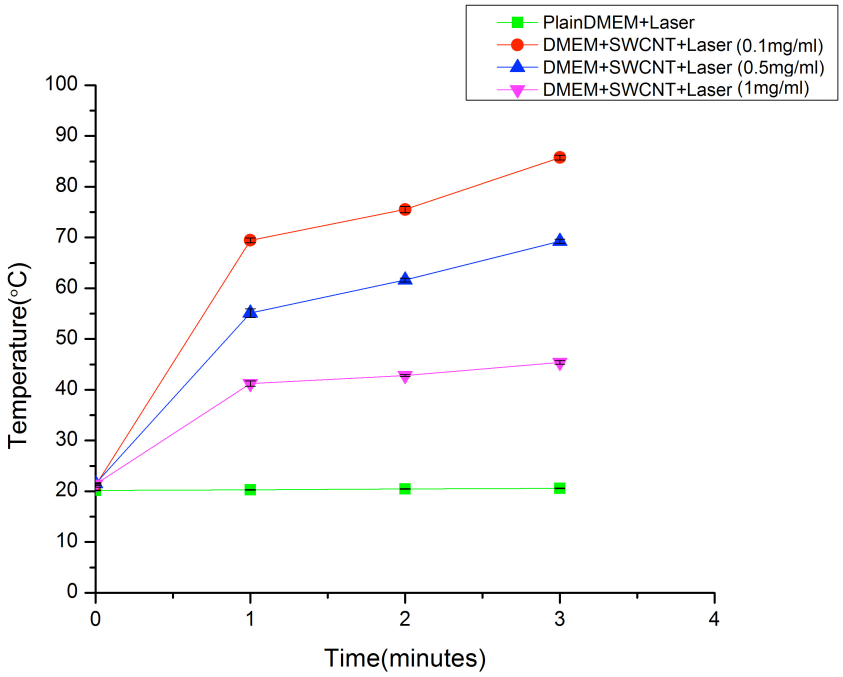

Figure 3a. Plots of temperature increase for suspensions of SWCNTs at various concentrations as a function of irradiation time using laser at 0.5-1 W/cm^2 for 3 min.

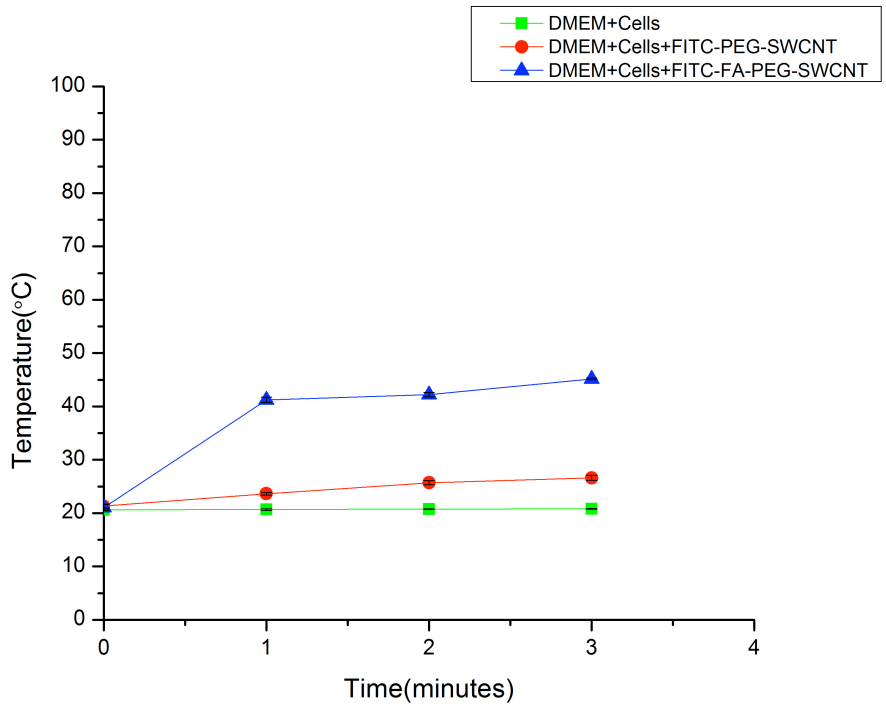

Figure 3b. In vitro temperature measurements using SWCNTs at a concentration of 0.1 mg/mL incubated with MCF7 cells during irradiation by an 800-nm laser at 0.5-1 W/cm^2 for 3 min.

Selective internalization of SWCNTs into cancer cells

Receptor mediated endocytosis is the most common pathway of endocytosis.[61, 62] It provides a means for the selective and efficient uptake of particles that may be present in the extracellular medium. Receptors are present on the cells for the uptake of different types of ligands like plasma proteins, enzymes, hormones and growth factors.[63] Here we investigate the uptake of folate-conjugated nanotubes into MCF7 cells that overexpresses folate receptors on the surface of cell membrane. The selective internalization and uptake of SWCNTs into cancer cells were recorded by confocal imaging to determine the intracellular fate of the nanotubes. Time-dependent cellular uptake of the nanotubes was studied for 1 h, 3 h and 5 h incubation periods (Figure 4a- f). After incubating the cells with DOX-FA-PEG-SWCNT for 1 h, the SWCNTs were initially seen attached to the plasma membrane of the cells, also the fluorescence intensity was very low. After 3 h of incubation, strong fluorescence was observed in the cytoplasm, indicating the entry of SWCNTs into cells. After 5 h, confocal images revealed decreased fluorescence inside cells, corresponding to the redistribution and discharge of SWCNTs out of the cells.[62] No fluorescence was observed in the nucleus for all cells, indicating the lack of SWCNTs translocating into the nucleus. The selective uptake of DOX-PEG-FA-SWCNT inside cancer cells clearly indicates that the folate receptor mediated endocytosis is more selective and efficient than the nonspecific endocytosis.

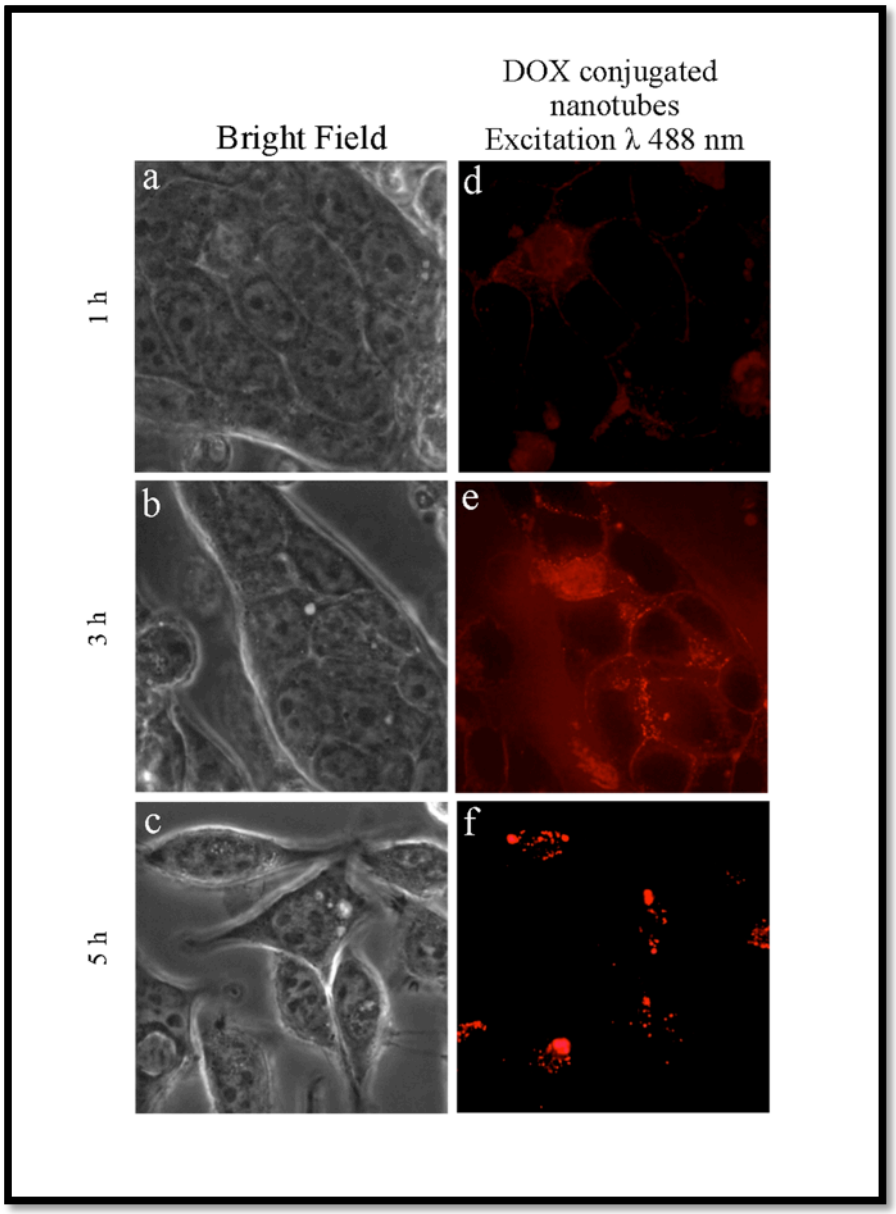

Figure 4. Confocal images of MCF7 cells treated with DOX-FA-PEG-SWCNTs at different incubation time intervals. (a, b, c) are bright field images of MCF7 cells and (d, e, f) are fluorescence images of MCF7 cells treated with DOX-FA-PEG-SWCNTs for 1, 3 and 5 h.

Cancer destruction using the NIR effect of SWCNTs

We have investigated the effects of SWCNTs on cancer cells during NIR laser treatment. After achieving confluence, MCF7 cells were incubated with FITC-PEG-

SWCNT and FITC-FA-PEG-SWCNT for 3 h, followed by irradiation with an 800 nm laser for 3 min. Figure 5 a- c shows the confocal images of MCF7 cells treated with FITC-PEG-SWCNT before and after laser irradiation. The images showed that the cells survived even after 3 min laser exposure, these results can be attributed to the low uptake of FITC-PEG-SWCNT into the MCF7 cells. From the confocal images of cancer cells with FITC-FA-PEG-SWCNT uptake before and after laser treatment, as shown in Figure 6 a- c, we could easily observe the breaking of cancer cells due to the hyperthermia effects in FITC-FA-PEG-SWCNT treated cells under laser excitation. Before laser treatment, the MCF7 cells have a clear dividing line between the nucleus and the cytoplasm, and the cells remain essentially intact. The SWCNTs mainly localize in cytoplasm, as evidenced by the presence of green fluorescence in cytoplasm. After the laser treatment, it is difficult to distinguish between the cytoplasm and nucleus since all cancer cells show distorted morphology of cells undergoing apoptosis. Also, green fluorescence in the cells undergoing apoptosis can been seen inside whole cells, thus indicating the damage of nuclear envelope caused by the hyperthermia effect of SWCNTs under laser irradiation. These results clearly state the high selectivity of FITC-FA-PEG-SWCNT on the NIR destruction of cancer cells. The selective destruction of cancer cells was further analyzed by Alamar blue assay. The studies were carried out in three sets (a) cancer cells + laser, (b) cancer cells + FITC-PEG-SWCNT + laser and, (c) cancer cells + FITC-FA-PEG-SWCNT + laser. Untreated cells were used as controls. All cells were irradiated with an 800 nm laser for 3 mins. The experiments were carried out for a time interval of 6 h, 12 h and 24 h. We observed that the cell viability of FITC-FA-PEG-SWCNT with laser treatment was 54, 27 and 5% at 6 h, 12 h and 24 h, respectively, when treated with a concentration of 0.1 mg/mL (Figure 7). The rate of viability of cells with only laser

treatment remained high, showing no obvious difference from the control group, indicating the NIR property of the laser where biological tissues are highly transparent. In case of cells treated with FITC-PEG-SWCNT, a high cell viability rate was observed. However the cell viability was drastically decreased in FITC-FA-PEG-SWCNT treated cells.

We also studied the combined cytotoxic effect of laser and DOX loaded SWCNTs. When the MCF7 cells were treated with DOX-FA-PEG-SWCNTs in the presence of laser irradiation for 3 min, the cell viability was reduced significantly. The confocal images clearly show apoptosis in the cancer cells treated with DOX-FA-PEG-SWCNTs after 3min laser exposure (Figure 8 a- c). The reason for this may be that the cell tolerance drops dramatically at a certain temperature during heat treatment.[58] Also, laser treatment application might have triggered the release of drug from the DOX-PEG-FA-SWCNTs, resulting in increased cell death. The cytotoxic effect of DOX-PEG-FA-SWCNTs in combination with laser on MCF7 cells was further analyzed by Alamar blue assay (Figure 9). From the results shown in Table 1, significant reduction in cell viability was observed, and the cell viability was 37%, 11% and 2% for 6 h, 12 h and 24 h, respectively. The inhibition rate of the cells under this mode was greater when compared to that of the cells treated with DOX free SWCNTs under laser. These results show that SWCNTs has a significant photothermal effect, and when combined with chemotherapy, it is ideal for cancer treatment, without causing toxicity to normal cells.

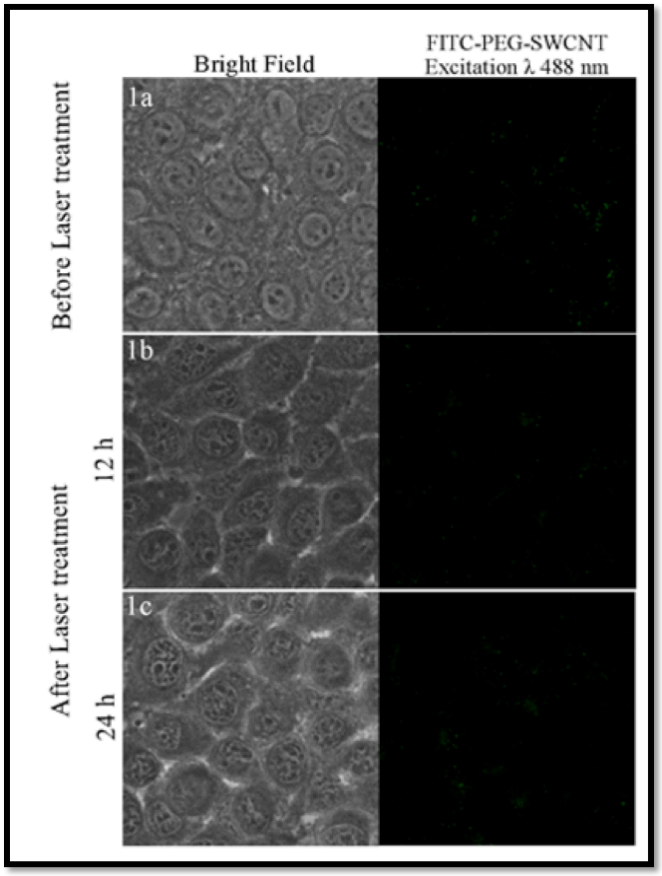

Figure 5. Confocal images of cancer cells (MCF7) treated with FITC-PEG-SWCNT (a) before laser treatment, (b) after 3 min laser treatment and viewed after 12 h, (c) confocal image viewed after 24 h.

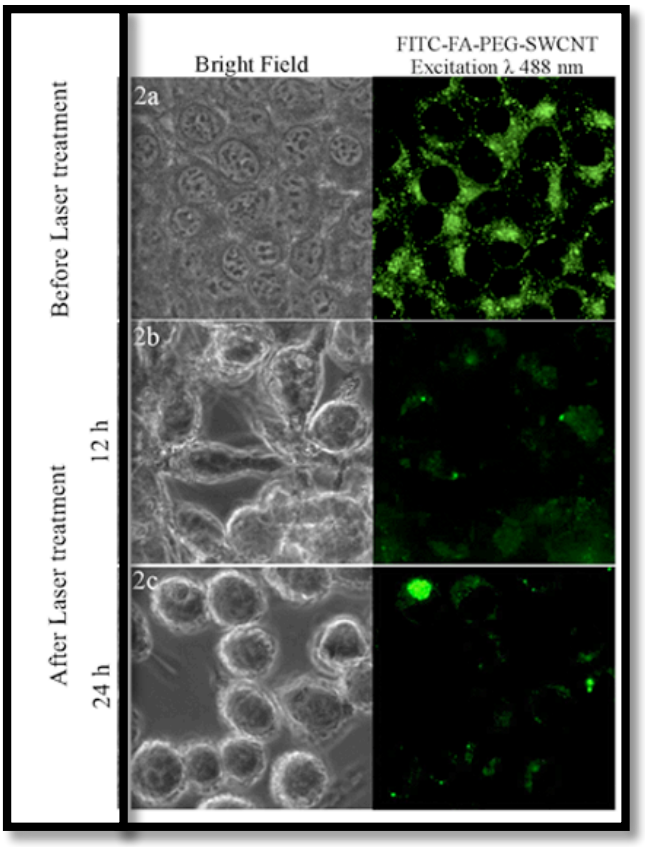

Figure 6. Targeted destruction of cancer cells by SWCNTs photothermal effect. Confocal images of cancer cells (MCF7) treated with FITC-FA-PEG-SWCNT (a) before laser treatment, (b) after 3 min laser treatment and viewed after 12 h. (c) confocal image viewed after 24 h.

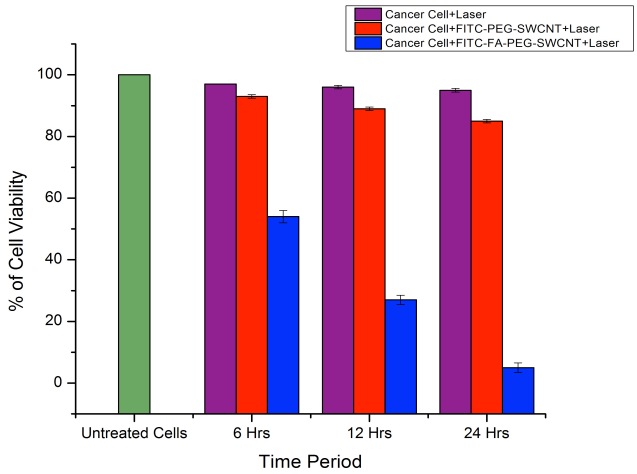

Figure 7. Results of cytotoxicity assay of FITC-PEG-SWCNT and FITC-FA-PEG-SWCNT after 3 min laser irradiation by an 800 nm laser on MCF7 cells.

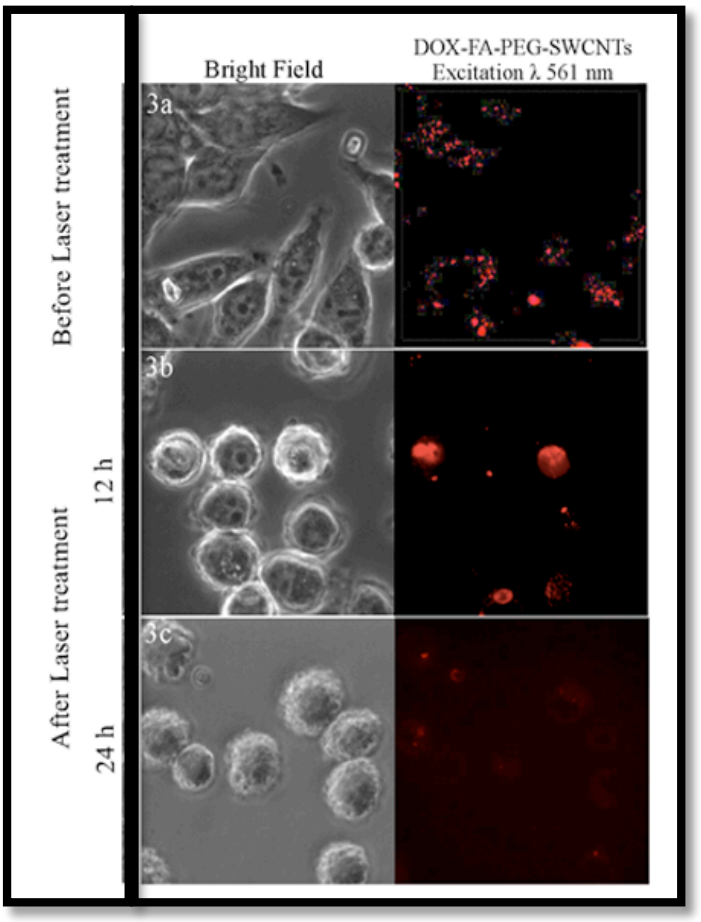

Figure 8. Targeted destruction of cancer cells by the photothermal effect of SWCNTs. Confocal images of cancer cells (MCF7) treated with DOX-FA-PEG-SWCNT (a) before laser treatment, (b) confocal image after 3 min laser treatment and viewed after 12 h (c) confocal image after 3 min laser treatment and viewed after 24 h.

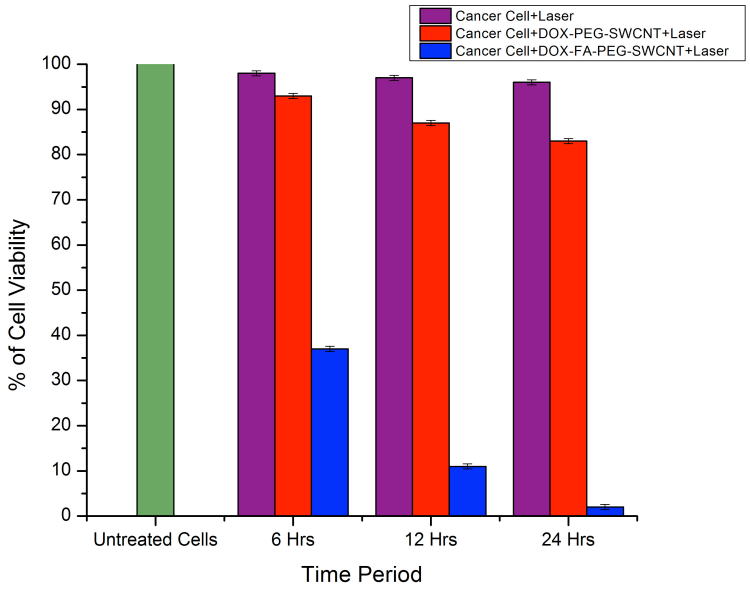

Figure 9. Results of cytotoxicity assay of DOX-PEG-SWCNT and DOX-FA-PEG-SWCNT after 3 min laser irradiation by an 800 nm laser on MCF7 cells.

Sample/Time	6h	12h	24h
Cancer cell + FITC-PEG-SWCNT + Laser	93%	89%	85%
Cancer cell + FITC-FA-PEG-SWCNT + Laser	54%	27%	05%
Cancer cell + DOX-PEG-SWCNT + Laser	93%	87%	83%
Cancer cell + DOX-FA-PEG-SWCNT + Laser	37%	11%	02%

Table 1. Results of Cytotoxicity Assay representing the percentage of cell viability of cancer cells treated with various modified SWCNTs at a concentration of 0.1 mg/mL after laser irradiation by an 800 nm laser at 0.5-1 W/cm^2 for 3 min and studied up to 24 h.

Conclusion

An ideal NDDS against cancer is expected to enter and destroy cancer cells while minimizing the side effects to normal tissues. Our results show that FA functionalized SWCNTs could be selectively internalized into cancer cells via a folate-folate receptor mediated pathway, without internalization into normal cells. Along with this obtained system (DOX-FA-PEG-SWCNT), we further demonstrate a photothermal technique for targeted cancer destruction by using the photothermal effect of SWCNTs. SWCNTs has a high optical absorbance in the NIR region, where biological tissues are highly transparent. From the observation of our data, it is clear that SWCNTs act efficiently to convert laser energy into heat after exposure to 800 nm laser irradiation in vitro. This advantage was used in selective photothermal therapy, for killing only cancer cells while sparing normal cells. Our results also showed that both, concentration of SWCNTs and time of laser, are controlling factors for thermally induced cytotoxicity. Also, the combined effect of targeted drug loaded DOX-FA-PEG-SWCNT with photothermal therapy was studied and we observed that the combined effect synergistically killed almost 95% of cancer cells at an accelerated rate. We conclude that this nanoscale drug delivery system is more selective and effective than the free drug, and results in enhanced therapeutic effects, when combined with photothermal therapy and reduced general toxicity. Considering these promising in vitro drug delivery results, the application of DOX-FA-PEG-SWCNT combined with NIR laser could be extended to enhance the efficiency of cancer therapy in the near future.

References

1. HL Wong, R Bendayan, AM Rauth, Y Li, XY Wu. Advanced Drug Delivery Reviews. (2007) 59, 491-504.

2. D Depan, J Shah, RDK Misra, J Shah. Materials science and engineering. (2011) C 3,1305-1312.

3. Z Ji, G Lin, Q Lu, et al. J Colloid Interface Science. (2012) 365,143-9.

4. F Alexis, JW Rhee, JP Richie, et al. Urology Oncology Seminars. O. I. (2008) 26, 74.

5. E Ando, R Kuromatsu, M Tanaka, et al. Journal of clinical gastroenterology. (2006) 40, 942-948.

6. S Jaracz, J Chen, LV Kuznetsova, I Ojima. Bioorganic and Medicinal Chemistry. (2005) 13, 5043-5054.

7. M Christoph, CD Drummond, ON Charles, et al. Cancer Research. (2005) 65, 11631-11638.

8. X Chen, X Wang, Y Wang, et al. Journal of Control Release. (2010) 145, 17-25.

9. X Wang, L Yang, M Zhuo, et al. Cancer Journal of Clinicians. (2008) 58, 97-110.

10. SD Weitman, RH Lark, LR Coney, et al. Cancer Research. (1992) 52, 3396-3401

11. AC Antony. Annual Review of Nutrition. (1996) 16, 501–521.

12. LU Yingjuan, S Philip. Advance Drug Delivery Reviews. (2002) 54, 675-693.

13. KM Maziarz, HL Monaco, F Shen, et al. Journal of Biological Chemistry. (1999) 274, 11086–11091.

14. D Peer, JM Karp, S Hong, et al. Nature Nanotechnology. (2007) 2, 751-60.

15. SM Moghimi, AC Hunter, JC Murray. The Journal of the Federation of American Socities for Experimental Biology. (2005) 19, 311-30.

16. M Youns, JD Hoheisel, T Efferth. Current Drug Targets. (2011) 12, 357-365.

17. NWS Kam, M O'Connell, JA Wisdom, HJ Dai. Proceedings of the National Academy of Sciences. (2005) 102, 11600.

18. N Shao, S Lu, E Wickstrom, B Panchapakesan. Nanotechnology. (2007) 18.

19. K Kostarelos, A Bianco, M Prato. Nature Nanotechnology. (2009) 4, 627–633.

20. PA Tran, L Zhang, TJ Webster. Advance Drug Delivery Reviews. (2009) 61, 1097-1114.

21. W Yang, P Thordarson, J Gooding, et al. Nanotechnology. (2007) 18 412001, 1-

22. L Lacerda, A Bianco, M Prato, K Kostarelos. Journal of Material Chemistry. (2008) 18, 17-22.

23. Z Liu, M Winters, M Holodniy, H Dai. Angewandte Chemie International Edition England. (2007) 46, 2023-7.

24. NWS Kam, TC Jessop, PA Wender, H Dai. Journal of American Chemical Society. (2004) 126, 6850-6851.

25. SF Chin, RH Baughman, AB Dalton, et al. Experimental Biology and Medicine. (2007) 232, 1236-44.

26. NW Kam, H Dai. Journal of American Chemical Society. (2005) 127, 6021-6.

27. L Zhuang, T Scott, W Kevin, H Dai. Nano Research. (2009) 2, 85-120.

28. R Singh, JW Lillard. Experimental and Molecular Pathology. (2009) 86, 215-223.

29. Z Liu, X Sun, N Nakayama-Ratchford, H Dai. ACS Nano. (2007) 1, 50–56.

30. J Chen, S Chen, X Zhao, et al. Journal of American Chemical Society. (2008) 130, 16778-85.

31. ML Schipper, N Nakayama-Ratchford, CR Davis, et al. Nature Nanotechnology. (2008) 3, 216 - 221

32. G Pastorin, W Wu, S Wieckowski, JP Briand, et al. Chemical Communications. (2006) 1182-4.

33. SJ Tans, MH Devoret, HJ Dai, et al. Nature. (1997) 386, 474–477.

34. Z Liu, C Davis, W Cai, et al. Proceedings of the National Academy of Science. (2008) 105,1410–1415.

35. HK Moon, SH Lee, HC Choi. ACS Nano. (2009) 3, 3707–3713.

36. K Welsher, Z Liu, SP Sherlock, H Dai, et al. Nature Nanotechnology. (2009) 4, 773–780.

37. Z Liu, S Tabakman, S Sherlock, H Dai. Nano Research. 2010; 3: 222–223.

38. Z Liu, R Peng, European Journal of Nuclear Medicine and Molecular Imaging. (2010) 37, 147–163.

39. S Ghosh, S Dutta, E Gomes, et al. ACS Nano. (2009) 3 2667–2673.

40. B Kang, DC Yu, YD Dai, et al. Small. (2009) 5, 1292–1301.

41. AD Zerda, C Zavaleta, S Keren, H Dai, SS Gambhir, Nature Nanotechnology. (2008) 3, 557–562.

42. LZ Xiang, Y Yuan, D Xing, et al. Journal of Biomedical Optics. (2009) 14.

43. K Welsher, Z Liu, H.Dai. Nano Letters. (2008) 8, 586–590.

44. MJ O'Connell, SM Bachilo, CB Huffman, RE Smalley. Science. (2002) 297, 593–596.

45. Z Amin, JJ Donald, A Masters. Radiology Easton, (1993) 187, 339-347.

46. LJ Anghileri, J Robert. CRC Press Boca Raton, FL (1986).

47. XH Huang, IH EL Sayed, W Qian, MA EL Sayed. Nano Letters. (2007) 7,1591.

48. NWS Kam, ZA Liu, HJ Dai, Angewandte Chemie International Edition. (2006) 45, 577.

49. MA Mamon, ME Itkis, S Niyogi, et al. Journal of American Chemical Society. (2001) 123, 11292-11293.

50. H Elnakat, M Ratnam, Frontiers in Bioscience. (2006) 11, 506-519.

51. G Minotti, P Menna, E Salvatorelli, et al. Pharmacological reviews. (2004) 56, 185-229.

52. KE Reinert. Nucleic acids research. (1983) 11, 10, 3411-3430.

53. WD Meriwether, NR Bachur. Cancer research. (1972) 32, 6, 1137-1142.

54. Mathias CJ, Wang S, Lee RJ. et al. J.Nucl.Med. (1996) 37, 1003-8.

55. HS Yoo, TG Park. Journal of Controlled Release. (2004) 100, 247-256.

56. H Huang, Q Yuan, JS Shah. et al. Advanced Drug Delivery Reviews. (2011) 63, 1332-1339.

57. V Srivani, CP Aby, MM Sheikh. et al. small. (2012) 1-14.

58. S Balasubramanian, GA Ravindran, N Yutaka. et al. Langmuir. 2012.

59. NR Nozomi, B Sarunya, S Xiaoming. et al. J AM CHEM SOC, (2007) 129, 9, 2448-2449.

60. W Lei, Z Mingyue, Z Nan. et al. International Journal of Nanomedicine. (2011) 6, 2641-2652.

61. RD Singh, V Puri, JT Valiyaveettil. Mol. Biol. Cell. (2003) 14, 3254.

62. K Bin, Y Decai, D Yaodong. et al. small. (2009) 11, 1292-1301.

63. RD Singh, V Puri, CL Wheatley. et al. Mol. Biol. Cell. (2002) 13, 230.

Chapter 5

Co-delivery of dual drugs using multifunctional carbon nanotubes for cancer therapy

Abstract

The use of single chemotherapeutic drug has shown some limitations in anti-tumor treatment, such as development of high toxicity, drug resistance, and limited regime of clinical uses. The combination of two or more therapeutic drugs is a feasible way to overcome the limitations of current treatment options. Co-delivery strategy has been proposed to minimize the amount of each drug and to achieve the synergistic effect in cancer treatment. Here, we present a dual drug delivery system consisting of PEG modified SWCNT conjugated with FA and loaded with two anticancer drugs doxorubicin (DOX) and paclitaxel (PTX). Independent and combined drug release behaviors of the drugs were studied. In vitro studies were done in MCF7 cells. A faster drug release was found to be associated with lower pH, which is advantageous for tumor targeted anticancer therapy. The nanocarrier containing the combination of anticancer drugs suppressed tumor cells growth more efficiently, demonstrating a highly synergistic anti-proliferative activity in MCF7 breast cancer cells. The effect of this DDS in combination with laser was also analyzed and enhanced destruction of breast cancer cells were observed. This nanocarrier seems to have important potential in clinical applications for co-delivery of multiple anti-tumor drugs with different properties.

Introduction

Currently available technologies have made enormous advancement in cancer research, but an adequate therapy remains elusive.[1] Existing chemotherapeutic drugs have disadvantages like severe undesirable side effects, low bioavailability or development of drug resistance. Overcoming these limitations requires effective delivery of chemotherapeutic drugs to tumor tissues with a minimal side effect to healthy tissues.[2] Over the past few decades, drug delivery systems (DDSs) have been developed and studied in great depth to improve the curative effect of drugs.[3-8] The discovery of carbon nanotubes has opened up new opportunities in the field of nanotechnology and nanoscience.[9-11] The interesting properties of carbon nanotubes, such as stability, inertness, and higher surface area-to-volume ratio suggest the potential utility of these materials as carriers in drug delivery systems requiring higher loadings of therapeutic agents.[12-14] The application of carbon nanotubes in drug delivery systems was apparent immediately after the first demonstration of the capacity of these materials to penetrate into cells.[15] Several in vitro studies have demonstrated that carbon nanotubes can effectively transport various molecules including drugs, peptides, and proteins into cells.[16-21] Modification of carbon nanotubes through functionalization of their external walls is a key step for biomedical applications because a wide variety of active molecules can be linked to a functionalized carbon nanotube.[22-26] Due to the hydrophilicity of polyethylene glycol (PEG), this polymer is used to functionalize carbon nanotubes in drug delivery systems to prepare stealth nanoparticles which can escape the reticuloendothelial systems.[27] Photothermal therapies for cancer have been widely investigated as a minimally invasive treatment modality in comparison with other methods. [28,29,30] Biological systems are known to be highly transparent in the near-infrared light

(NIR). An intrinsic property of SWCNTs is their strong optical absorbance in the NIR region, which could release significant heat and enhance thermal destruction of cells during NIR laser irradiation. [31-36] A synergistic combination of two drugs as a promising strategy to overcome undesirable toxicity and other side effects that limit the utility of many potential drugs is demonstrated.[37-39] Co- delivery systems, containing different drugs loaded into it can simultaneously deliver the drugs to the tumor cells, and have been proposed to minimize the amount of drug used, while achieving synergistic therapeutic effect in treating cancers.[40, 41] PTX and DOX are drugs with different anticancer mechanisms.[42, 43, 44] DOX is a hydrophilic compound, which binds to DNA by intercalation and induces a series of biochemical events inducing apoptosis in a number of different tumor cells. [45] PTX, a naturally occurring antimitotic agent, is a highly hydrophobic drug, which can inhibit microtubule disassembly and promote the formation of unusually stable microtubules, thereby disrupting normal dynamic reorganization of the microtubule network required for mitosis and cell proliferation, and in turn causing apoptosis. [46] Clinical studies have shown that the incorporation of DOX and PTX increases tumor regression rates relative to the individual drugs and has been used as a first-line treatment for metastatic breast cancer. [42]

In this report, a targeted drug delivery system for cancer chemotherapy based on single walled carbon nanotubes functionalized with PEG (SWCNT-PEG) and conjugated to folate as a targeting moiety and loaded with the commonly used potent chemotherapy drugs, (PTX) and DOX, to produce a DOX-PTX-FA-PEG-SWCNT conjugate was developed. Here, a co-delivery strategy has been proposed to minimize the amount of each drug and to achieve the synergistic effect for breast cancer therapy. Studies on drug release and cellular uptake of the co-delivery system

demonstrated that both drugs were effectively taken up by the breast cancer cells and suppressed tumor cells growth more efficiently than the individual delivery of either DOX or PTX at the same concentrations, indicating a synergistic effect. SWCNTs have a strong optical absorbance in the near-infrared (NIR) region. These optical properties of SWCNTs provide an opportunity for selective photothermal ablation for cancer treatment. In our in vitro experiments, laser effect was combined with DOX-PTX-FA-PEG-SWCNT conjugates and an enhanced killing of breast cancer cells was observed.

Experimental details

Paclitaxel and Doxorubicin Hydrochloride were obtained from Wako Chemicals (Osaka, Japan). The SWCNTs (length 0.5-100 μm, diameter of 1-2 nm), DSPE-PEG_{2000}-NH_2-FA (1,2-distearoyl-sn-glycero-3-phosphoethanolamine-N-(polyethylene glycol-2000) folate) were obtained from Sigma Aldrich, Japan. Concentrated acids and all other reagents used were supplied from Fisher Scientific (Fairlawn, NJ). Cell cultures chemicals - Lyso-tracker, Trypan Blue, Trypsin (0.25%), Dulbecco's modified Eagle's medium (DMEM) and fetal bovine serum (FBS) was purchased from Sigma-Aldrich, USA and Gibco, Japan. Invitrogen, USA, supplied Alamar Blue stain. All chemicals used for this work were of reagent grade.

Purification of SWCNTs

Purification of SWCNTs was carried out according to an already reported procedure[47]. The SWCNTs (30 mg) were added to a solution containing 96% H_2SO_4 and 70% HNO_3 (3:1, V/V; 120 mL) and subjected to sonication at 0˚C for 24 h. Then extensive washing of the SWCNTs with deionized water was carried out and filtered through a microporous filtration membrane (0.22 μm). After filtration, they were

redispersed in HNO_3 (2.6 M, 200 mL) and refluxed for 24 h, and collected by filtration and washed with ultrapure water to neutrality. The obtained product was then dried at 50°C for 24 h.

Preparation of PEGylated SWCNTs

Purified SWCNT (0.2 mg) was sonicated in (0.10 mL) of dimethyl formamide (DMF) for 2 h to give a homogenous suspension. Oxalyl chloride (0.008 mL) was added drop wise to the purified SWCNT suspension at 0˚C under N_2 atmosphere. The mixture was stirred at 0˚C for 2 h and then at room temperature for another 2 h. Finally, the temperature was raised to 70˚C and the mixture was stirred overnight on a magnetic stirrer to remove excess oxalyl chloride. Folate conjugated PEG (FA-PEG) dispersed in chloroform and methanol was used for bio-conjugation. FA-PEG (0.2 mM) was added to the SWCNT suspension and the mixture was stirred at 100˚C for 5 days. After it was cooled to room temperature, the mixture was filtered through a 0.2 μm pore-size membrane and washed thoroughly with ethyl alcohol and deionized water DI water. The PEGylated SWCNTs were collected on the membrane and dried overnight under vacuum[48].

Formulation of drug loaded PEGylated SWCNTs

SWNTs (300 nmol/L, 0.05 mg/mL) with PEG-NH2 functionalization were reacted with 0.3 mmol/L of the modified PTX (dissolved in DMSO) in the presence of 5 mmol/L 1-ethyl-3-(3-dimethylaminopropyl) carbodiimide hydrochloride (EDC) and 5 mmol/L N-hydroxysulfo- succinimide (Sulfo-NHS). The solution was supplemented with PBS (Phosphate buffered saline) at pH 7.4. After 6 h reaction, the resulting SWCNT-PTX was purified to remove unconjugated PTX by filtration through 5 kDa molecular weight cut off filters and followed by extensive washing.[49]

DOX loaded PEGylated nanotubes were prepared for anticancer treatment. The drug loading efficiency and its release profile from the PEGylated nanotubes were studied. Dox hydrochloride (15 mg) was stirred with the PEGylated nanotubes (5 mg) dispersed in a PBS buffered solution of pH 7.4 (10 mL) and stirred for 16 h at room temperature in dark condition to synthesize the targeted drug delivery system (DOX-FA-PEG-SWCNTs). Unbound excess DOX was removed by repeated centrifugation and washing with water until the filtrate was no longer red (red color corresponds to free DOX). Then, the resulting DOX-FA-PEG-SWCNT complexes were finally centrifuged at 12,000 rpm for 10 min, the supernatant was decanted and the DOX-FA-PEG-SWCNT complexes were freeze dried[50].

Particle characterization studies

Particle morphology of pristine and purified SWCNTs was characterized using field emission transmission electron microscope (TEM)(JEM 2200 FS, JEOL, Japan). One drop of nanotube suspension was placed on carbon coated copper grid after hydrophilizing the grid for 30 seconds in TEM grid hydrophilizer (JEOL DATUM, HDT-400) and dried thoroughly. The prepared product was analyzed under TEM, and tubular nature of the SWNTs was observed. The shape and surface morphology of both pristine and purified nanotubes were analyzed using a high-resolution scanning electron microscope (SEM) (JSM-7400F, JEOL, Japan) at an accelerating voltage of 3-5 kV. For atomic force microscopy (AFM) (Asylum Research, MFP-3D-CF AFM), the sample was deposited on a glass surface and vacuum dried. The sample was characterized under tapping mode. The presence of FA-PEG on FA-PEG-SWCNT was confirmed from the surface chemistry analyzed by X-ray photoelectron spectroscopy (XPS) (AXIS His-165 Ultra, Kratos Analytical, Shimadzu Corporation, Japan). Five microliters of the sample was applied on a clean silicon substrate and

dried in vacuum. The zeta potential (Zetasizer Nano, Malvern Instruments Ltd) of pristine SWCNT, purified SWCNT and PEGylated SWCNT was studied to understand the change in their surface potential due to bio functionalization. The PTX and DOX conjugation to the PEGylated SWCNTs was determined by UV/Vis absorption spectrophotometry (Shimadzu UV-3100).

Drug loading and in vitro release studies

Initially, a standard curve was plotted using a series of standard paclitaxel and doxorubicin solutions in PBS, to facilitate the determination of the exact amount of the drugs loaded onto the nanotubes. The amount of drug (paclitaxel and doxorubicin) loaded onto the nanotubes was quantified spectrophotometrically with the help of UV/ Vis absorption spectrometer at an absorbance of 227 nm for paclitaxel and at 490 nm for doxorubicin.[51, 52, 53] 100 µL of the drug-loaded samples were drawn before and after centrifugation, to calculate the amount of DOX loaded onto the nanotubes and the loading efficiency of the drug used. The following formulae were used for the calculations:

$$\text{Amount of drug loaded} = \text{Total amount of drug used} - \text{the amount of drug in the supernatant} \quad (1)$$

$$\text{Drug loading efficiency}(\%) = \frac{A_{total\ drug} - A_{free\ drug}}{A_{total\ drug}} \times 100 \quad (2)$$

Where, A total drug is the initial drug concentration and A free drug is the free drug concentration in the supernatant.

Later, the in vitro drug release profile of PTX from PTX-PEG-SWCNT, DOX from DOX-PEG-SWNT, and PTX and DOX from PTX-DOX-PEG-SWCNT conjugates,

were studied at the physiological temperature of 37°C and pH of 7.4, and 4.0 in PBS. Drug loaded particles (1 mg) were dissolved in PBS (5 ml) and maintained at 37°C under continuous shaking at 100 rpm for 3 days. At particular time intervals, 1 mL of the sample in buffer was taken, centrifuged and the concentration of released PTX and DOX in the supernatant was estimated by UV/Vis spectrophotometer at 227 nm and 490 nm, respectively. An equal volume of fresh PBS was replaced in the above suspension to maintain the sink conditions. All experiments were performed in triplicates.

Cell culture studies

Breast adenocarcinoma cells (MCF7) and mouse connective tissue (L929) fibroblast cells were procured from RIKEN Bioresource Center, Japan. Breast cancer cell lines (MCF7) and mouse fibroblast cell lines (L929) were cultured in T25 flasks and maintained separately in monolayers to 80% confluency in DMEM, supplemented with 10% FBS and 1% penicillin-streptomycin solution in a 5% CO_2 humidified atmosphere at 37 °C. For use in experiments, the respective cells were trypsinized, counted and loaded onto their respective plates for testing. Cells were seeded into 96 well plates for cytotoxic studies and in 33 mm glass base dish for confocal studies. For cytotoxicity studies, 5000 cells per well were seeded and grown for 24 h and for confocal studies, 30,000 cells per glass base dish were plated also grown for 24h before treating them with the modified nanotubes.

Cellular imaging studies

The internalization of PTX-DOX-FA-PEG-SWCNT and PTX-DOX-PEG-SWCNT with cancer MCF7 and control L929 cells was investigated by confocal laser scanning microscopy (CLSM). MCF7 and L929 cells were seeded in a 35 mm glass based dish at a density of 1.6 X 10^4 cells/mL. The plates were incubated at 37°C and grown to

70% confluency. PTX-DOX-FA-PEG-SWCNT and PTX-DOX-PEG-SWCNT at concentration of 0.1 mg/mL were added to the cells and again incubated for 3 h, rinsed with PBS, and stained with Lysotracker as per the instructions of the manufacturer, to mark the location of lysosomes. Nanotubes gain entry into the cells by means of endosome-mediated transport. The cells were again washed and placed in fresh cell medium, viewed and imaged.

In vitro cell viability studies

The cell viability of PTX-FA-PEG-SWCNT, DOX-FA-PEG-SWCNT and PTX-DOX-FA-PEG-SWCNT in comparison with free PTX and free DOX were studied by means of Alamar Blue assay. MCF7 cells were exposed to three different concentrations (0.1, 0.5 and 1.0 mg/mL) of the above five samples for 72 h. Experiments were conducted in triplicates. The alamar blue assay evaluates the proliferation and metabolic activity of cells. In living cells, the mitochondrial reductase enzymes are active and reduce Alamar blue to form a different colored product form the blue dye. This reducing ability of the cells explains the active metabolism that takes place within the cells. When the samples added to the cells are toxic in nature, the reducing ability of the cells to reduce the dye decreases. The fluorescence intensity of Alamar blue assay was quantified at 590-620 nm to determine the cell viability.

The percentage of cell viability was calculated using the following formula:

$$\% \text{ of cell viability} = \frac{A \text{ sample}}{A \text{ control}} \times 100$$

where, $A\,\text{sample}$ is the absorbance of the sample used and $A\,\text{control}$ is the absorbance of control sample used.

Cancer destruction using the NIR effect of SWCNTs

In this study, the combined destructive effect of dual drug delivery system (PTX-DOX-FA-PEG-SWCNT) along with the effects of laser was also studied. SWCNTs can act efficiently to convert the 800 nm laser energy into heat to destroy target cells. The effect of NIR laser was studied using MCF7 cancer cell lines. Untreated cells were used as controls. Cells were seeded at a density of 1.6 X 10^4 cell/mL in 35 mm petri dishes. After 24 h of growth, MCF7 cells, with PTX-DOX-FA-PEG-SWCNT at concentration of 0.1 mg/mL were added to the cells and again incubated for 3 h, rinsed with PBS, and stained with Lysotracker as per the instructions of the manufacturer, to mark the location of lysosomes. The cells were again washed and placed in fresh cell medium and irradiated by 800 nm laser at 0.5-1 W/cm^2 for 3 min. All the experiments were conducted at room temperature. The cells were viewed under a confocal microscope before and after laser treatment using a 100X oil objective and 488/561 nm excitations.

Cytotoxicity assays of nanotubes under laser irradiation in vitro studies

The in vitro cytotoxicity profile of the MCF7 cells with PTX-DOX-FA-PEG-SWCNT after laser irradiation was studied using Alamar Blue assay. MCF7 cells were exposed to concentration of 0.1 mg/mL for the above sample for 72 h duration. Untreated cells were used as controls. Experiments were conducted in triplicates. The fluorescence intensity of Alamar blue assay was quantified at 590-620 nm.

Results and Discussions

In this chapter, we describe a dual drug delivery system using anticancer drugs paclitaxel and doxorubicin, conjugated to PEGylated SWNTs, was synthesized.

Particle characterization analysis

TEM, SEM and AFM were used for the surface morphology characterization of the purified nanotubes. On TEM and SEM observations, we found that the purified nanotubes were well dispersed and in small bundles as compared to the pristine SWCNTs, which were bundled or aggregated with black metal catalyst and amorphous carbon particles. We also observed a decrease in the concentration of metal particles and amorphous carbon in the purified nanotubes when compared to pristine SWCNTs (Figure 1, 2).

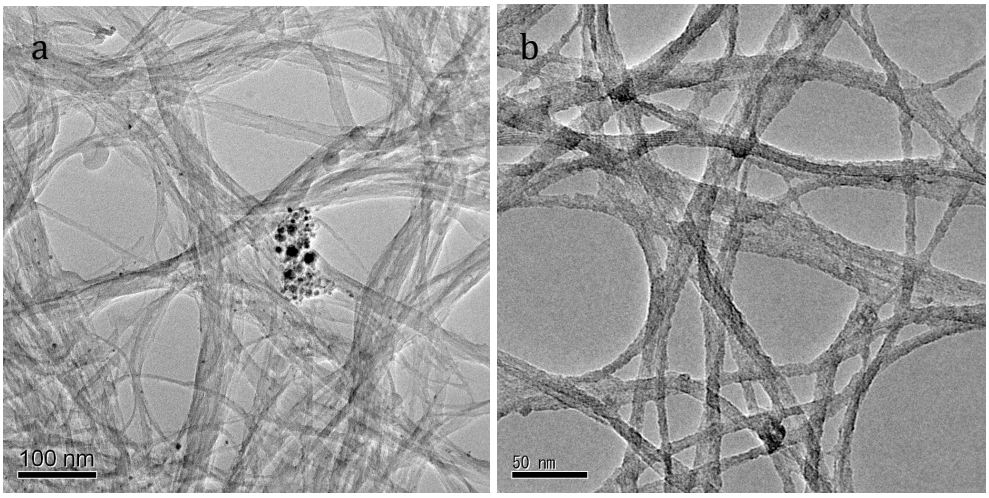

Figure 1. Transmission electron microscopy (TEM) images of (a, b) pristine and (c, d) purified SWCNTs.

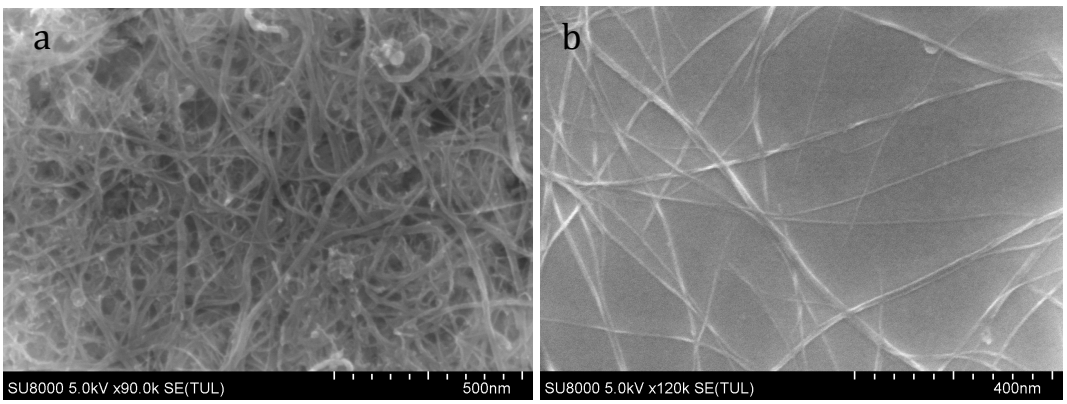

Figure 2. Scanning electron microscopy (SEM) image of (a) pristine and (b) purified SWCNTs.

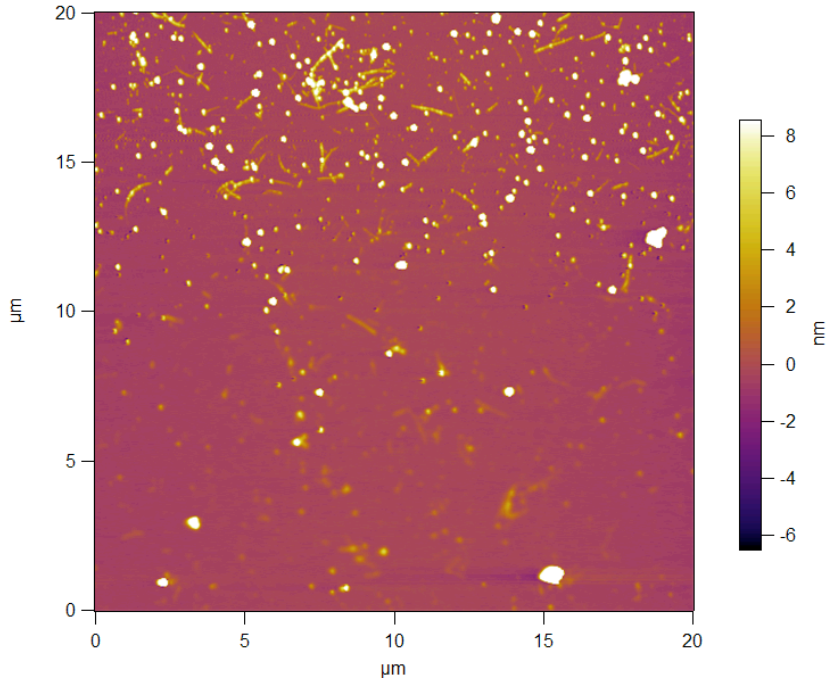

Figure 3. Atomic force microscopy (AFM) image of PEGylated SWCNTs.

AFM was used to analyze the effect of PEGylation on the morphology of SWCNTs. We observed uniformly distributed and well dispersed PEGylated SWCNTs. (Figure 3).

To investigate the uniformity of the PEGylation process, we measured the zeta potential of the pristine, purified and PEGylated nanotubes. The zeta potential measures the potential at the interface between a solid surface and the liquid medium.

Particles	Zeta Potential
Pristine SWCNT	-22.7 mV
Purified SWCNT	-53.6 mV
PEGylated SWCNT	-30.1 mV

Table 1. Zeta potential analysis of pristine, purified and PEGylated SWCNTs

The pristine SWCNT has a zeta potential of (-22.7 mV). The zeta potential has an increase of (-53.6 mV) for purified SWCNTs and this may be due to the existence of many COO^- groups on the sidewalls of SWCNTs. [54] A change in the zeta potential to (-30.1 mV) was observed for PEGylated nanotubes. PEGylated SWCNTs has less negative potential than purified SWCNTs since the PEGylation converts the carboxylic acid groups into esters.[48] Table 1 shows the zeta potential shift for different samples. The shift towards more negative potential for PEGylated SWCNTs clearly proves the proper conjugation of PEG moieties on to the SWCNTs.

Electron Spectroscopy for Chemical Analysis (ESCA) was used to analyze the surface elemental compositions of the oxidized SWCNTs. The attachment of FA-PEG to oxidized SWCNTs was confirmed by nitrogen peak. The wide spectrum obtained clearly shows the peaks corresponding to carbon, oxygen and nitrogen. Nitrogen peak is absent in oxidized SWCNTs and the presence of nitrogen peak in the PEGylated SWCNTs [55] confirms the PEGylation of the oxidized SWCNTs with the PEG (Figure 4).

Drug loading and drug release studies

The amount of drug (PTX and DOX) loaded onto the nanotubes was quantified spectrophotometrically by UV/Vis absorption spectroscopy by obtaining the absorption values of standard drug concentrations and correlating them. The loading efficiency of paclitaxel and doxorubicin was 53% and 59% respectively. The drug release behavior of PTX and DOX from DOX-PTX-FA-PEG-SWCNT was examined at 37°C in PBS at two different pH conditions - 7.4 and 4.0, respectively, with a continuous shaking of 100 rpm for 72 h.

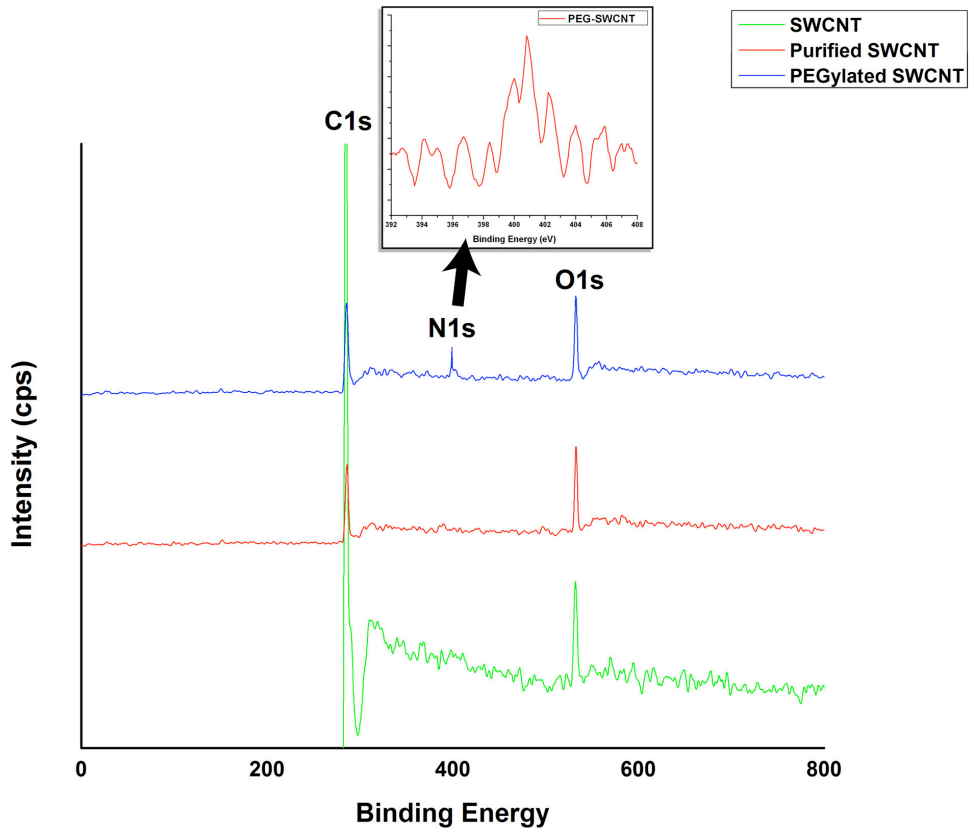

Figure 4. X-ray photoelectron spectroscopy (XPS) peaks of SWCNTs. Inset correspond to N1s signal spectra of PEGylated SWCNTs that has been shown separately outside.

The drug release curves (Figure 5, 6) reveal that the release of both the drugs (PTX and DOX) from the PEGylated nanotubes is markedly influenced by the pH value. When the pH is higher (pH 7.4), the release rate is slower. As the pH value is decreased (pH 4.0), the release rate is accelerated.

The release behavior of PTX from DOX-PTX-FA-PEG-SWCNT at pH 7.4 showed a short-term release behavior in 8 h although the initial release rates were greater between 0 and 8 h, no initial burst of PTX was observed. After 8 h, the release rates were much lower, with very minimal drug release up to 72 h. In case of DOX released from DOX-PTX-FA-PEG-SWCNT under pH 7.4, an initial burst of drug release is

seen in 4 h, followed by a very slow rate of drug release for 6 h and then sustained drug delivery behavior in the following hours with very minimal drug release up to 60 h before reaching the stationary phase. An enhanced drug release profile of PTX was observed at pH 4.0 within the same time period of 8 h. We observed an initial burst of drug release within 24 h, followed by a more sustained release of the drug till 54 h. For DOX at pH 4.0, an initial burst of drug release up to 6 h, followed by a sustained release pattern till 72 h was observed. In addition, similar release profiles obtained from both PTX and DOX indicated that the co-delivery system provided a synergistic effect. The above results can be ascribed to the hydrogen-bonding interaction between DOX and SWCNT which is stronger under neutral conditions, resulting in a controlled release.[55, 56] However, under acidic conditions, the drug release pattern shows higher amount of DOX release, as the amine ($-NH_2$) groups of DOX get protonated resulting in the partial dissociation of hydrogen-bonding interaction; hence, the DOX released from SWCNTs is much higher. This efficient loading and release of DOX indicates strong π-π stacking interaction between SWCNT and DOX. However, the drug release pattern for paclitaxel can be due to the hydrolysis of ester bonds to release paclitaxel in phosphate-buffered solutions.[53]

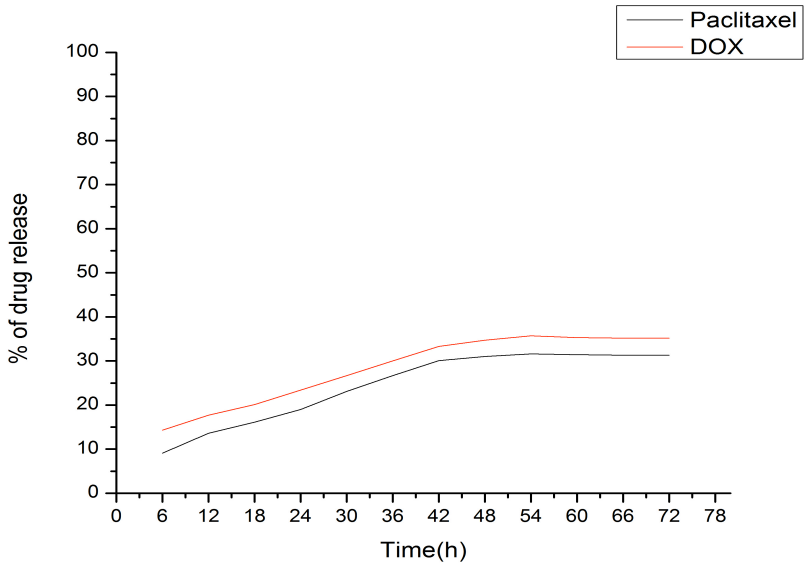

Figure 5. In vitro drug release profile of PTX and DOX from DOX-PTX-FA-PEG-SWCNT in phosphate buffered saline at pH 7.4.

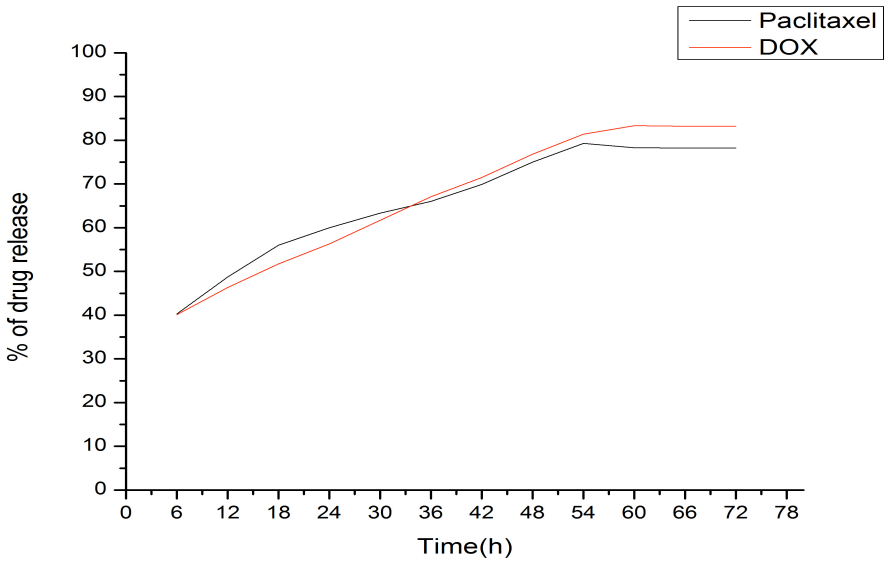

Figure 6. In vitro drug release profile of PTX and DOX from DOX-PTX-FA-PEG-SWCNT in phosphate buffered saline at pH 4.0.

Cellular imaging studies

To confirm the cellular uptake of the nanotubes and their localization within the cells, confocal laser scanning microscopy was performed. As shown in the Figure 7(a-c) and (d-f), the images confirm the accumulation of nanotubes within the lysosomes after 3 h of incubation with MCF7 cancer cells. The amount of DOX-PTX-PEG-SWCNTs accumulated within the MCF7 cells was less as observed by the low fluorescence intensity in the cancer cells, as compared to the folate targeted nanotubes DOX-PTX-FA-PEG-SWCNTs which showed a very strong fluorescence intensity in the cancer cells, indicating the significant role of folate in endosomal mediated cell uptake. Folate-negative L929 cells were used as a control. No fluorescence was observed in the nucleus of all the cells, which had taken up SWCNTs, indicating that no SWCNTs were translocated into the nucleus. To further confirm the endosome-mediated pathway of the nanotubes, lysosomal staining was performed using Lysotracker dye. The overlapping signals of red from the DOX-FA-PEG-SWCNT and green from lysosomes confirm the receptor-mediated endosomal uptake of the nanotubes into the cells.

In vitro cell viability studies

To study the enhanced drug effect brought about by the increased cellular uptake of the nanotubes due to folate conjugation in comparison with free PTX and free DOX, time dependent in vitro cytotoxicity assays were performed.

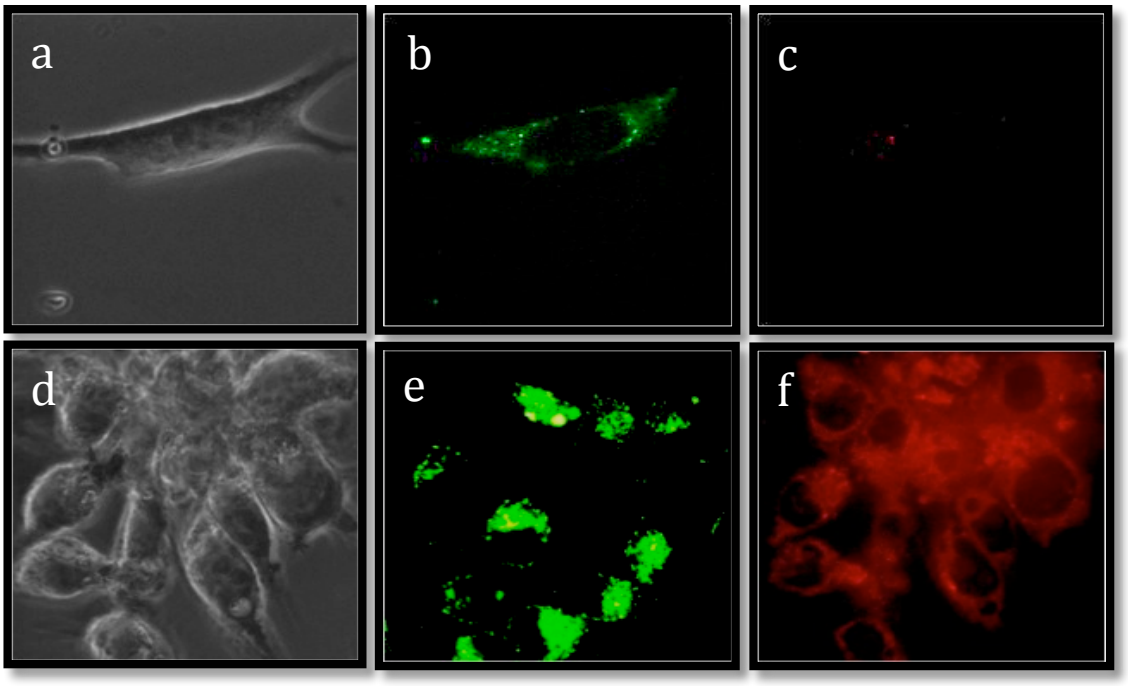

Figure 7. Confocal laser microscopy (CLSM) images showing the selective internalization of SWCNTs by L929 and MCF7 cells (a, d) Bright field images of the cells treated with nanotubes, (b, e) green fluorescence of the lysosomal staining of the cells with lysotracker dye, (c, f) red fluorescence of DOX conjugated nanotubes internalized in the cells.

The tumor cells were treated with DOX-PTX-FA-PEG-SWCNTs, PTX-FA-PEG-SWCNTs, DOX-FA-PEG-SWCNTs, free PTX and free DOX for 72 h. The assays were performed in triplicate. Three different concentrations of each of the above test samples were used. The percentage of cell viability measured for each of the samples was calculated using Alamar blue assay. As shown in Figure 8, co-delivery of PTX and DOX significantly reduced cell viability. Free single drug and single drug-loaded nanotubes induced similar cytotoxicity, demonstrating that the triggering mechanism for the release of the drug from the endosomes/lysosomes into the cytosols is highly efficient. Moreover when compared to single drug loaded nanotubes, the nanotubes

with dual drug (PTX- DOX) loaded showed the highest anti-tumor activity in the tumor cells. It is suggested that the synergistic effect might result from the combination of individual anti-tumor mechanism for each drug. DOX binds to DNA by intercalation, and motivates a series of biochemical events inducing apoptosis in tumor cells, and PTX can inhibit microtubules disassembly and promote the formation of unusually stable microtubule, thereby disrupting normal dynamic reorganization of the microtubule network required for mitosis and cell proliferation, and in turn causing cell apoptosis. Treating cancer cells using PTX and DOX together might achieve the best synergistic effects and accelerate tumor cell death with the highest anti-tumor efficacy.

Cancer destruction using the NIR effect of SWCNTs

The effect of SWCNTs on cancer cells during NIR laser treatment was investigated. MCF7 cells were incubated with DOX-PTX-FA-PEG-SWCNTs and DOX-PTX-PEG-SWCNTs for 3 h, followed by irradiation with an 800 nm laser for 3 min. Figure 9 shows the confocal images of MCF7 cells treated with DOX-PTX-FA-PEG-SWCNT before and after laser irradiation. The breaking of cancer cells due to the hyperthermia effects of SWNTs inside the cells can be observed and all cancer cells show distorted morphology of cells undergoing apoptosis. Figure 10 shows the confocal images of MCF7 cells treated with DOX-PTX-PEG-SWCNTs before and after laser irradiation. The images showed that the cells survived even after 3 min of laser exposure, which might be attributed to the low uptake of DOX-PTX-PEG-SWCNTs into the MCF7 cells, confirming the significant role of folate in the enhanced drug delivery to the tumor cells.

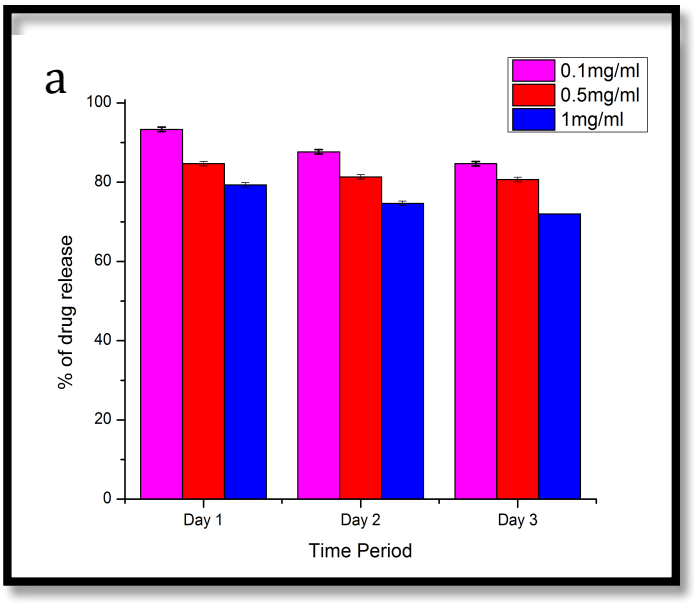

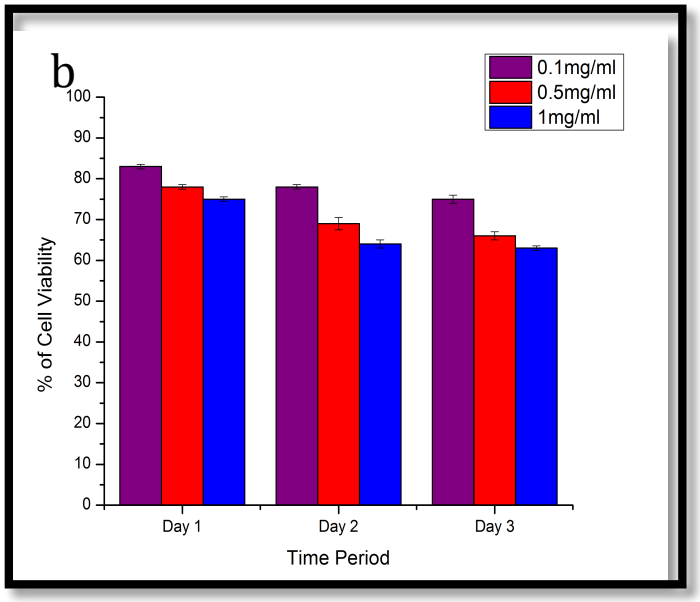

Figure 8 (a, b). A three-day cytotoxicity assay of (a) plain PTX and (b) plain DOX on MCF7 cells.

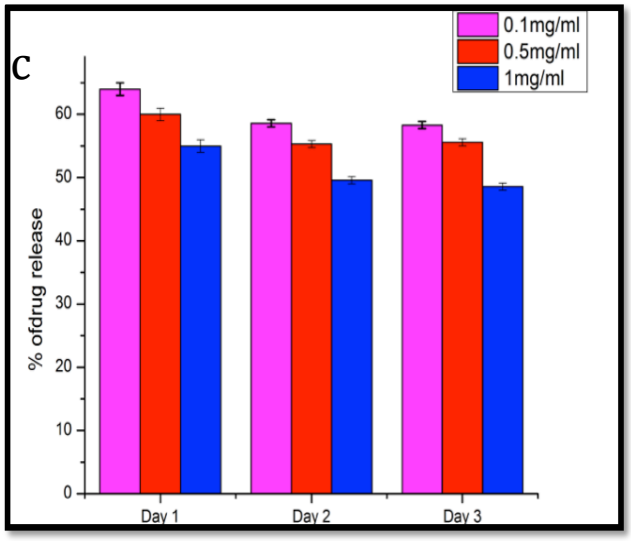

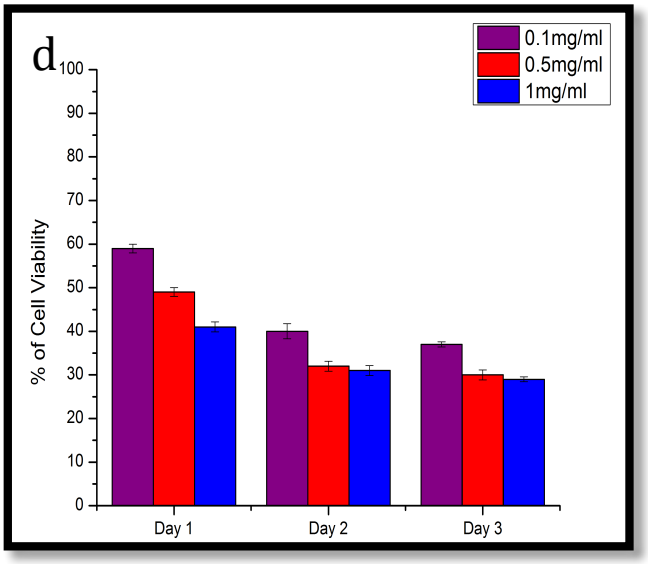

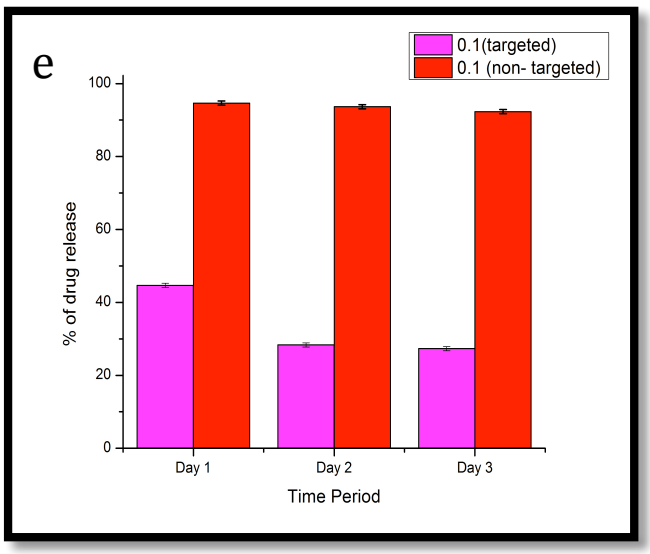

Figure 8 (c, d, e). A three-day of cytotoxicity assay of (a) PTX-FA-PEG-SWCNT, (b) DOX-FA-PEG-SWCNT and (c) PTX-DOX-FA-PEG-SWCNT on MCF7 cells.

The combined cytotoxic effect of laser and DOX loaded SWCNTs on cancer cells were further analyzed by Alamar blue assay. DOX-PTX-FA-PEG-SWCNTs + laser and DOX-PTX-PEG-SWCNTs + laser were incubated with MCF7 cells. Untreated cells were used as controls. All cells were irradiated with 800 nm laser for 3 mins. The experiments were carried out for 48 h. As shown in Figure 11, in case of cells treated with DOX-PTX-FA-PEG-SWCNTs a decreased rate of cell viability was observed. However, the cell viability rate was high for DOX-PTX-PEG-SWCNTs. This indicated that the targeted nanotubes were highly specific to folate receptors overexpressed in MCF7 cells.

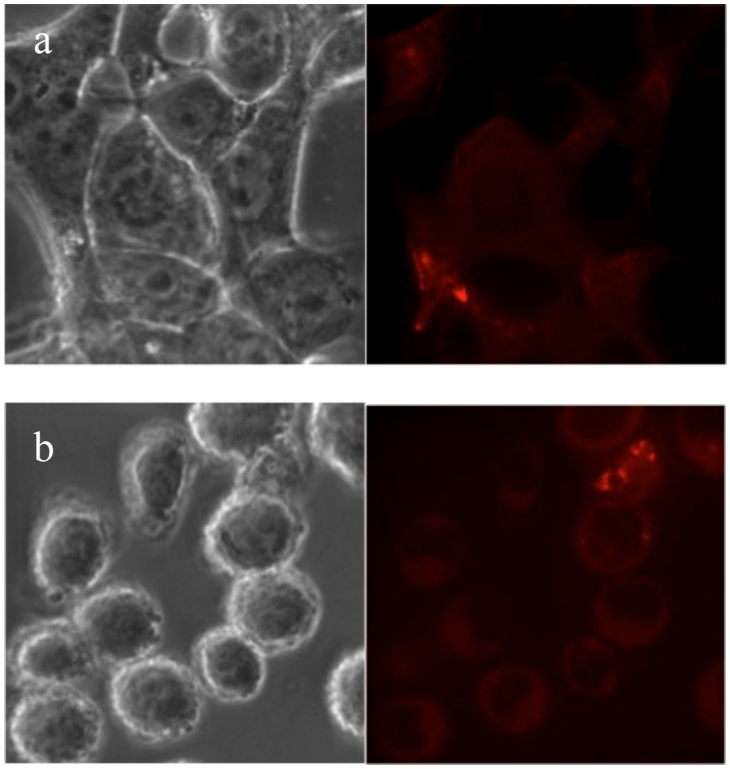

Figure 9. Confocal images of MCF7 cells treated with DOX-PTX-FA-PEG-SWCNT (a) before laser treatment (b) after 3 min laser treatment and viewed after 24 h.

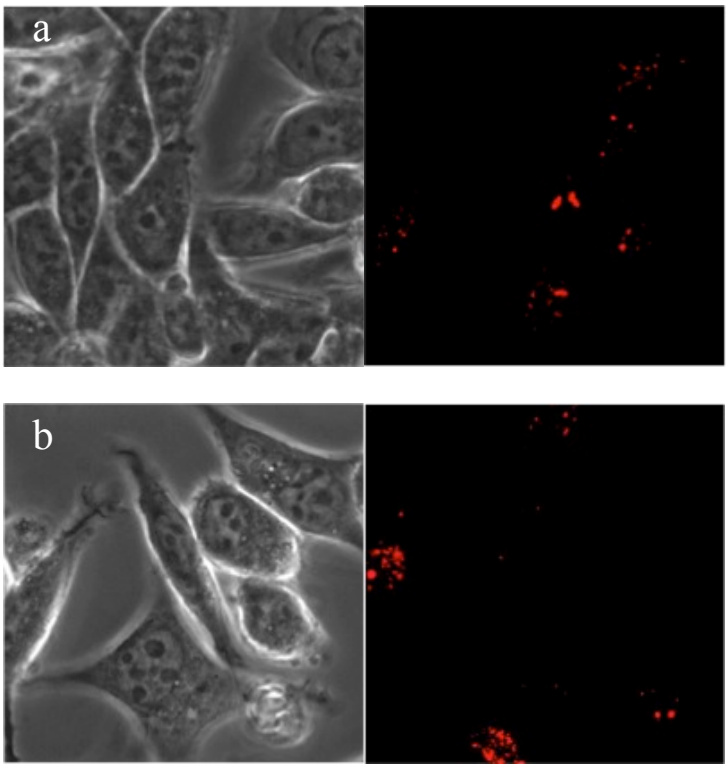

Figure 10. Confocal images of MCF7 cells treated with DOX-PTX-PEG-SWCNT (a) before laser treatment (b) after 3 min laser treatment and viewed after 24 h.

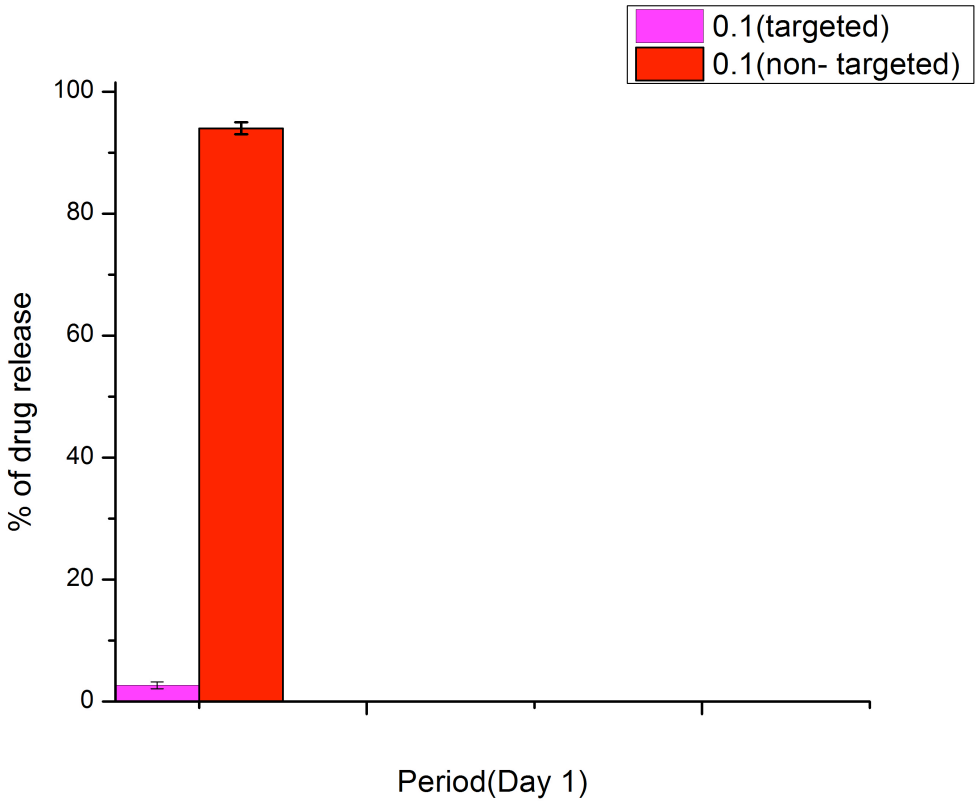

Figure 11. Results of cytotoxicity assay of DOX-PTX-FA-PEG-SWCNT and DOX-PTX-PEG-SWCNT after 3 min laser irradiation by an 800 nm laser on MCF7 cells.

Conclusion

We have synthesized a targeted carrier by combining the merits of PEGylated SWCNTs and further functionalized these nanotubes with tumor specific folate receptors to co-deliver PTX and DOX for pH responsive drug release in tumor therapy. These nanotubes possessed a high drug-loading yield. The releases of PTX and DOX at neutral pH were slow and sustained, however the drug releases were much faster in acidic environment. Studies on drug release and cellular uptake of the co-delivery system demonstrated that both drugs were effectively taken up by the cells and released simultaneously. Furthermore, the co-delivery nanocarrier suppresses tumor cells growth more efficiently than the individual delivery of either

PTX or DOX at the same concentrations, indicating a synergistic effect. Also, due to the presence of folate, efficient cellular targeting of the tumor cells was exhibited by the nanotubes that resulted in enhanced cytotoxicity in the selected tumor cells, avoiding toxicity to normal cells.

References

1. J Luo, NL Solimine, SJ Elledge. Cell. (2009) B6, 823-837.

2. W Hai, Z Ying, W Yan. et al. Biomaterials. (2011) 32, 8281-8290.

3. G Fundueanu, M Constantin, P Ascenzi. Biomaterials. (2008) 29, 2767–75.

4. DP Huynh, MK Nguyen, BS Pi. et al. Biomaterial. (2008) 29, 2527–34.

5. YC Wang, XQ Liu, TM Sun. et al. J Control Release. (2008) 128, 32–40.

6. K Nakamura, Y Maitani, AM Lowman. et al. J Control Release. (1999) 61, 329–35.

7. P Satya, M Meenakshi, S Wei. Adv. Drug delivery reviews. (2011) 63, 1340-1351.

8. Z Sobhani, R Dinarvand, F Atyabi. et al. International Journal of Nanomedicine. (2011) 6, 705–719.

9. D Pantarotto, R Singh, D McCarthy. et al. Angewandte Chemie. (2004) 43, 39, 5242–5246.

10. C Klumpp, K Kostarelos, M Prato. et al. Biochimica Biophysica Acta. (2006) 1758, 3, 404–412.

11. A Merkoc. Microchimica Acta. (2006) 152, 157–174.

12. N Ashok Kumar, HS Ganapathy, JS Kim. et al. European Polymer Journal. (2008) 44, 3, 579–586.

13. Z Liu, S Tabakman, K Welsher. et al. Nano Research. (2009) 2, 2, 85–120.

14. S Matsumura, K Ajima, M Yudasaka. et al. Molecular Pharmaceutics. (2007) 4, 5, 723–729.

15. M Endo, M Strano, P Ajayan. Berlin/Heidelberg: Springer-Verlag. (2008) 13–62.

16. T Murakami, K Ajima, J Miyawaki. et al. Molecular Pharmaceutics. (2004) 1, 6, 399–405.

17. SJ Son, X Bai, SB Lee. Drug Discovery Today. (2007) 12, 15, 16, 650–656.

18. X Wang, J Ren, X Qu. Chem Med Chem. (2008) 3, 6, 940–945.

19. Z Liu, X Sun, RN Nakayama. et al. ACS Nano. (2007) 1, 50–56.

20. MR McDevitt, D Chattopadhyay, BJ Kappel. et al. Journal of Nuclear Medicine. (2007) 48, 7, 1180–1189.

21. N Venkatesan, J Yoshimitsu, Y Ito. et al. Biomaterials. (2005) 26,34, 7154–7163.

22. W Yang, P Thordarson, JJ Gooding. et al. Nanotechnology. (2007) 18, 1–12.

23. Y Guo, D Shi, H Cho. et al. Advanced Functional Materials. (2008) 18, 17, 2489–2497.

24. G Pastorin, W Wu, S Wieckowski. et al. Chemical Communications (Camb). (2006) 11, 1182–1184.

25. Y Ren, G Pastorin. Advanced Materials. (2008) 20, 11, 2031–2036.

26. K Teker, R Sirdeshmukh, K Sivakumar. et al. Nanobiotechnology. (2005) 1, 2, 171–182.

27. M Foldvari, M Bagonluri. Nanomedicine. (2008) 4, 3, 183–200.

28. Z Amin, JJ Donald, A Masters. et al. Radiology. (1993) 187, 339-347.

29. CP Nolsoe, S Torp. Radiology. (1993) 187, 333-337.

30. TJ Vogl, MG Mack, PK Miller. et al. European Radiology. (1999) 9, 1479-1487.

31. N Huang, H Wang, J Zhao. et al. Lasers Surgical Medicine. (2010) 42, 9, 638–648.

32. X Liu, H Tao, K Yang. Biomaterials. (2011) 32, 1, 144–151.

33. X Zheng, F Zhou. J Xray Science and Technology. (2011) 19, 2, 275–284.

34. HK Moon, SH Lee, HC Choi. ACS Nano. (2009) 3, 11, 3707–3713.

35. JT Robinson, K Welsher, SM Tabakman. et al. Nano Research. (2010) 3, 11, 779–793.

36. NW Kam, M O'Connell, JA Wisdom. et al. Proceedings of National Academy of Science U S A. (2005) 102, 33, 11600–11605.

37. J Lehar, AS Krueger, W Avery. et al. Nat Biotechnology. (2009) 27, 659-66.

38. WG Jr Kaelin. Nature Review Cancer. (2005) 5, 689-98.

39. CT Keith, AA Borisy, BR Stockwell. Nature Review Drug Discov. (2005) 4, 71-8.

40. W Xiao, X Chen, L Yang. et al. International Journal of Pharmaceutics. (2010) 393, 119-26.

41. N Wiradharma, YW Tong, YY Yang. Biomaterials. (2009) 30, 3100-9.

42. F Ahmed, RI Pakunlu, A Brannan. et al. Journal of Control Release. (2006) 116, 150-8.

43. L Han, R Huang, J Li. et al. Biomaterials. (2011) 32, 1242-52.

44. DL Gustafson, AL Merz, ME Long. Cancer Letters. (2005) 220, 161-9.

45. S Lee, M Baek, HY Kim. et al. Biotechnology Letters. (2002) 24, 1147-51.

46. Y Huang, KR Johnson, JS Norris. et al. Cancer Research. (2000) 60, 4426-32.

47. J Liu, AG Rinzler, H Dai. et al. Fullerene Pipes. Science. (1998) 280, 1253-1256.

48. Z Bin, H Hui, Y Aiping. et al. Journal of American Chemical Society. (2005) 127, 8197-8203.

49. HM Deutsch, JA Glinski, M Hernandez. et al. Journal of Medicinal Chemistry. (1989) 32, 788–792.

50. XK Zhang, LJ Meng, QG Lu. et al. Biomaterials. (2009) 30, 6041-6047.

51. H Huang, Q Yuan, JS Shah. et al. Advanced Drug Delivery Reviews. (2011) 63, 1332-1339.

52. GJ Yan, C Jinping, J Jiefu. et al. International journal of Nanomedicine. (2011) 6, 2889-2898.

53. L Zhuang, C Kai, D Corrine. et al. Cancer Research. (2008) 68, 16, 6652-6660.

54. GJ Yan, C Jinping, J Jiefu. et al. International journal of Nanomedicine. (2011) 6, 2889-2898.

55. C Senlin, J Yugui, W Zhiqiang. et al. Langmuir. (2008) 24, 9233–9236.

56. D Depan, J Shah, RDK Misra. Material Science and Engineering (2011) 31, 1305-1312.

57. Z Liu, X Sun, NR Nakayama. et al. ACS Nano. (2007) 1, 50–56.

Chapter 6

Nano-carriers for therapeutic applications

Introduction

Nanotechnology has been exploited extensively to enhance the pharmacokinetic properties and therapeutic index of myriad of drugs. The therapeutic advantages of nanotechnology-derived drug delivery over current treatment modalities include lower drug toxicities improved bioavailability, reduced cost of treatment and increased patient adherence to treatment. Due to advantages of targeted drug delivery systems enhanced cytotoxicity in selected tumor cells, with minimal cytotoxicity to normal cells can be achieved. Thus enhancing the therapeutic efficacy of cancer therapy.

AS1411 Aptamer tagged PLGA-Lecithin- PEG nanoparticles for tumor cell targeting and drug delivery

Liposomes and polymers are widely used as drug carriers for controlled release, since they offer many advantages like increased treatment effectiveness, reduced toxicity and bio-degradability. In this work, anticancer drug loaded PLGA –lecithin-PEG nanoparticles were synthesized and were functionalized with AS1411 Anti-nucleolin aptamers for site specific targeting against tumor cells, which overexpresses nucleolin receptors. Drug loading studies indicated that under the same drug loading, the aptamer-targeted nanoparticles show enhanced cancer killing effect when compared to the non- targeted nanoparticles. In addition, the PLGA-lecithin-PEG nanoparticles exhibited high encapsulation efficiency and superior, sustained drug release than the drug loaded in plain PLGA nanoparticles. The results confirmed that AS1411 aptamer-PLGA-lecithin-PEG nanoparticles are potential carrier candidates for differential targeted drug delivery.

Chapter 7

Conclusion and future prospects

Nanotechnology has great potential in developing efficient cancer therapeutics. We have synthesized CNT encapsulated chemotherapeutic agents and targeted it for site-directed drug delivery. In this final chapter, we are presenting the major observations of our work.

1. Nano delivery systems hold great potential to overcome many of the present obstacles of drug delivery. Carbon nanotubes have been proposed and actively explored as multipurpose innovative carriers of drugs for drug delivery and diagnostic applications. They have many unique physical, mechanical and electronic properties, and these distinct and exceptional properties have made it possible to exploit CNTs as drug delivery systems for biomedical applications. CNTs are promising carriers of both small drug molecules as well as macromolecules such as genes and proteins. Functionalization of CNTs with an organic moiety has made possible their use in diagnostics for imaging as well as for targeting purposes, especially in cancer therapy. Nanotube drug delivery holds future promise for high treatment efficacy with low drug doses, combined with minimal side effects for cancer therapy.

Even though CNTs are playing a larger and most promising role in the field of nano-medicine, more research is required to guarantee safety in drug delivery. Functionalized CNTs have been considered biocompatible and safe for drug and bio-molecular delivery applications, as they are soluble in physiological media and are nontoxic. They have shown no accumulation in the tissues and can be readily excreted through the renal route. Toxicity studies are critical to establish the full in vivo potential of CNTs for drug delivery before their actual application and marketing. In order to understand the toxic impact of the systemic delivery of carbon nanotubes in

greater detail, more extensive toxicity, safety and efficacy studies in animal models and in humans over a longer time frame need to be performed. The effects of CNT aggregation, size, length, functionalization, metal impurities on the toxicological safety require more thorough research. Functionalization of SWCNTs and its effects on aggregation and consequent genotoxicity also needs to be evaluated. Overall, the use of CNTs for delivery of drugs and biomolecules is a significant development in the field of therapeutic nano-medicine.

2. We successfully synthesized a highly effective targeted NDDS based on PEG functionalized SWCNTs and then further functionalization was facilitated with a targeting group (FA) and an anticancer drug (Doxorubicin). The obtained system (DOX-FA-PEG-SWCNT) displays excellent stability under physiological conditions. It was found that it could also effectively release DOX at reduced pH typical of the tumor environment of intracellular lysosomes and endosomes. We conclude that this nanoscale drug delivery system is more selective and effective than the free drug and it should result in enhanced therapeutic effects, with reduced general toxicity and hence reduced side effects in patients. Considering these positive in vitro drug delivery results, the application of DOX-FA-PEG-SWCNT could be extended to enhance the efficiency of cancer therapy in vivo.

3. With this obtained system- (DOX-FA-PEG-SWCNT), we further demonstrate a photothermal technique for targeted cancer destruction by using the photothermal effect of SWCNTs. SWCNTs has a high optical absorbance in the NIR region, where biological tissues are highly transparent. From the observation of our data, it is clear that SWCNTs act efficiently to convert laser energy into heat after exposure to 800 nm laser irradiation in vitro. This advantage was used in selective photothermal therapy, for killing only cancer cells while sparing normal cells. Our results also

showed that both, concentration of SWCNTs and time of laser, are controlling factors for thermally induced cytotoxicity. Also, the combined effect of targeted drug loaded DOX-FA-PEG-SWCNT with photothermal therapy was studied and we observed that the combined effect synergistically killed almost 95% of cancer cells at an accelerated rate. We conclude that this nanoscale drug delivery system is more selective and effective than the free drug, and results in enhanced therapeutic effects, when combined with photothermal therapy and reduced general toxicity. Considering these promising in vitro drug delivery results, the application of DOX-FA-PEG-SWCNT combined with NIR laser could be extended to enhance the efficiency of cancer therapy in the near future.

4. We have synthesized a targeted carrier by combining the merits of PEGylated SWCNTs and further functionalizing these nanotubes with tumor specific folate receptors to co-deliver PTX and DOX for pH responsive drug release in tumor therapy. These nanotubes possessed a high drug-loading yield. The releases of PTX and DOX at neutral pH were slow and sustained, however the drug releases were much faster at acidic environment. Studies on drug release and cellular uptake of the co-delivery system demonstrated that both drugs were effectively taken up by the cells and released simultaneously. Furthermore, the co-delivery of nano-carrier suppresses tumor cell growth more efficiently than by the individual delivery of either PTX or DOX at the same concentrations, indicating a synergistic effect. Also, due to the presence of folate, efficient cellular targeting of tumor cells was exhibited by the nanotubes, which resulted in enhanced cytotoxicity in the selected tumor cells, avoiding toxicity to normal cells.

5. Anticancer drug loaded PLGA-lecithin-PEG nanoparticles were synthesized and were functionalized with AS1411 Anti-nucleolin aptamers for site specific targeting

against tumor cells, which overexpresses nucleolin receptors. Drug loading studies indicated that under the same drug loading, the aptamer-targeted nanoparticles show enhanced cancer killing effect when compared to the non- targeted nanoparticles.

Developments of anticancerous nanoparticles have been considered as one of the promising therapeutic applications in the growing field of nanotechnology. Cancer nanotechnology exerts its application through the development of nanocarriers with multiple functionalities which can be targeted to tumors, and which can act as controlled delivery vehicles for improved therapy efficacy. These advances will hopefully open new pathways and innovations in the field of nanoscience and nanotechnology.

Acknowledgments

First and foremost, I would like to thank God Almighty for his continuous blessings and immense care throughout my life.

I am deeply indebted to my husband Andrew Jeyathilagar who was with me in the entire journey and with his words of support and encouragement; I got the strength to come to this level. I couldn't have achieved any of this without you. Each step, you guided me, stood by me, with deep understanding. Words aren't enough to convey what you mean to me. **I owe a lot to my little Queen Anika Melissia for whom I dedicate this Thesis**. Her sacrifice is more than anything I did in these three years.

I am grateful to my dad Col. Jeyamohan Kandaswamy, my mom Niruparani Jeyamohan, and my sister Dr. Tarani for their invaluable support and unconditional love and encouragement without which I could not have achieved any of these. And also I want to express my gratitude to my in-laws Dr. Jeyathilagar Duraiswamy and Dr. Thamilmani Jeyathilagar for their constant prayers and their words of confidence.

I owe my deepest gratitude to Prof. Sakthi Kumar and Prof. Toru Maekawa, my principal supervisors of my research work. I am extending my sincere and heartfelt thanks to Prof. Sakthi Kumar for the opportunity he gave me to be a part of his research team, for the excellent mentoring of my research and production of the thesis and unconditional help whenever the situation called for. His incredible patience, friendly and understanding nature went a long way to make this research

happen. His sincere and timely advices and constant encouragement was a driving force to do this PhD. I am grateful to Prof Toru Maekawa, Director, Bio-Nano Electronics Research Center who ensured availability of all facilities required for the work and provided immense encouragement and showered generous appreciation during my research.

I would like to express my sincere thanks to Prof. Y. Yoshida for his help and support in my scholarship application process and research study.

I extend my sincere appreciation to Prof. H. Morimoto, for his timely help. I recollect with gratitude the cooperation and help provided by Dr. Y. Nagaoka, Dr. T. Hasumura, Dr. T. Fukuda, Dr. Y. Nakajima, Mr. Y. Hayasaki to conduct my experiments and to operate and analyze the results with the help of various sophisticated equipments.

I wish to express my sincere thanks to Mr. K. Hirakawa, the technical manager for his great help and support in operating electron microscopy. I wish to thank all the staff and students of Bio-Nano Electronics Center and chemistry laboratories.

I am grateful to non-teaching staff of Toyo University for their never-ending support with the administrative work. Ms. Y. Tsuburaya, Ms. Y. Kawagoe, Ms. M. Koizumi, Ms. A. Tanaka, Ms. N. Tomita, Ms. T. Natsue, Mr. H. Akasu and Ms. N. Setojima are gratefully remembered for all the kind help.

I am deeply indebted to Yuko Tsuburaya San for her motherly affection and support, which provided me the strength and stability during my study. I am

grateful to her in providing me all the help and cooperation during my study at Toyo University.

I am thankful to the librarians and security staff members of Toyo University for their kind support. Thanks to Mr. Hirayama and Mr. Maekawa for their timely delivery of chemicals and apparatus.

I wish to extend my warmest thanks to all my colleagues - Dr. Saino H V, Dr. Remya N, Dr. Baiju N, Dr. Brahateeshwram D, Dr. Srivani V, Dr. Aby C P, Dr. Ashwathy Ravindran, Dr. Sreejith R, Dr. Sheikh M, and Dr. Ankur B. Mr. Siva B, Mr. Vivek P, Ms. Neha C, Ms. Archana M R and Mr. Anil for their cooperation and teamwork.

Words are not enough to express my gratefulness to my dear friends Dr. Athulya Aravind and Dr. Anila Mathew who stood by me at times of hardship as well as happiness and guided me during the various stages of my work.

I remember all my friends in japan who were so supportive all these three years and especially I want to shower my gratitude to my friends Ambily Justin, Sudha Vinoth, Kavitha Manikandaraja and Lavanya Senthamil, who were so understanding and gave their wholehearted support whenever I needed. Spending time with them gave me the much-needed relaxation during my stressful days. My gratitude is also goes to another little angel Eva Justin, friend of my daughter for her help in spending time with my daughter whenever I come late or engaged in my work.

There is a special person whom I am deeply indebted and thankful. Anitha Ayappan Pillai, whom I look to as my Friend, Philosopher and Guide. Without her guidance or encouragement I wouldn't have joined this course. She was a constant source of encouragement whom I discuss anything which troubles me. Whenever I talk with her I always gain confidence and strength from each and every word she speaks. I am happy she came into my life at the right time as a guiding light for my career. Thank you chechi.

My gratitude also goes to the CWAJ (College Women's Association in Japan), Japan and Otsuka Toshimi Scholarship foundation for providing their financial support in the form of a scholarship to complete my research.

Prashanti Jeymohan

Publications

1. Athulya Aravind, **Prashanti Jeyamohan**, Remya Nair, Srivani Veeranarayanan, Yutaka Nagaoka, Yasuhiko Yoshida, Toru Maekawa, D. Sakthi Kumar. AS1411 Aptamer Tagged PLGA-Lecithin-PEG nanoparticles for tumor cell targeting and drug delivery. Biotechnology and Bioengineering, 2012, DOI: 10.1002/bit.24558.

2. **Prashanti Jeyamohan**, Takashi Hasumura, Yutaka Nagaoka, YasuhikoYoshida, Toru Maekawa, D.Sakthi Kumar. Accelerated killing of cancer cells using multifunctional SWCNTs based system for targeted drug delivery in combination with photothermal therapy. International Journal of Nanomedicine, 2013 (Accepted).

3. **Prashanti Jeyamohan**, YasuhikoYoshida, Toru Maekawa, D.Sakthi Kumar. Opportunities and challenges of single walled carbon nanotubes in cancer therapy (Review, to be submitted).

4. **Prashanti Jeyamohan**, Takashi Hasumura, Yutaka Nagaoka, YasuhikoYoshida, Toru Maekawa, D.Sakthi Kumar. Co-delivery of dual drugs using multifunctional carbon nanotubes for cancer therapy. Biotechnology and Bioengineering, 2013 (to be submitted).

Conferences

1. **Prashanti Jeyamohan,** Sanal Sukuvihar, Yasuhiko Yoshida, Toru Maekawa, D. Sakthi Kumar. *Carbon nanotubes mediated cancer therapy* (poster). India-Japan Synposium in Emerging Technologies, Tokyo, Japan. October 7, 2011.

2. **Prashanti Jeyamohan**, Athulya Aravind, Srivani Veeranarayanan, Aby Cheruvathoor Poulose, Yasuhiko Yoshida, Toru Maekawa, D. Sakthi Kumar. *Functionalized Single-walled Carbon Nanotubes as Nanocarriers Against Breast Cancer* (Poster). 9th International Symposium on Bioscience and Nanotechnology, December 10, 2011, Toyo University, Tokyo, Japan.

3. **Prashanti Jeyamohan**, Athulya Aravind, Yasuhiko Yoshida, Toru Maekawa, D. Sakthi Kumar. *Single walled nanotubes as drug delivery vehicles (Poster)*. 3rd India-Japan Symposium on Frontiers in Science & Technology: Successes & Emerging Challenges, September 20, 2012, Tokyo, Japan**.**

4. **Prashanti Jeyamohan,** Ankur Baliyan, Takashi Hasumura, Yutaka Nagoaka, Yasuhiko Yoshida, Toru Maekawa, D. Sakthi Kumar. *Cancer-cell Targeting using Single-Walled Carbon Nanotubes for Cancer Photothermal Therapy (Poster).* BNERC and IJAA joint International Symposium on Advanced Science and Technology, December 7, 2012, Toyo University, Tokyo, Japan.

APPENDIX I

GLOSSARY

NDDS	Nano Drug Delivery System
DDS	Drug Delivery System
TEM	Transmission Electron Microscope
SEM	Scanning Electron Microscopy
AFM	Atomic Force Microscope
XPS	X-ray Photoelectron Spectroscopy
UV-Vis	Ultraviolet-Visible Spectrometer
CLSM	Confocal Laser Scanning Microscopy
ESCA	Electron Spectroscopy for chemical analysis
NIR	Near Infrared
IR	Infra red
CNTs	Carbon Nanotubes
SWCNTs	Single Wall Carbon Nanotubes
MWCNTs	Multiwall Carbon Nanotubes
SWCNT-COOH	Carboxylic acid functionalized SWCNTs
DOX-FA-PEG-SWCNTs	Doxorubicin and folate conjugated
HNO_3	Nitric acid
H_2SO_4	Sulfuric acid
NHS	N-hydro succinimide
DSC	Disuccinimide carbonate
DMF	Dimethylformamide
NaOH	Sodium Hydroxide

dd.H_2O	Double Distilled Water
DI	Distilled Water
MWCO	Molecular weight cut off
AB	Alamar Blue
FITC	Fluorescein Isothiocyanate
DMEM	Dulbecco's Minimal Essential Medium
PBS	Phosphate buffered saline
FBS	Foetal Bovine Serum
PEG	Polyethylene Glycol
FA	Folic acid
DSPE-PEG_{2000}-NH_2 folate	1, 2-distearoyl-sn-glycero-N-carboxy (polyethylene glycol)$_{2000}$ aminefolate
DOX	Doxorubicin
PTX	Paclitaxel
MCF7	Human Breast Adenocarcinoma
L929	Mouse Fibroblast Cells
CO_2	Carbondioxide